NASA/TM-2003-212413

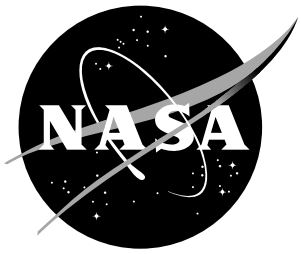

Survey of Primary Flow Measurement Parameters at the NASA Langley Transonic Dynamics Tunnel

David J. Piatak
Langley Research Center, Hampton, Virginia

June 2003

The NASA STI Program Office . . . in Profile

Since its founding, NASA has been dedicated to the advancement of aeronautics and space science. The NASA Scientific and Technical Information (STI) Program Office plays a key part in helping NASA maintain this important role.

The NASA STI Program Office is operated by Langley Research Center, the lead center for NASA's scientific and technical information. The NASA STI Program Office provides access to the NASA STI Database, the largest collection of aeronautical and space science STI in the world. The Program Office is also NASA's institutional mechanism for disseminating the results of its research and development activities. These results are published by NASA in the NASA STI Report Series, which includes the following report types:

- TECHNICAL PUBLICATION. Reports of completed research or a major significant phase of research that present the results of NASA programs and include extensive data or theoretical analysis. Includes compilations of significant scientific and technical data and information deemed to be of continuing reference value. NASA counterpart of peer-reviewed formal professional papers, but having less stringent limitations on manuscript length and extent of graphic presentations.

- TECHNICAL MEMORANDUM. Scientific and technical findings that are preliminary or of specialized interest, e.g., quick release reports, working papers, and bibliographies that contain minimal annotation. Does not contain extensive analysis.

- CONTRACTOR REPORT. Scientific and technical findings by NASA-sponsored contractors and grantees.

- CONFERENCE PUBLICATION. Collected papers from scientific and technical conferences, symposia, seminars, or other meetings sponsored or co-sponsored by NASA.

- SPECIAL PUBLICATION. Scientific, technical, or historical information from NASA programs, projects, and missions, often concerned with subjects having substantial public interest.

- TECHNICAL TRANSLATION. English-language translations of foreign scientific and technical material pertinent to NASA's mission.

Specialized services that complement the STI Program Office's diverse offerings include creating custom thesauri, building customized databases, organizing and publishing research results ... even providing videos.

For more information about the NASA STI Program Office, see the following:

- Access the NASA STI Program Home Page at ***http://www.sti.nasa.gov***

- E-mail your question via the Internet to help@sti.nasa.gov

- Fax your question to the NASA STI Help Desk at (301) 621-0134

- Phone the NASA STI Help Desk at (301) 621-0390

- Write to:
  NASA STI Help Desk
  NASA Center for AeroSpace Information
  7121 Standard Drive
  Hanover, MD 21076-1320

NASA/TM-2003-212413

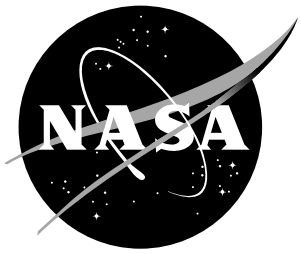

Survey of Primary Flow Measurement Parameters at the NASA Langley Transonic Dynamics Tunnel

David J. Piatak
Langley Research Center, Hampton, Virginia

National Aeronautics and
Space Administration

Langley Research Center
Hampton, Virginia 23681-2199

June 2003

Available from:

NASA Center for AeroSpace Information (CASI)
7121 Standard Drive
Hanover, MD 21076-1320
(301) 621-0390

National Technical Information Service (NTIS)
5285 Port Royal Road
Springfield, VA 22161-2171
(703) 605-6000

Table of Contents

Abstract

An assessment of the methods and locations used to measure the primary flow conditions in the NASA Langley Transonic Dynamics Tunnel was conducted during calibration activities following the facility conversion from a Freon-12 heavy-gas test medium to R-134a. A survey of stagnation pressure, plenum static pressure, and stagnation temperature was undertaken at many pertinent locations in the settling chamber, plenum, and contraction section of the wind tunnel and these measurements were compared to those of the existing primary flow measurement systems. Local flow velocities were measured in the settling chamber using a pitot probe. Results illustrate that small discrepancies exist between measured primary tunnel flow conditions and the survey measurements. These discrepancies in tunnel stagnation pressure, plenum pressure, and stagnation temperature were found to be approximately $\pm 1-3$ *psf and* $2-3$ *degrees Fahrenheit. The propagation of known instrument errors in measured primary flow conditions and its impact on tunnel Mach number, dynamic pressure, flow velocity, and Reynolds number have been investigated analytically and shown to require careful attention when considering the uncertainty in measured test section conditions.*

Nomenclature

f	re-entry flap setting, deg
M	Mach number
p	pressure, psf
R	Reynolds number
T	temperature, ^{o}F
q	dynamic pressure, psf
x	R-134a purity ratio
γ	Ratio of specific heats
ρ	density, slug/ft^3
μ	viscosity, lb$_f$-s/ft^2

Abbreviations:

CLST4	Ceiling station 4 plenum pressure
CT	Centerline tube
EWST1	East wall station 1 plenum pressure
FLST2	Floor station 2 plenum pressure
Sta1	Vane D station 1
RTD	Resistance temperature device

TC	Thermocouple
TS	Tunnel station, ft
VC	Vane C
VD	Vane D
WWST3	West wall station 3 plenum pressure

Subscripts:

i	initial, wind-off condition
m	main flap
n	nose flap
o	stagnation condition
pl	plenum

Introduction

The NASA Langley Transonic Dynamics Tunnel (TDT) is a continuous-flow transonic wind tunnel that was specifically designed for the testing of aeroelastic wind-tunnel models in a heavy gas or air test medium. The TDT has a 16-ft square slotted test section that is capable of Mach numbers from near 0 to 1.2. Stagnation pressures can be varied in the facility from pressures below 50 psf up to atmospheric pressure and dynamic pressure can be varied up to a value of 300 psf for an air test medium, and up to 550 psf for heavy gas testing.

The TDT is a unique facility for testing aeroelastic models large enough to allow the accurate scaling of mass and stiffness distributions from the full-scale vehicle to the model. Besides matching such important model structural and mass properties, it is imperative for high-subsonic and transonic flutter models that full-scale Mach numbers be matched because of compressibility effects. In addition, other dimensionless quantities such as reduced frequency and Froude number may need to be matched to adequately represent full-scale flight conditions. Using reasonable model construction capabilities, it is not possible to match Mach number, Froude number, and reduced frequency simultaneously for most flight vehicles using air as a test medium in a wind tunnel. However, it may be possible to match these dimensionless parameters by testing in a heavy gas.

Recently, the TDT has undergone a conversion from Freon-12 as a test medium to R-134a for environmental purposes. Because of the change in test medium, it was necessary to determine the TDT performance envelope and document various test section flow parameters before regular testing resumed. Over the period of a year, an exhaustive calibration effort involving sidewall, centerline, boundary-layer, and test section core (survey rake) measurements was completed. Turbulence measurements were also made using the sting-mounted survey rake. In addition to these measurements, an assessment of the methods and locations used to measure TDT primary flow conditions was conducted. Primary tunnel flow parameters include stagnation pressure, plenum static pressure, stagnation temperature, and R-134a gas purity. These flow parameters are used to determine calculated test section conditions such as freestream Mach number, Reynolds number, speed of sound, medium density, medium viscosity, and flow velocity. References 1 and 2 describe the TDT heavy gas conversion project and the calibration of the facility.

This paper will focus on the measurement of these primary flow parameters and attempt to assess the methods and locations used to measure them at the TDT.

Facility Description

The TDT is a continuous-flow transonic wind tunnel that has many unique features that make it well suited for aeroelastic testing. The facility is capable of attaining Mach numbers between near zero to 1.2 in both air and R-134a as a test medium. Stagnation pressures can be varied in the facility from pressures below 50 psf up to atmospheric pressure. Dynamic pressure, an important parameter in aeroelastic testing, can be varied up to a value of 300 psf for an air test medium, and up to 550 psf for heavy gas testing. Figures 1 and 2 illustrate the configuration of the TDT and figures 3 and 4 show the operating envelope for air and heavy gas test mediums.

Referring to figures 1 and 2, the major components of the TDT include a steel pressure shell, settling chamber, contraction section, slotted test section with plenum chamber, diffuser section, electric drive system with 47-blade fan, and a high-volume gas handling system for heavy gas operations. The 16-ft square test section with cropped corners is surrounded by a 60ft diameter plenum chamber and has three transonic slots in both the ceiling and the floor to provide adequate area for flow expansion and subsequently to avoid choked flow above the speed of sound (M=1). The transonic slot shapes are designed to provide a nearly gradient free region of flow at transonic speeds in the vicinity of a model. Additional slots are located on the tunnel walls for the purpose of reducing model blockage effects. During operations above a Mach number of 0.85, hinged re-entry flaps are progressively opened to allow flow that exits the test section through the transonic slots to re-enter the main flow in the diffuser section.

Primary Flow Conditions

The primary flow conditions of the TDT consist of stagnation pressure, plenum chamber pressure, stagnation temperature, and R-134a gas purity. From these primary measurements, test section Mach number, dynamic pressure, speed of sound, flow velocity, and Reynolds Number are determined. Thus the flow conditions in the test section are adequately defined. If the test

medium was air or pure R-134a, then Mach number based on the measured stagnation pressure and plenum pressure could be determined by the equation

$$M_{pl} = \sqrt{\frac{2}{\gamma - 1}\left[\left(\frac{p_o}{p_{pl}}\right)^{\frac{\gamma-1}{\gamma}} - 1\right]}$$

where γ is the appropriate value for pure air or R-134a. The actual test section free-stream Mach number would then be determined by applying empirical data from the calibration of the transonic test section such that

$$M_\infty = f\left(M_{pl}\right).$$

Historically, empirical corrections to Mach number have not been applied to the calculated plenum Mach number at the TDT because calibration studies have shown that there is little appreciable difference between free-stream Mach number, M_∞, and plenum Mach number, M_{pl}.

During testing in heavy gas it is typically not possible to achieve 100 percent pure R-134a in the tunnel circuit. Therefore, an iterative process has been developed to determine TDT operating conditions based on the four primary flow measurements using real-gas equations and accounting for air/R-134a gas mixtures. This process is described in Reference 3.

Existing TDT Primary Flow Measurement Systems

The measurement locations for each primary flow parameter are illustrated in Figure 5. Stagnation pressure is measured on the west wall of the settling chamber at tunnel station 0 at the beginning of the contraction section by a pressure probe that extends 2 ft from the wall at the tunnel vertical centerline. Plenum chamber pressure is measured from an open orifice between the outer shell of the control room and the plenum chamber west wall. This location is well suited for measuring plenum chamber pressure since it is protected from unsteady flow near the test section slots. Stagnation pressure and plenum pressure tubing lead to a pair of Ruska Series 6000 direct reading pressure gages. These gages are located at the vertical centerline of the wind

tunnel to minimize buoyancy effects. Table 1 lists the quoted accuracy of the Ruska system and other TDT instrumentation.

Referring to Figure 5, stagnation temperature is measured in the settling chamber on turning vane C near the tunnel centerline using a type J thermocouple. It appears that the thermocouple units have been in operation since the conversion of the 19ft Pressure Tunnel to the present TDT configuration in the mid 1950's. These stagnation temperature thermocouples are located 3 feet downstream of the tunnel cooling coils and at one time were used as part of a system to automatically control tunnel temperature. This control system is no longer used by the facility. It was realized that this location may not be ideal due to its proximity to the tunnel cooling coils and further investigation was conducted as part of this study.

The fourth primary tunnel flow parameter that is measured is the purity of the R-134a test medium. Calculated tunnel parameters such as γ, ρ, and μ are dependant on R-134a test medium purity and thus are all other calculated tunnel parameters. R-134a purity is measured using a Servomex infrared gas analyzer whose accuracy is listed in Table 1. Gas is sampled from the tunnel circuit downstream of the test section on the west wall of the diffuser section on the test section vertical centerline (see Figure 5).

TDT Flow Measurement Survey Instrumentation

To assess and document trends in the primary flow parameters measured at locations in the settling chamber and plenum of the TDT, instrumentation was developed and installed to conduct a flow survey of stagnation pressure, plenum pressure, and stagnation temperature. In addition to these measurements, pitot-static measurements were made in the settling chamber and contraction section to assess local flow velocities.

Stagnation, Plenum Chamber, and Static Pressure

Stagnation pressure instrumentation consisted of nine probes mounted in a 3-by-3 grid on turning vane D in the settling chamber just prior to the contraction section of the wind tunnel. Figure 6 illustrates the arrangement of the probes on vane D. Each probe consisted of a 4.5 ft long, 0.5 inch diameter steel tube which was mounted on the turning vane shelves and oriented downstream parallel to the flow. A 0.25 inch diameter steel tube which was mounted within the

0.5 inch tube was bent ninety degrees, extended 1.5 feet perpendicular to the 0.5 inch tube and the flow, and finally bent another ninety degrees parallel to the flow to measure stagnation pressure. Figure 7 shows a pressure probe mounted to turning vane D in the settling chamber. All nine stagnation pressure probes were connected via flexible tubing to an Electronic Pressure Scanner (ESP) module mounted to the center turning vane shelf. The ESP module was rated at 1 psi of differential pressure and therefore required an additional stagnation pressure probe for this reference pressure. This reference probe was mounted on the west wall of the settling chamber where the primary stagnation pressure measurement is made (see Figure 5). Table 1 lists the accuracy of the 1-psid ESP module.

In addition to the instrumentation described above, stagnation and static pressure measurements were also acquired in the contraction section using a pitot-static probe mounted to a centerline tube that extended along the test section centerline and into the contraction section. Figure 8a shows the centerline tube mounted in the TDT test section and contraction section. The pitot-static probe on the centerline tube is identified in Figure 8b. The centerline tube stagnation and static pressure measurements were acquired using a 1-psid ESP module referenced to the plenum static pressure. At this measurement location, flow velocity was well below the speed of sound and therefore no oblique shock waves were present at the tip of the probe.

Plenum chamber pressure was surveyed at four locations around the test section of the TDT. Flexible pressure tubing terminated at locations 6 ft above and below the test section and at locations to the east of the test section on the end of the east platform (Figures 1-2) and west of the test section on the outer control room chamber. Beyond locating the pressure tubing several feet from the test section walls, no attempt was made to shield the measurement points from the unsteady effects of slot flow. ESP modules (1-psid) referenced to tunnel primary plenum pressure were used to conduct the survey.

Centerline tube static pressures are also reported and compared to the measured plenum chamber pressure measurements. Static pressure orifices were located along the length of the centerline tube and static pressures were measured using 1 and 5 psid ESP modules referenced to plenum chamber pressure. In this report, the average centerline tube static pressure from TS 70 to TS 74 is presented.

Stagnation Temperature

Total, or stagnation, temperature was measured at locations on turning vanes C and D in the settling chamber and in the test section for this survey. Figure 6 illustrates the locations where stagnation temperature was measured on turning vane D. Stagnation temperature was also measured on vane C near the tunnel primary stagnation temperature measurement location (see Figure 5) and in the test section on the centerline tube. Figure 8 shows the stagnation cup in which stagnation temperature was measured near the nose of the centerline tube in the contraction section of the TDT.

Two methods of temperature measurement were employed: type-T thermocouples and Resistance Temperature Device (RTD). Type-T thermocouples were chosen for fast response time while the RTD was chosen for stability and accuracy of temperature measurements. Figure 9 shows the mount used for RTD and thermocouple instrumentation on vane D. Table 1 lists the typical accuracy of type-T thermocouples and each RTD.

Settling Chamber Flow Velocity

The local velocity of the flow in the settling chamber was measured for the purpose of confirming the assumption that static temperature measurements made in the settling chamber can be assumed to be nearly identical to stagnation conditions. This assumption is valid when local Mach number is sufficiently small ($M < 0.2$). A pitot probe was mounted to turning vane D in the settling chamber and both local static and stagnation pressure were measured using a 1-psid ESP module.

Re-entry Flap Schedule

During operations above $M = 0.85$, double-hinged re-entry flaps are progressively opened to allow flow that exits the test section through the transonic slots to re-enter the main flow in the diffuser section, downstream of the test section. All data presented have been recorded at the standard re-entry flap settings defined in table 2.

Survey Results

Results presented were acquired during TDT calibration testing using the instrumentation described above at a variety of tunnel conditions in both air and R-134a as a test medium. During R-134a testing, the percentage of the gas in the tunnel was maintained above 90 percent.

Measurements of stagnation pressure and plenum pressure are presented as differential pressures measured by the differential ESP modules referenced to primary tunnel stagnation and plenum chamber pressure measurement locations respectively. This simplifies comparison to primary flow parameters measured by the TDT Ruska pressure gages. All stagnation temperature data are presented in degrees Fahrenheit and as a differential temperature for convenience and pitot probe velocity data are presented in feet per second.

Stagnation Pressure Results

Differential stagnation pressure results from the flow survey are presented in this section for set wind-off tunnel pressures and at constant dynamic pressures. Constant wind-off pressure results contain differential stagnation pressure data from the nine probes mounted to turning vane D of the TDT. Constant dynamic pressure results contain both vane D stagnation pressure data and centerline tube stagnation pressure data.

Constant wind-off tunnel pressure results in air. Differential stagnation pressure results from turning vane D probes are presented in this section versus test section Mach number for several wind-off tunnel pressures. Results presented in figures 10-13 have been acquired at wind-off (starting) stagnation pressures of 200 psf, 400 psf, 700 psf, 1200 psf, and 2200 psf (atmospheric pressure) in air as the test medium.

Constant dynamic pressure results in air. As discussed above, differential stagnation pressure data were obtained at constant dynamic pressure using both vane D instrumentation and instrumentation located at the nose of the centerline tube within the contraction section of the TDT. Figures 14 and 15 present results of these measurements for dynamic pressures of 125 psf and 200 psf in air as a test medium.

Constant wind-off pressure results in R-134a. Figures 16 through 21 illustrate the measured vane D differential stagnation pressures at wind-off tunnel stagnation pressures of 200 psf, 500 psf, 700 psf, 1000 psf, 1400 psf, and 1800 psf for a test medium of R-134a.

Constant dynamic pressure results in R-134a. Differential stagnation pressure measurements from the centerline tube total probe located in the contraction section of the TDT is presented in this section at constant values of dynamic pressure for an R-134a test medium. Figures 22 through 24 illustrate the measured centerline-tube probe differential stagnation pressures for constant tunnel dynamic pressures of 100 psf, 225 psf, and 350 psf respectively. An instrumentation failure during testing precluded acquiring vane D differential stagnation pressure measurements at higher dynamic pressures.

Plenum Chamber Pressure Results

Plenum static pressure results from the flow survey are presented in this section for several wind-off pressures and for constant dynamic pressures. Constant wind-off tunnel pressure results contain differential stagnation pressure data from the four stations surrounding the test section of the TDT. Constant dynamic pressure results contain data from both the four static pressure measurements around the test section and the centerline tube stagnation pressure measurements.

Constant wind-off pressure results in air. Figures 25 through 28 illustrate the differential plenum chamber static pressures versus Mach number at four points around the test section: above, below, to the west near the control room chamber, and on the end of the east platform. Data are presented for wind-off stagnation pressures of 200 psf, 400 psf, 700 psf, 1200 psf and atmospheric pressure.

Constant dynamic pressure results in air. Figures 29 through 30 illustrate plenum chamber differential pressures versus test section Mach number at four measurement points around the test section and also the averaged differential pressure from TS 70 to TS 74 along the east and west side of the centerline probe. The data are presented for constant dynamic pressures of 125 psf and 200 psf.

Constant wind-off pressure results in R-134a. Figures 31 through 36 show differential plenum static pressures versus test section Mach number at the four measured points surrounding the test section. Results are presented for wind-off pressures of 200 psf, 500 psf, 700 psf, 1000 psf, 1400 psf, and 1800 psf.

Constant dynamic pressure results in R-134a. Plenum chamber differential static pressures and centerline tube static pressures for measurements at constant dynamic pressures of 100, 225, and 350 psf are shown figures 37 through 39.

Stagnation Temperature Results

Stagnation temperature data measured on vane D, vane C, and on the centerline tube are presented in this section. Figure 6 illustrates the vane D stagnation temperature instrumentation stations and Figure 8 shows the stagnation cup near the nose of the centerline tube that contains a thermocouple. As previously discussed, vane D stagnation temperature instrumentation consists of both RTD's and thermocouples. Stagnation temperature data are presented for constant dynamic pressures of 125 psf and 200 psf in air and for constant dynamic pressures of 100 psf, 225 psf, and 350 psf in R-134a.

Constant dynamic pressure results in air. Figures 40-49 illustrate the stagnation temperatures measured in air at a constant dynamic pressure of 125 psf on vane D, vane C, centerline tube, and at the primary tunnel measurement location on vane C. The measurements at vane D are plotted against the measurement location on the turning vane (see Fig. 6). The remaining single-point temperature measurements are plotted as constants across the abscissa for easy comparison to the vane D values. Each figure presents data at a discrete Mach number: 0.3, 0.5, 0.6, 0.7, 0.8, 0.85, 0.9, 0.95, 1.05, and 1.15. For each vane D measurement station, both the thermocouple and RTD measurement are presented. The discrepancies between the thermocouple and RTD measurement at each station is within the range of accuracy listed in Table 1 for each instrument. Figure 50a illustrates the stagnation temperature trend versus Mach number in air at a constant dynamic pressure of 125 psf. Figure 50b presents the average differential temperature (T-To) versus Mach number. This average includes only RTD measurements on vane D.

Figure 51 through 57 illustrate the stagnation temperatures measured in air at a constant dynamic pressure of 200 psf. Again, data from vane D, vane C, centerline tube, and at the primary tunnel measurement location is presented at discrete Mach numbers for each figure. Those Mach numbers include: 0.39, 0.7, 0.8, 0.85, 0.9, 1.0, and 1.05. Figures 58a and 58b present stagnation temperature trends and averaged vane D RTD stagnation temperature versus Mach number for a constant dynamic pressure of 200 psf in air.

Constant dynamic pressure results in R-134a. Figures 59 through 66 present stagnation temperatures measured in R-134a at a constant dynamic pressure of 100 psf. Data from vane D, vane C, centerline tube, and at the primary tunnel measurement location is presented at discrete Mach numbers for each figure. Those Mach numbers include: 0.5, 0.7, 0.8, 0.9, 0.95, 1.05, 1.1, and 1.19. Figures 67a and 67b illustrate the stagnation temperature trend and average vane D RTD stagnation temperature versus Mach number in R-134a at a constant dynamic pressure of 100 psf.

Stagnation temperature results in R-134a at a constant dynamic pressure of 225 psf are presented in Figures 68 through 75 at the following Mach numbers: 0.5, 0.6, 0.7, 0.9, 0.95, 1.0, 1.05, and 1.1. Figures 76a and 76b illustrate the stagnation temperature trends and average vane D RTD stagnation temperature versus Mach number for constant 225 psf dynamic pressure in R-134a.

Figures 77 through 83 present stagnation temperature results measured in R-134a at a constant dynamic pressure of 350 psf at the following Mach numbers: 0.8, 0.9, 0.95, 1.0, 1.05, 1.1, and 1.2. Figures 84a and 84b illustrate the stagnation temperature trends and average vane D RTD stagnation temperature versus Mach number in R134a at a constant dynamic pressure of 350 psf.

Settling Chamber Flow Velocity

The flow velocity at vane D in the settling chamber was measured using a pitot probe mounted to the vane at approximately 7 ft above the floor. Figures 85 through 88 present vane D flow velocities versus test section Mach number in air wind-off tunnel pressures of 200 psf, 400 psf, 700 psf, 1200 psf, and atmospheric pressure. Figures 89 through 94 present vane D flow velocities versus test section Mach number in R-134a at wind-off tunnel pressures of 200 psf, 500 psf, 700 psf, 1000 psf, 1400 psf, and 1800 psf.

Analytical Study of Tunnel Parameter Error Propagation

An analytical study of the propagation of tunnel parameter measurement errors into calculated tunnel parameters that include Mach number, dynamic pressure, and velocity has been carried out using the R-134a/air mixture equations as discussed in Reference 3. Using the known

measurement accuracy listed in Table 1, deviation errors in calculated parameters were calculated at Mach numbers between 0.1 and 1.2 at constant stagnation pressures of 50 psf, 200 psf, 600 psf, 1000 psf, 1400 psf, 1800 psf, and 2200 psf. Data is presented for uncertainty errors in measured stagnation and plenum pressure (Ruska pressure gage error), stagnation temperature, and gas purity. Stagnation and plenum pressure uncertainty error was represented as a percent increase in stagnation pressure and a percent decrease in plenum pressure to represent a worst-case scenario. Figure 95 illustrates the trend in Ruska error applicable to stagnation and plenum pressures versus the measure pressure as described in Table 1.

Error Propagation in Air

Figures 96 through 98 show the Mach number, dynamic pressure, and velocity error and corresponding percent error versus test section Mach number for lines of constant stagnation pressure due to the uncertainty error in the Ruska stagnation and plenum pressure measurement in an air test medium. At each reference Mach number, deviations of stagnation and plenum pressure were made with respect to the reference values of stagnation and plenum pressure. The resulting error in each flow parameter due to these deviations are reported in the figures. As can be seen in Figs. 96-98, relatively large values of percent error (up to 45%) are found at low Mach numbers and low stagnation pressures.

Figures 99 through 101 illustrate the sensitivity of Mach number, dynamic pressure, and velocity to the uncertainty in the primary tunnel stagnation temperature measurement. In each figure the calculated parameter error is shown versus Mach number for lines of constant stagnation pressure. Mach number, dynamic pressure, and velocity are rather insensitive to errors in measured tunnel stagnation temperature.

Error Propagation in R-134a

Figures 102 through 104 show the sensitivity of calculated tunnel parameters due to the uncertainty error in the Ruska stagnation and plenum pressure measurement in a R-134a test medium. In each figure the calculated parameter error is presented versus test section Mach number for lines of constant stagnation pressure. As in the air case, the R-134a test medium results show that for lower Mach numbers and stagnation pressures the percent error in Mach number and velocity can be appreciable.

Figure 105 through 107 illustrate the sensitivity of Mach number, dynamic pressure, and velocity to the uncertainty in the primary tunnel stagnation temperature measurement. Similar to the air test medium case, the calculated tunnel parameters are shown to be rather insensitive to the uncertainty error in the primary tunnel stagnation temperature measurement.

Figure 108 through 110 show the calculated tunnel parameter error versus Mach number for lines of constant stagnation pressure in R-134a due to a 2% uncertainty error in the R-134a gas purity measurement system. Dynamic pressure and tunnel velocity are shown to be rather insensitive to the 2% error in the R-134a gas purity measurement listed in Table 1. Mach number error is shown to approach 0.0007 at higher Mach numbers. Due to the current manual method in which R-134a purity is updated at the TDT, larger errors can easily be anticipated and the Mach number error could then approach 0.001-0.003.

Because of the manual method utilized at the TDT, a 5% error in R-134a gas purity measurement was also considered. Figures 111 through 113 illustrate the calculated tunnel parameter error versus Mach number for lines of constant stagnation pressure in R-134a due to a 5% gas purity measurement error. At high Mach numbers the error is shown to approach Mach 0.0016.

Conclusions

A survey of primary flow measurements has been conducted at the TDT as part of a facility calibration effort. Stagnation pressure, plenum pressure, and stagnation temperature surveys have been conducted at various locations in the tunnel circuit and the results have been documented for future reference. This flow survey has identified small discrepancies between the flow survey measurements and the primary tunnel parameter measurements; stagnation pressure: 1-2 psf, plenum pressure: 1-3 psf, and stagnation temperature: up to 4 degrees Fahrenheit. In addition to the flow survey, results have been presented from an analytical study of the propagation of primary parameter measurement error into the calculated tunnel parameters such as Mach number, dynamic pressure, and velocity in the test section. This analytical study has shown that appreciable errors can be present in Mach number and velocity at conditions of low stagnation pressure and Mach number due to uncertainties in tunnel primary pressure measurements and at high Mach numbers in R-134a due to gas purity measurement uncertainties.

Recommendations

It is recommended that a new method of measuring tunnel stagnation temperature be implemented on turning vane D using a high accuracy RTD in place of the type J thermocouple on vane C. This recommendation comes in response to the fact that the observed temperature data presented in this study shows that the primary tunnel stagnation temperature measurement is consistently lower than the average vane D stagnation temperature. Also, the aging system used to currently measure stagnation temperature in the TDT failed during calibration testing and required repair and re-calibration. Furthermore, the vane C thermocouple currently used to measure tunnel temperature is directly behind the cooling coils used to control tunnel temperature. The proximity of the thermocouple to the cooling coils suggests that local temperature fluctuations in the flow near the tubes could bias the measurement. Locating the primary tunnel temperature measurement to turning vane D would allow more thorough mixing of the flow prior to the measurement location.

Secondly, it is recommended that a reliable, automated system be investigated for measuring the R-134a gas purity within the TDT during heavy gas testing. Error propagation studies have shown that as little as 3-5% error in R-134a gas purity can result in as much as a 0.0016 error in Mach number which can be significant for certain performance tests.

Finally, rather large errors were identified by the analytical study due to Ruska primary stagnation and plenum pressure measurement uncertainty errors at low Mach numbers and low stagnation pressures. It is recommended that these errors be carefully considered when testing at these conditions.

References

1. Cole, S.R.; and Rivera, J.A., Jr.: The New Heavy Gas Testing Capability in the NASA Langley Transonic Dynamics Tunnel. Presented at the Royal Aeronautical Society Wind Tunnels and Wind Tunnel Test Techniques Forum, Churchill College, Cambridge, UK, April 14-16, 1997.

2. Corliss, J.M.; and Cole, S.R.: Heavy Gas Conversion of the NASA Langley Transonic Dynamics Tunnel. 20th AIAA Advanced Measurement and Ground Testing Technology Conference, Albuquerque, NM, June 15-18, 1998 (AIAA Paper 98-2710).
3. Kvaternik, R.G.: Computer Programs for Calculating the Isentropic Flow Properties for Mixtures of R-134a and Air. NASA TM-2000-210622, November, 2000.

Tables

Table 1. Instrument accuracy.

Instrument	Range	Accuracy, percent full-scale	Accuracy
Ruska pressure gages	0-2200 psf	+/- 0.016% RDG +/- 0.008% FS	At p_o=200 psf: 0.208 psf At p_o =500 psf: 0.256 psf At p_o =1000 psf: 0.336 psf At p_o =1500 psf: 0.416 psf At p_o =2200 psf: 0.528 psf
Type J thermocouple (tunnel T_o)	32^o-1380^o F	N/A	+/- 4^o F
R-134a purity gage	0-100%	+/- 2%	+/- 2%
ESP	0-1 psid	+/- 0.1%	+/- 0.144 psf
Type T thermocouple (Vane D)	32^o-660^o F	N/A	+/- 1.8^o F
RTD	0^o F to 200^o F	+/- 0.25%	+/- 0.5^o F

Table 2. Re-entry flap schedule.

Mach Range	Main Flap	Nose Flap
M=0.00 – 0.85	0.00 deg	0.00 deg
M=0.85 – 0.95	0.00 deg	0.75 deg
M=0.95 – 1.05	1.50 deg	0.75 deg
M=1.05 – 1.2	5.25 deg	0.75 deg

Figures

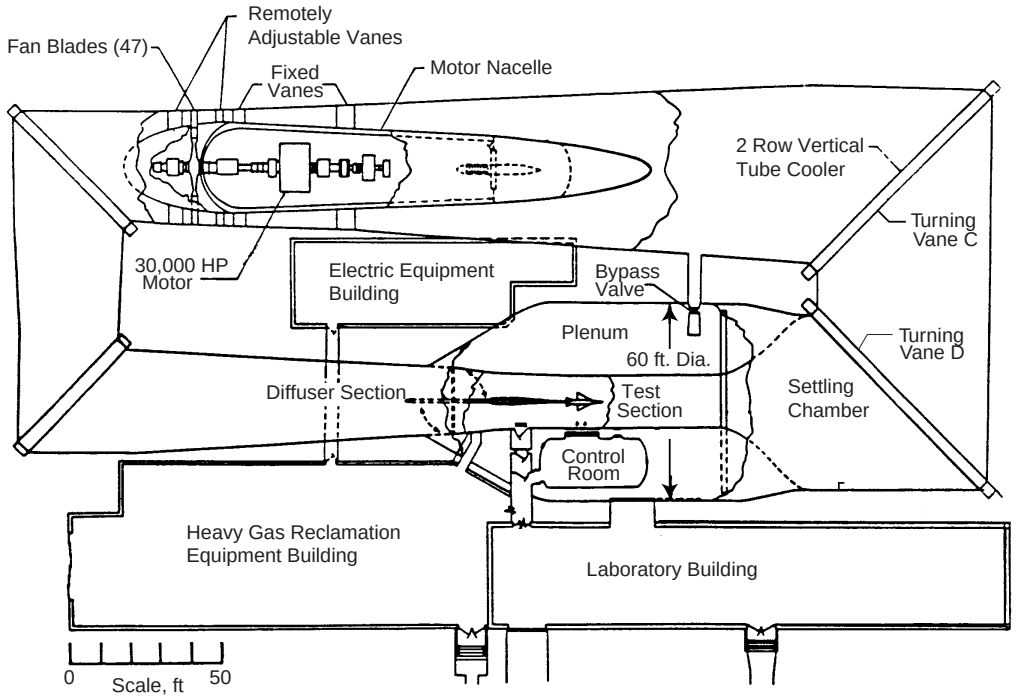

Figure 1. Plan view of the TDT.

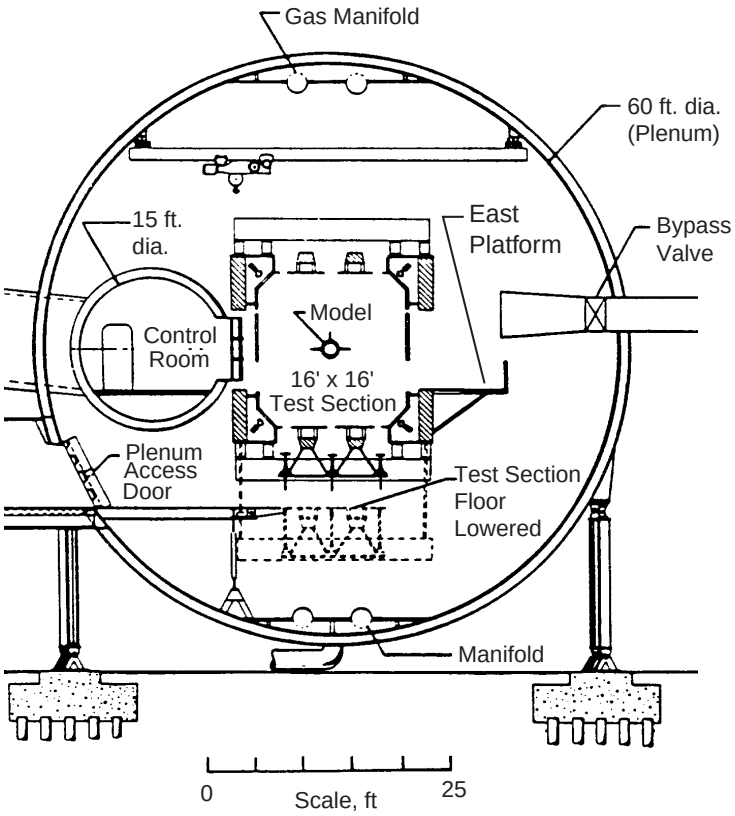

Figure 2. Cross-section of TDT test section.

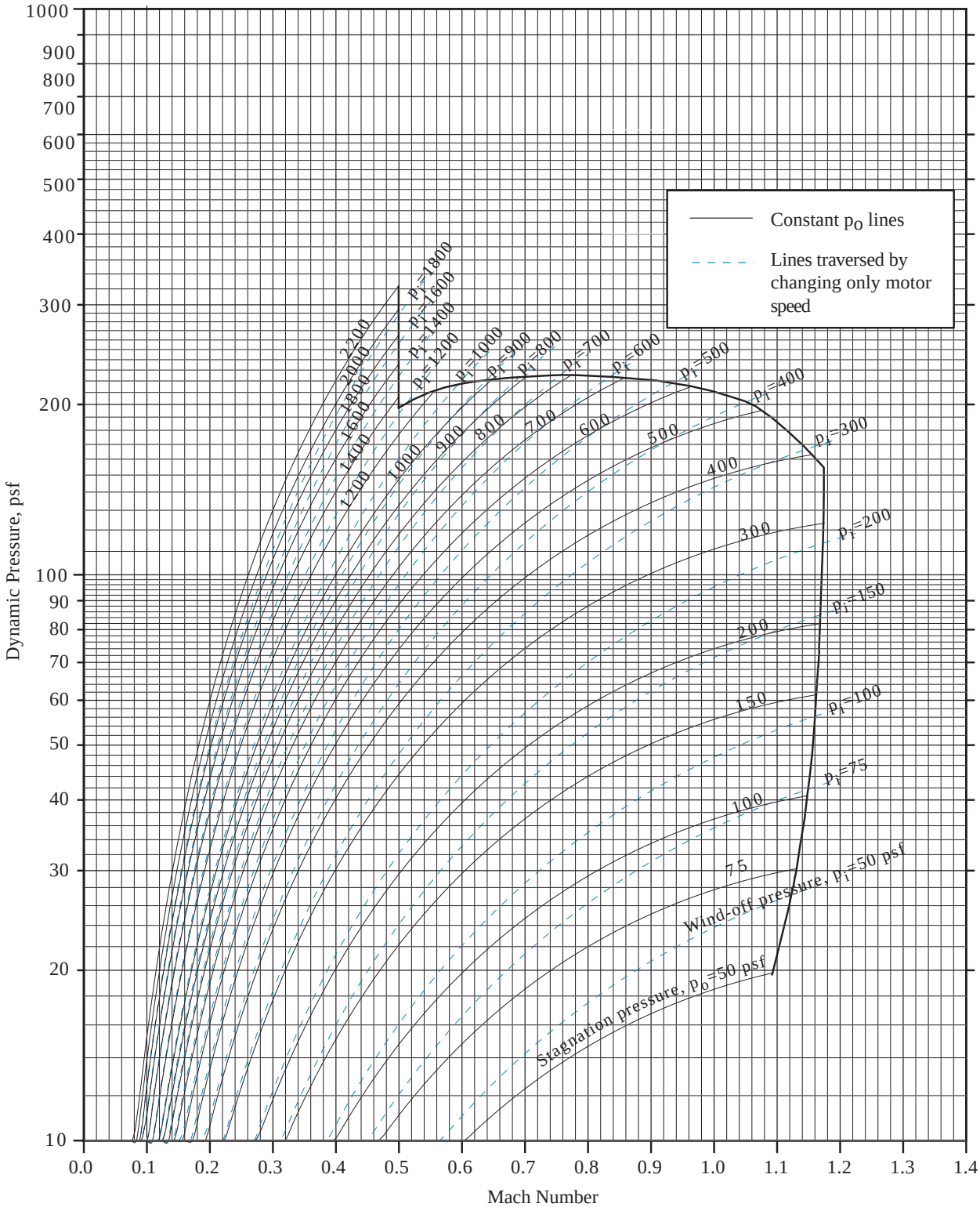

Figure 3. TDT operating envelope for air.

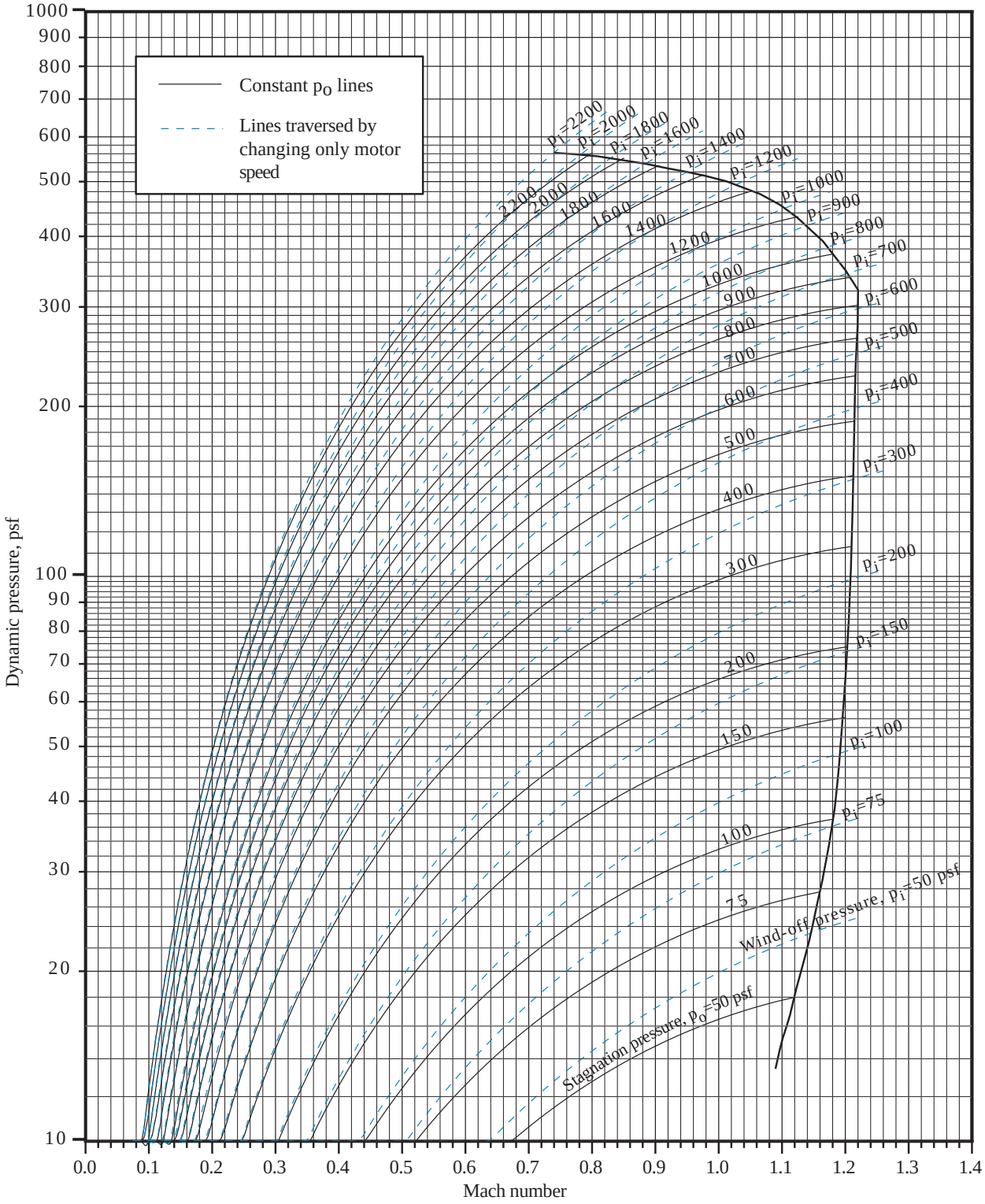

Figure 4. TDT operating envelope for R-134a heavy gas test medium.

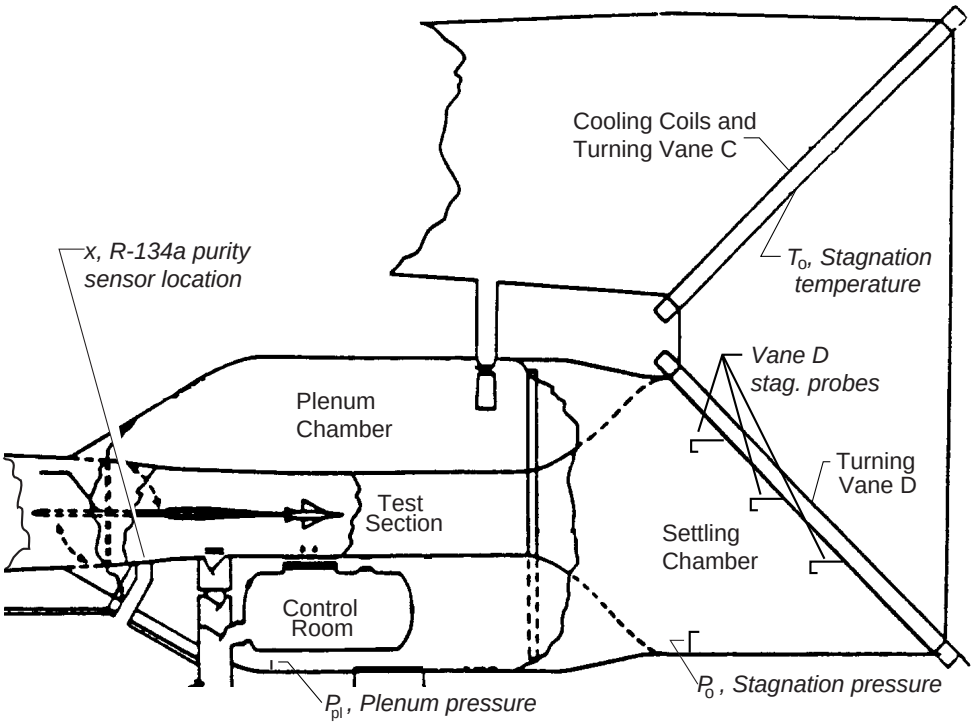

Figure 5. Plenum chamber and settling chamber of TDT.

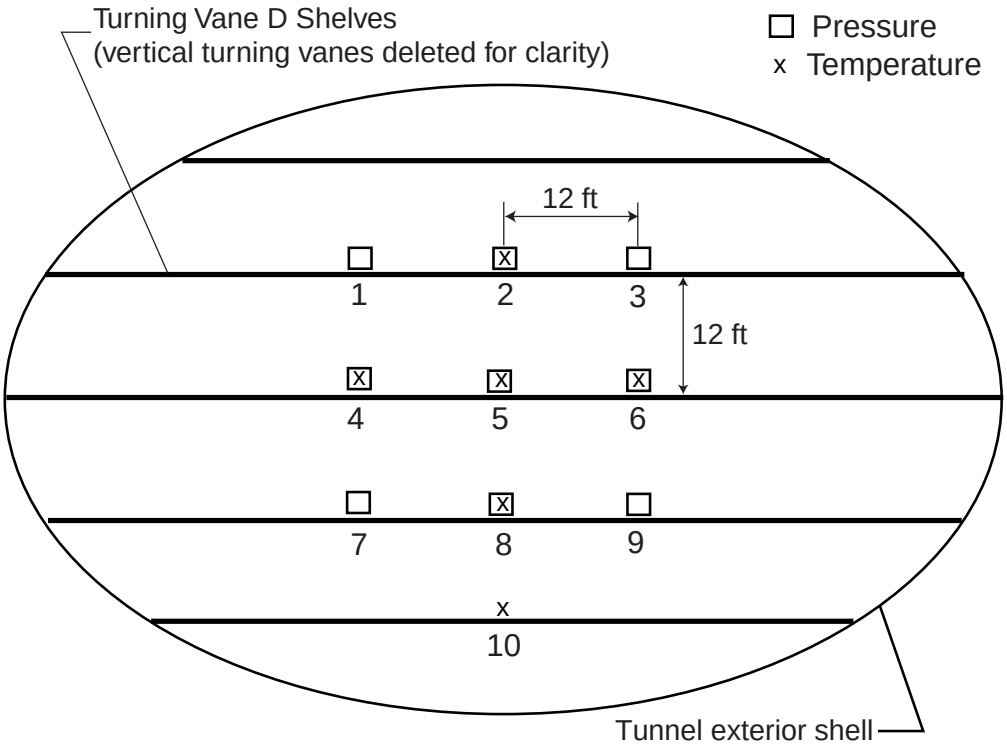

Figure 6. Turning vane D stagnation pressure and temperature instrumentation grid.

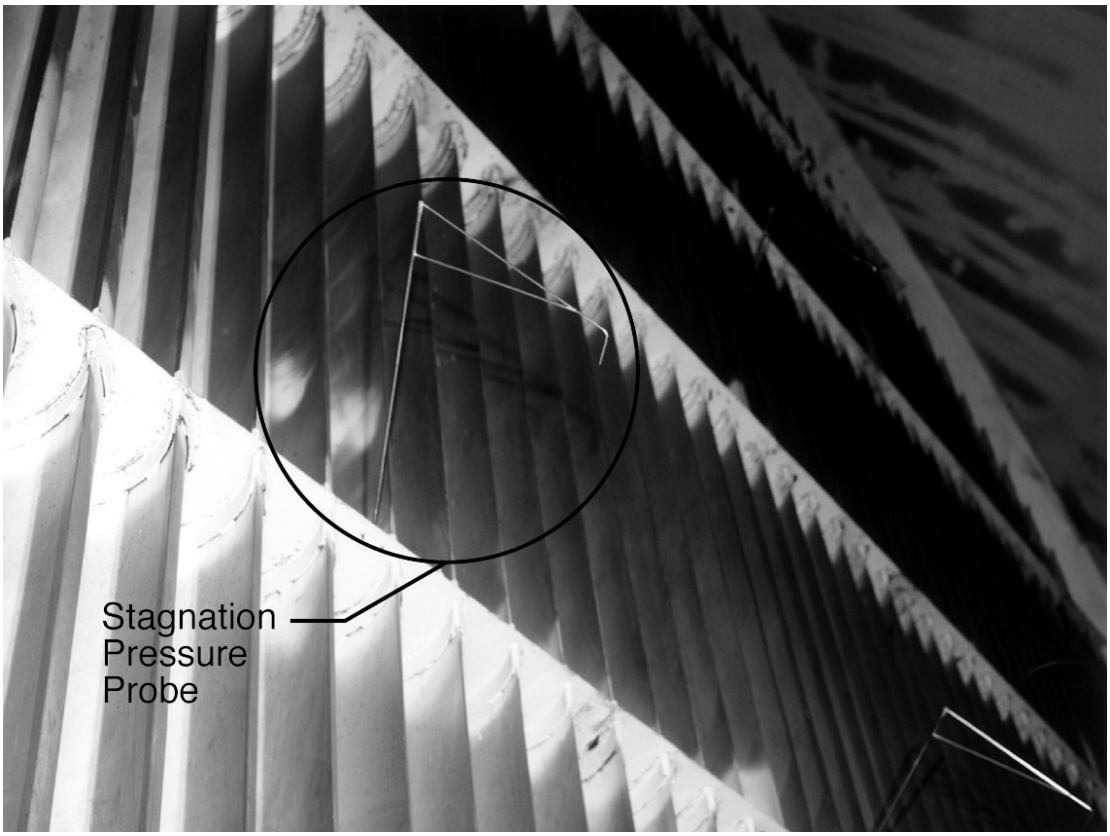

Figure 7. Stagnation pressure probe mounted to turning vane D.

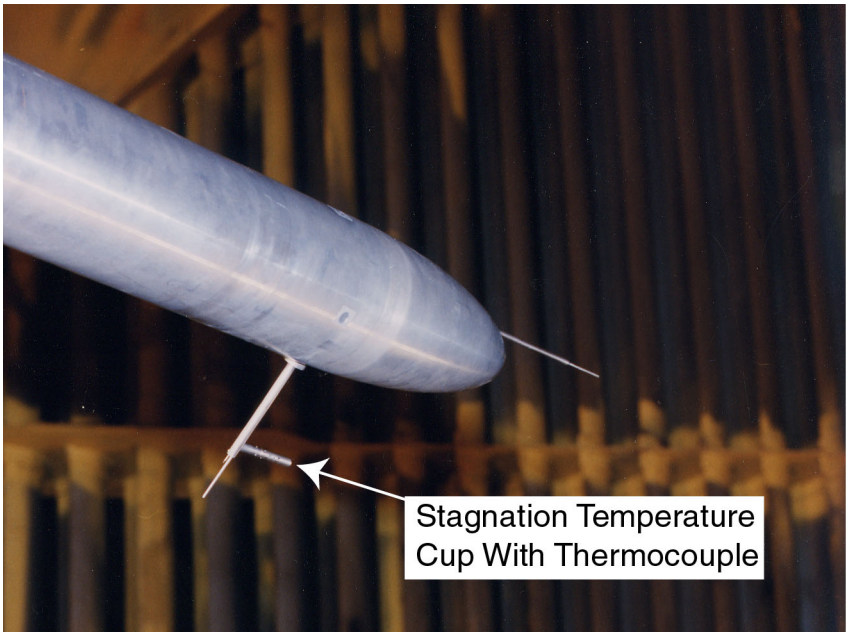

Figure 8. Stagnation temperature measurement on upstream nose of centerline tube within contraction section.

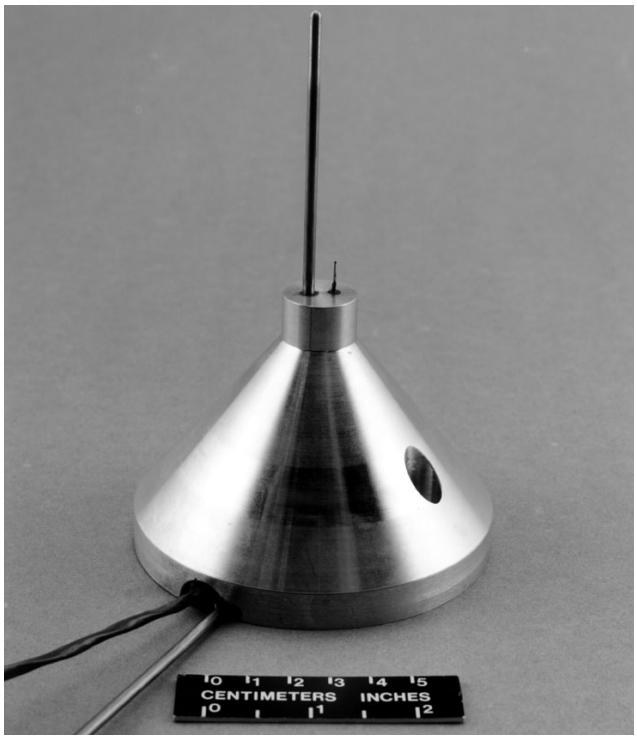

Figure 9. Thermocouple and RTD mount unit.

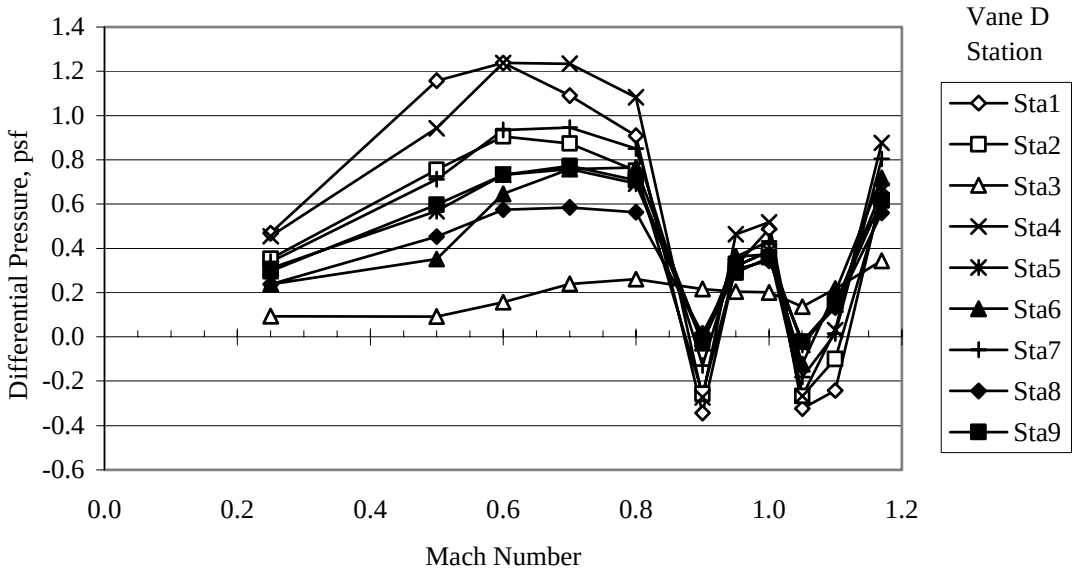

Figure 10. Vane D differential stagnation pressure versus test section Mach number in air for a wind-off tunnel pressure of 200 psf.

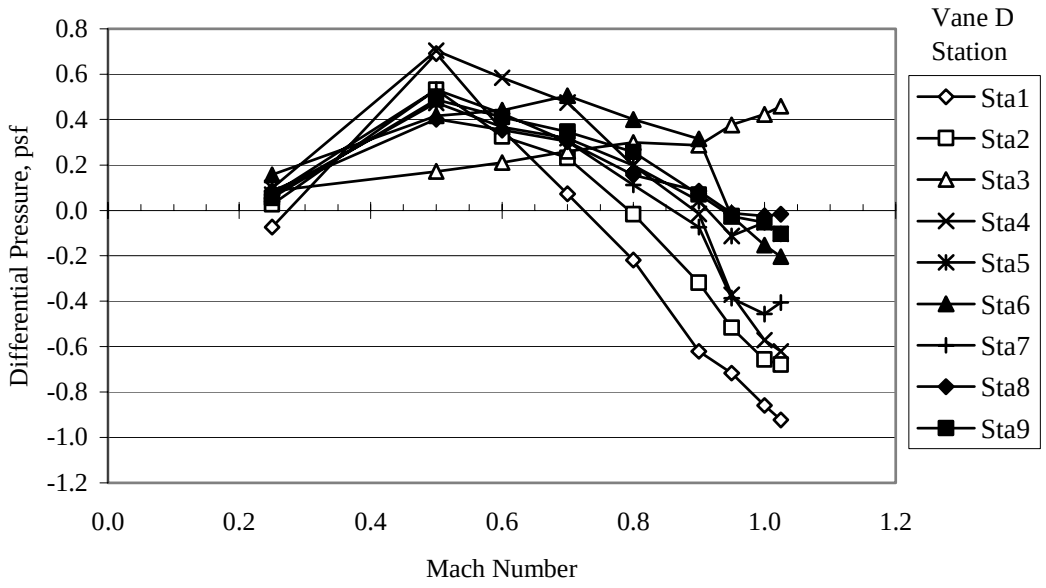

Figure 11. Vane D differential stagnation pressure versus test section Mach number in air for a wind-off tunnel pressure of 400 psf.

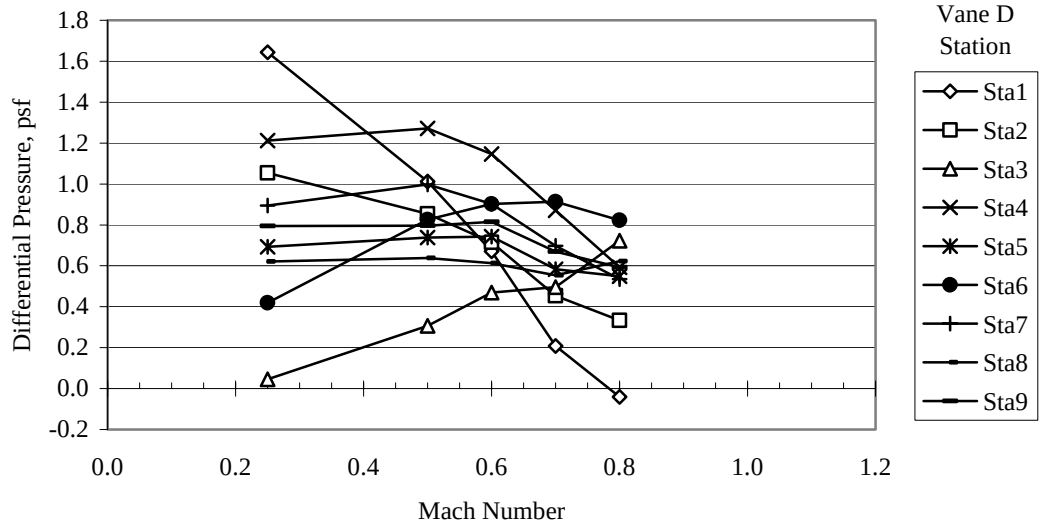

Figure 12. Vane D differential stagnation pressure versus test section Mach number in air for a wind-off tunnel pressure of 700 psf.

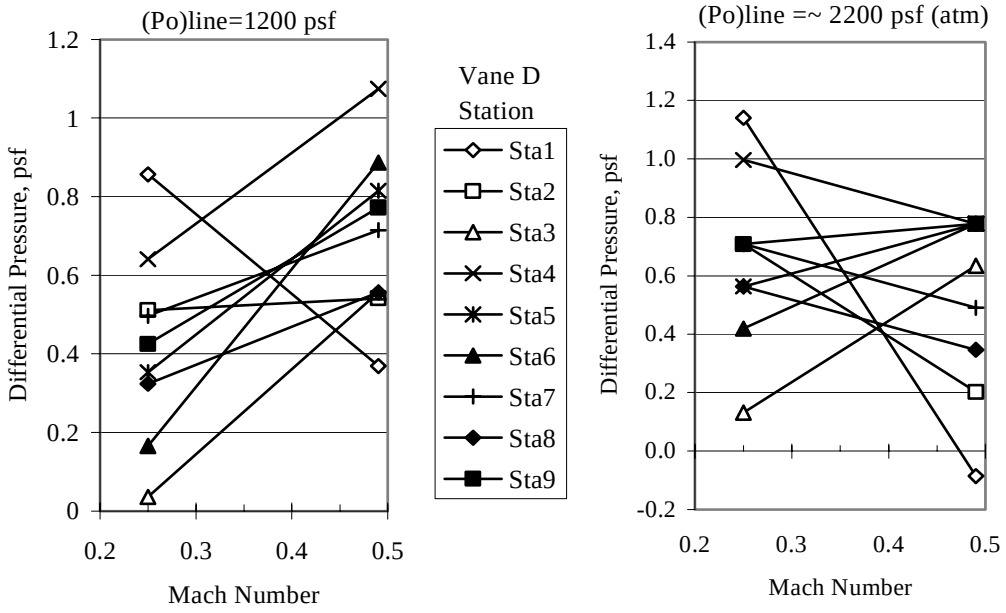

Figure 13. Vane D differential stagnation pressure versus test section Mach number in air for a wind-off tunnel pressure of 1200 psf and atmospheric pressure.

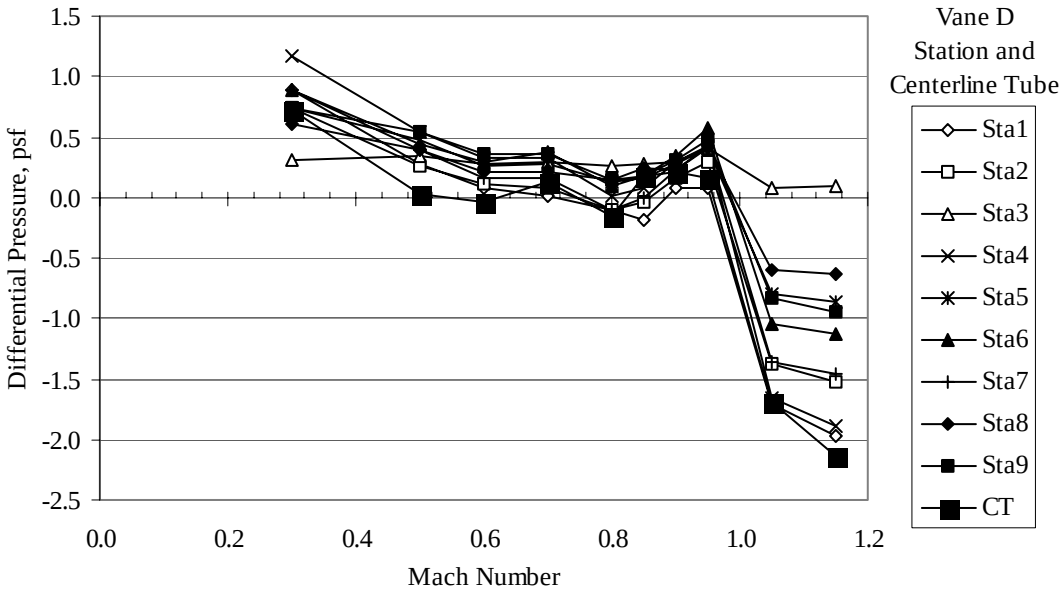

Figure 14. Vane D and centerline tube differential stagnation pressure versus test section Mach number in air for constant dynamic pressure of 125 psf.

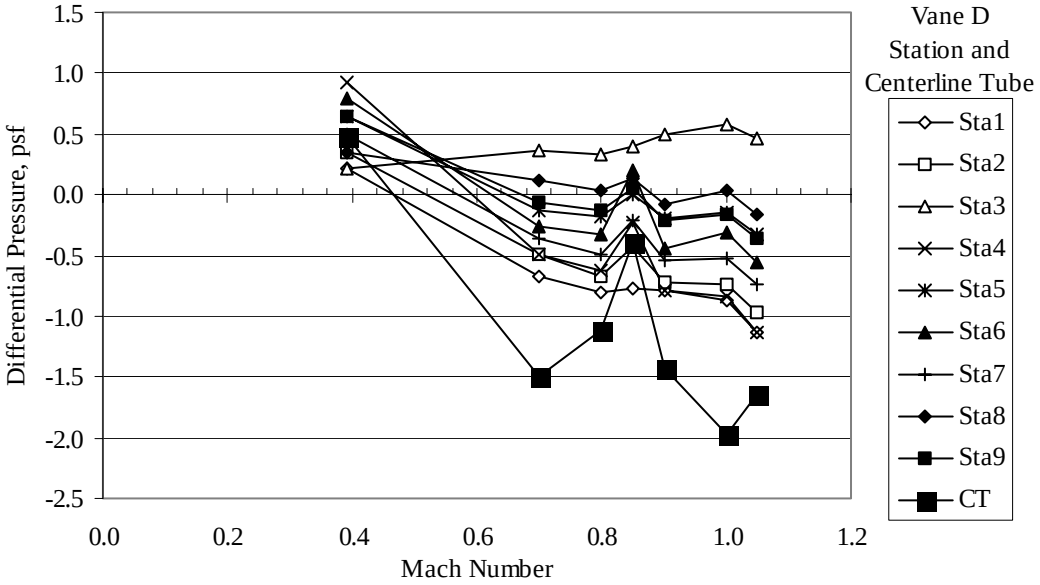

Figure 15. Vane D and centerline tube differential stagnation pressures versus test section Mach number in air for constant dynamic pressure of 200 psf.

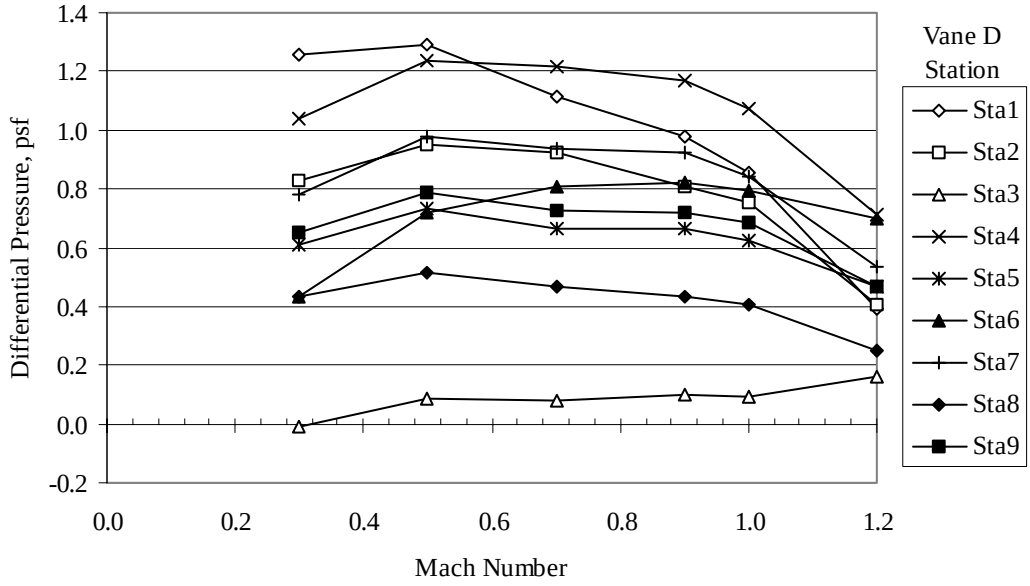

Figure 16. Vane D differential stagnation pressures versus test section Mach number in R-134a for wind-off tunnel pressure of 200 psf.

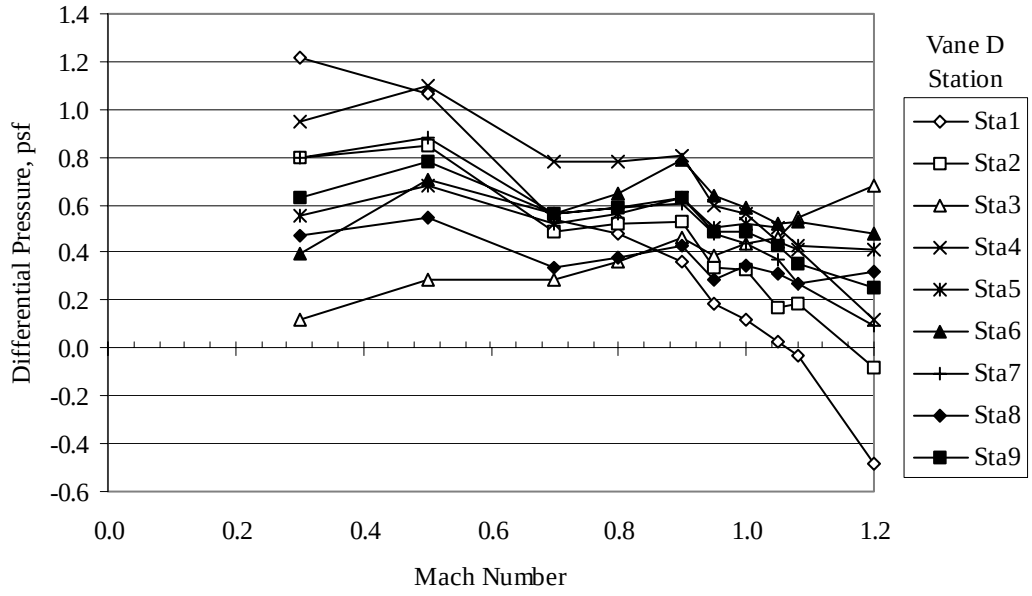

Figure 17. Vane D differential stagnation pressures versus test section Mach number in R-134a for wind-off tunnel pressure of 500 psf.

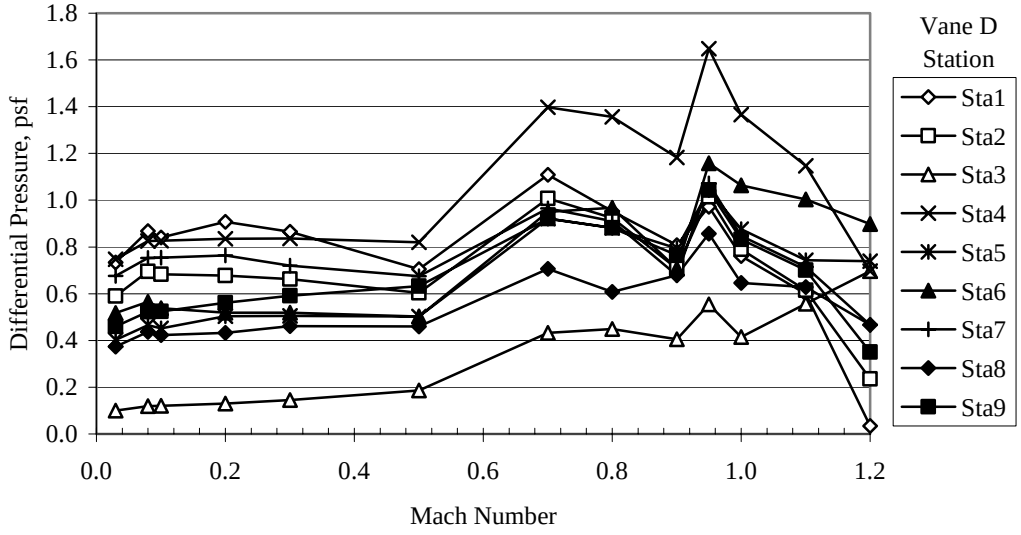

Figure 18. Vane D differential stagnation pressures versus test section Mach number in R-134a for wind-off tunnel pressure of 700 psf.

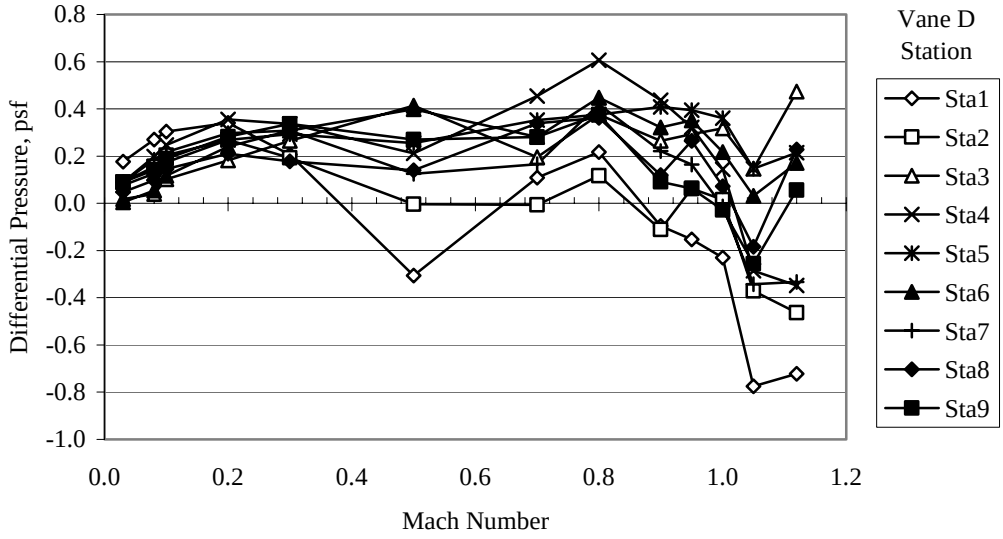

Figure 19. Vane D differential stagnation pressures versus test section Mach number in R-134a for wind-off tunnel pressure of 1000 psf.

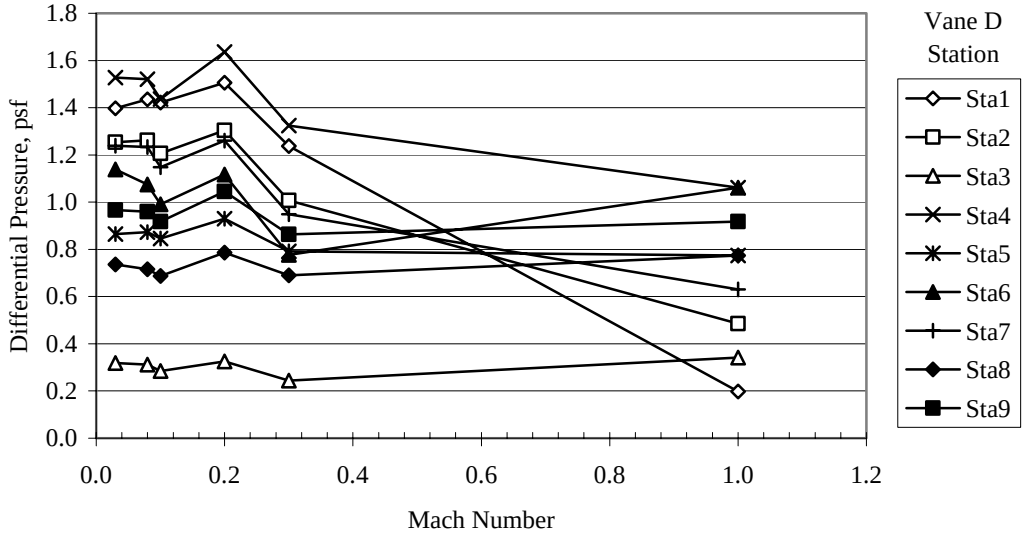

Figure 20. Vane D differential stagnation pressures versus test section Mach number in R-134a for wind-off tunnel pressure of 1400 psf.

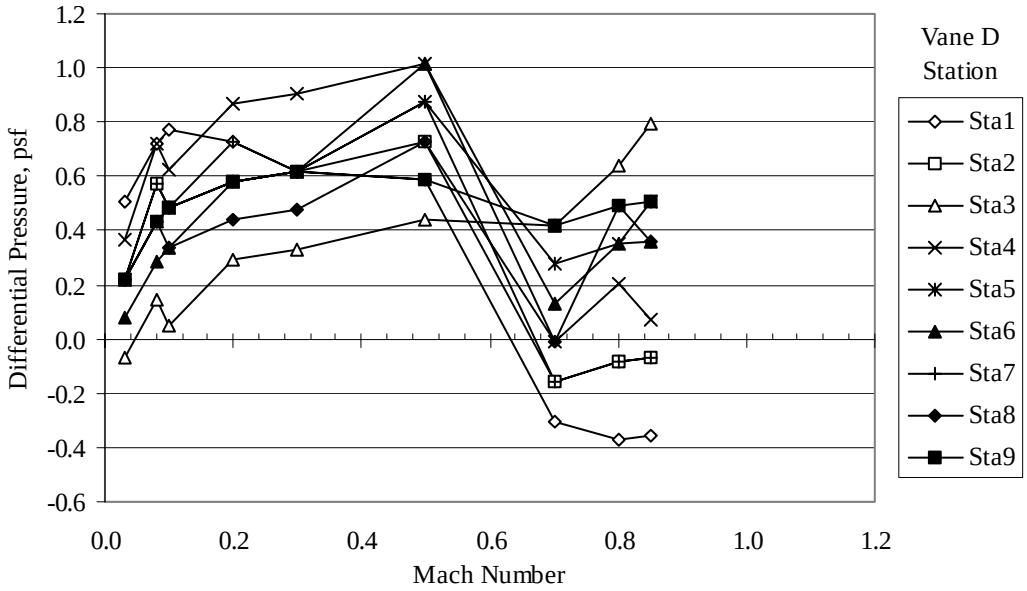

Figure 21. Vane D differential stagnation pressures versus test section Mach number in R-134a for wind-off tunnel pressure of 1800 psf.

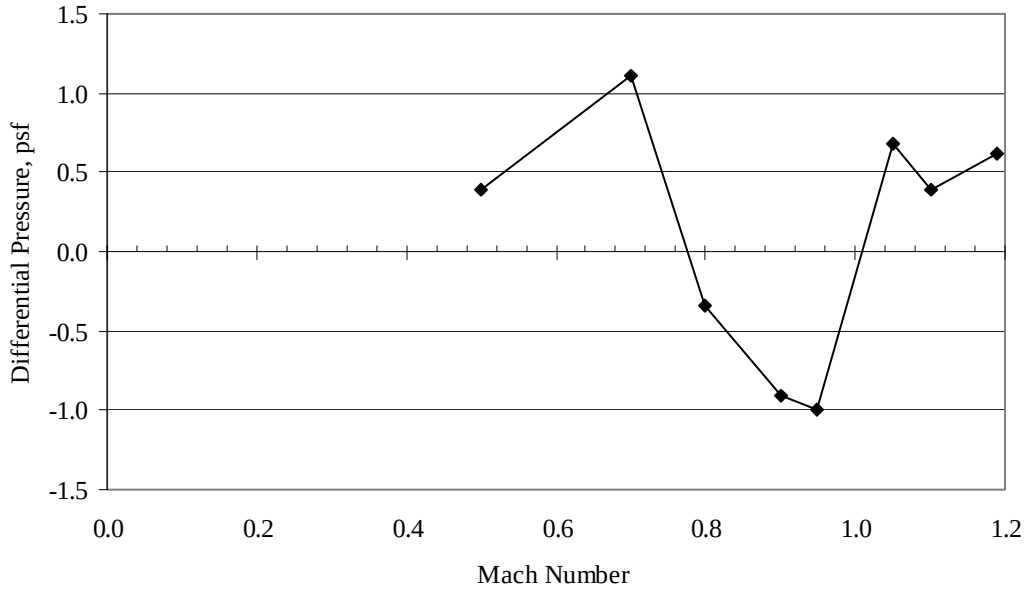

Figure 22. Centerline tube differential stagnation pressure versus test section Mach number in R-134a for constant tunnel dynamic pressure of 100 psf.

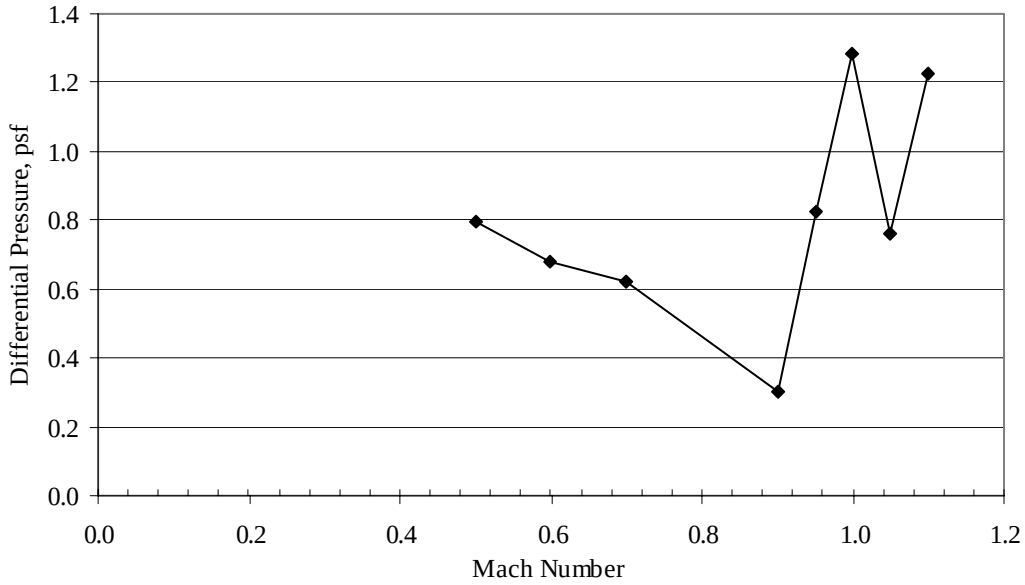

Figure 23. Centerline tube differential stagnation pressure versus test section Mach number in R-134a for constant tunnel dynamic pressure of 225 psf.

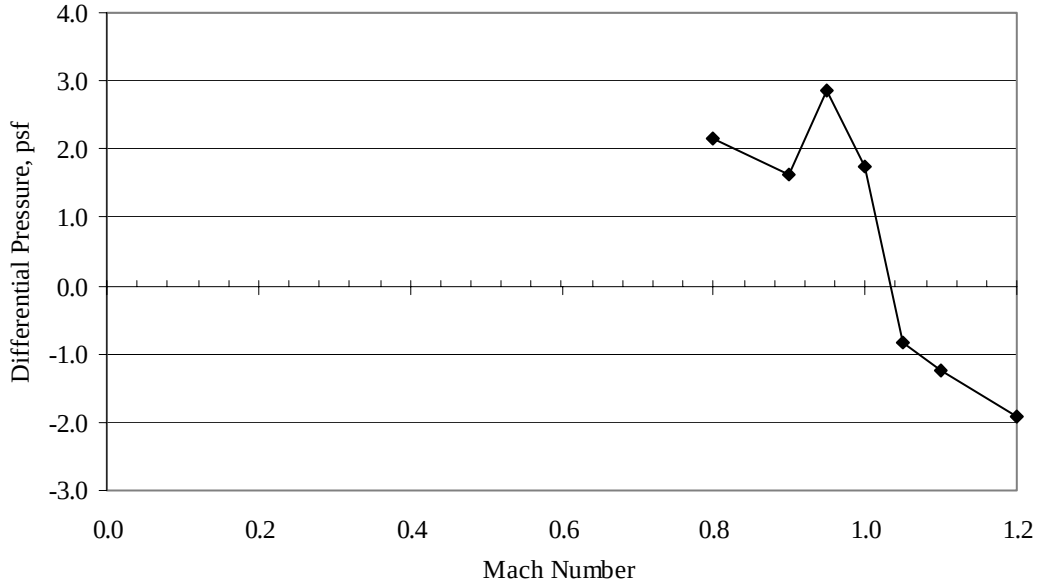

Figure 24. Centerline tube differential stagnation pressure versus test section Mach number in R-134a for constant tunnel dynamic pressure of 350 psf.

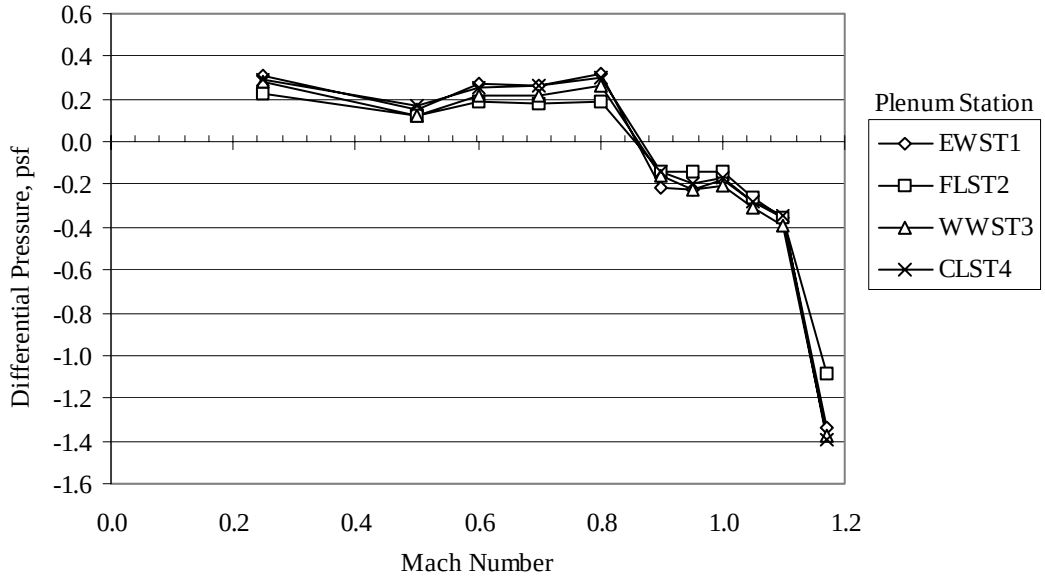

Figure 25. Plenum chamber differential static pressures versus Mach number in air for wind-off tunnel pressure of 200 psf.

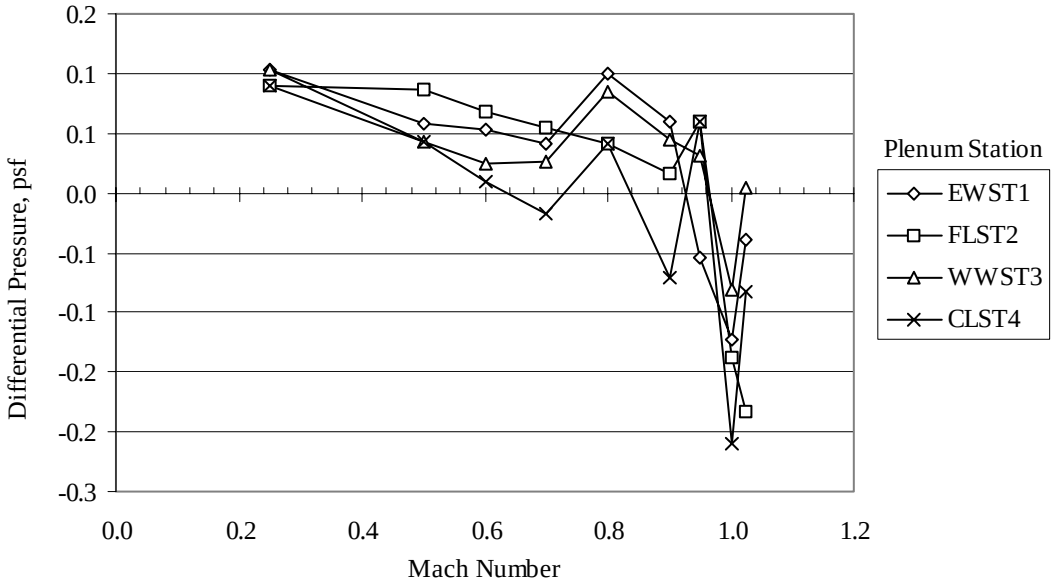

Figure 26. Plenum chamber differential static pressures versus Mach number in air for wind-off tunnel pressure of 400 psf.

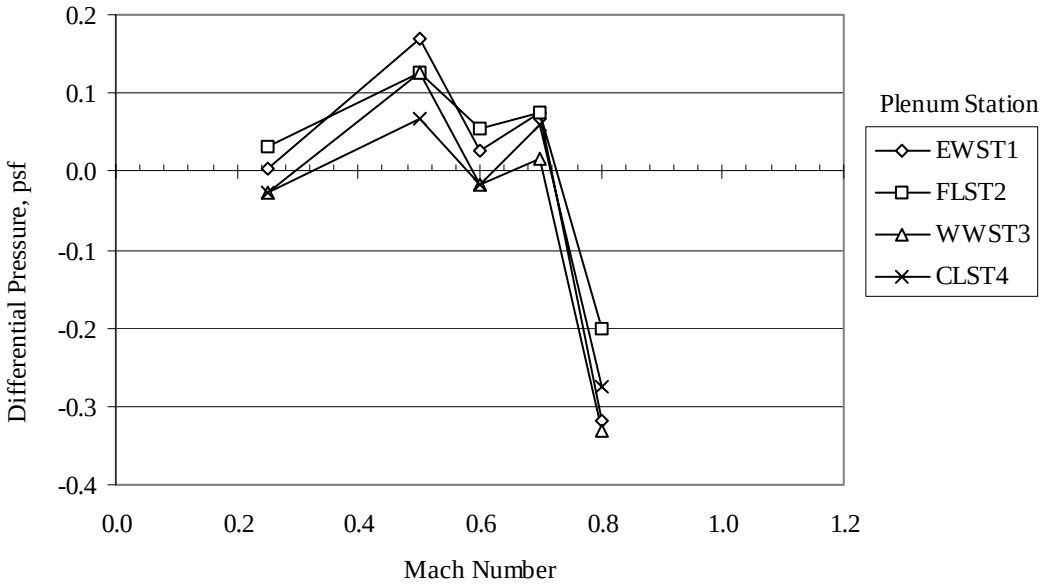

Figure 27. Plenum chamber differential static pressures versus Mach number in air for wind-off tunnel pressure of 700 psf.

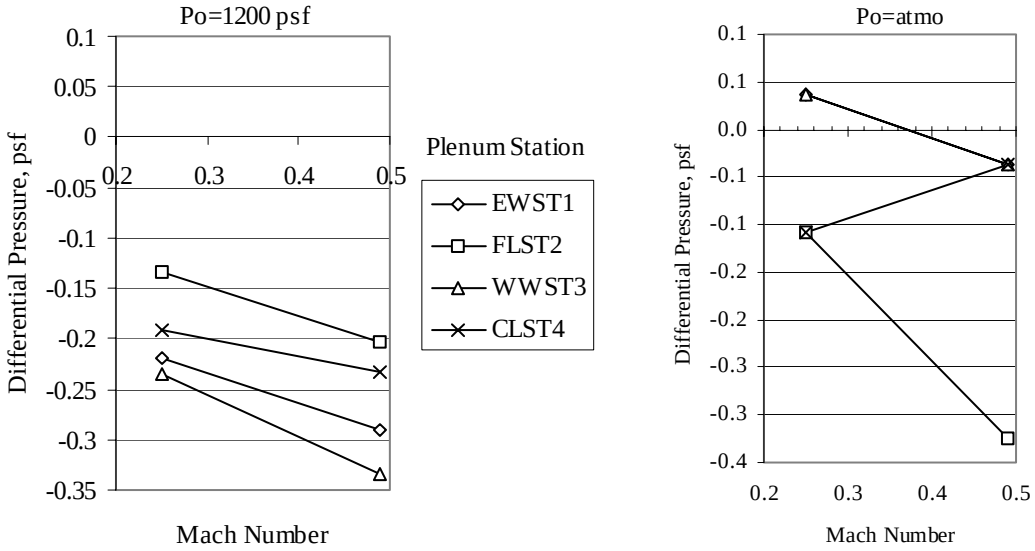

Figure 28. Plenum chamber differential static pressures versus Mach number in air for wind-off tunnel pressures of 1200 psf and atmospheric pressure.

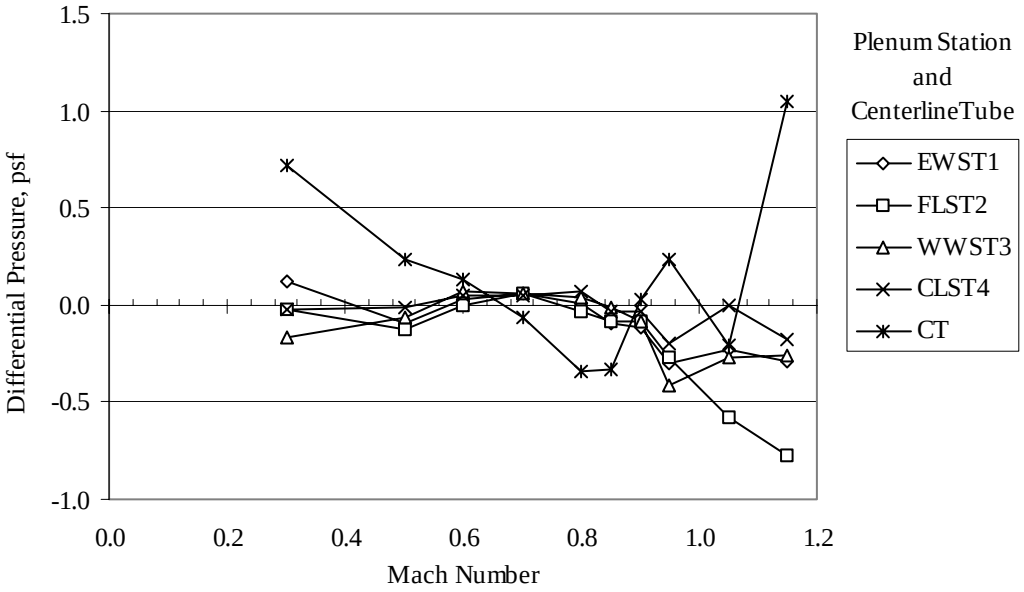

Figure 29. Plenum chamber and centerline tube differential static pressures versus Mach number in air for constant tunnel dynamic pressures of 125 psf.

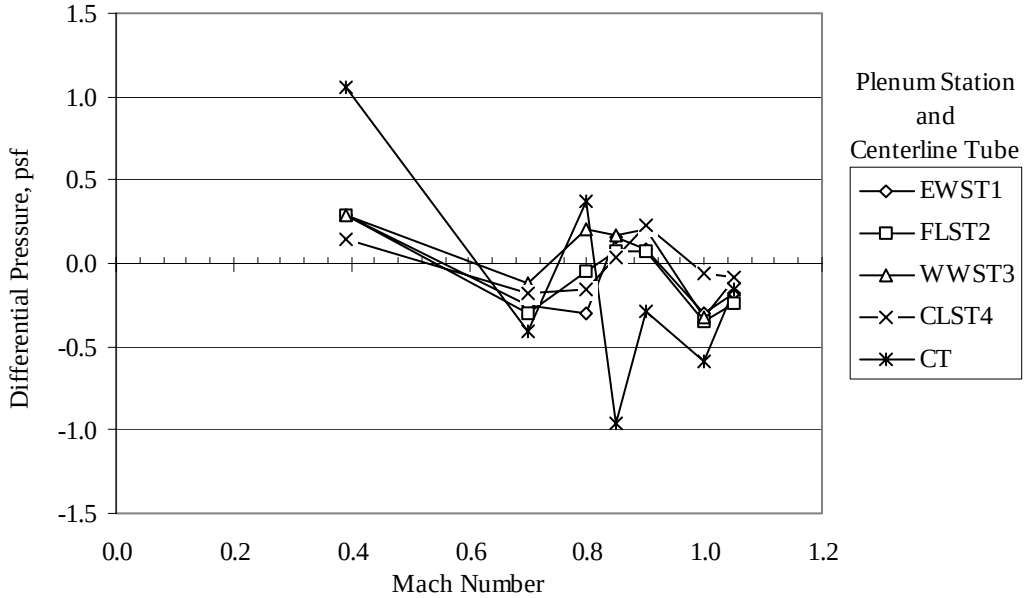

Figure 30. Plenum chamber and centerline tube differential static pressures versus Mach number in air for constant tunnel dynamic pressures of 200 psf.

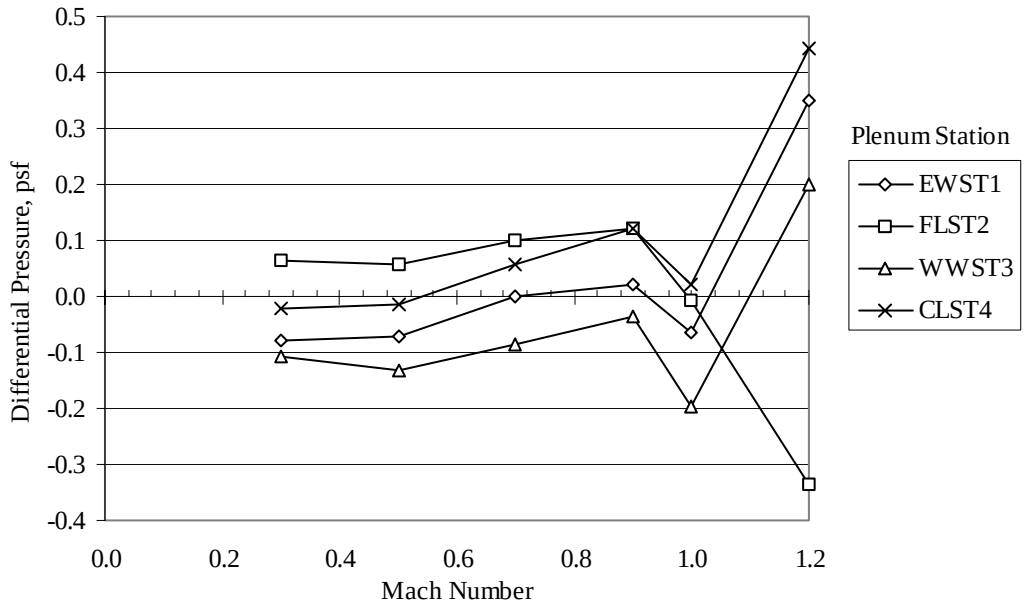

Figure 31. Plenum chamber differential static pressures versus Mach number in R-134a for wind-off tunnel pressure of 200 psf.

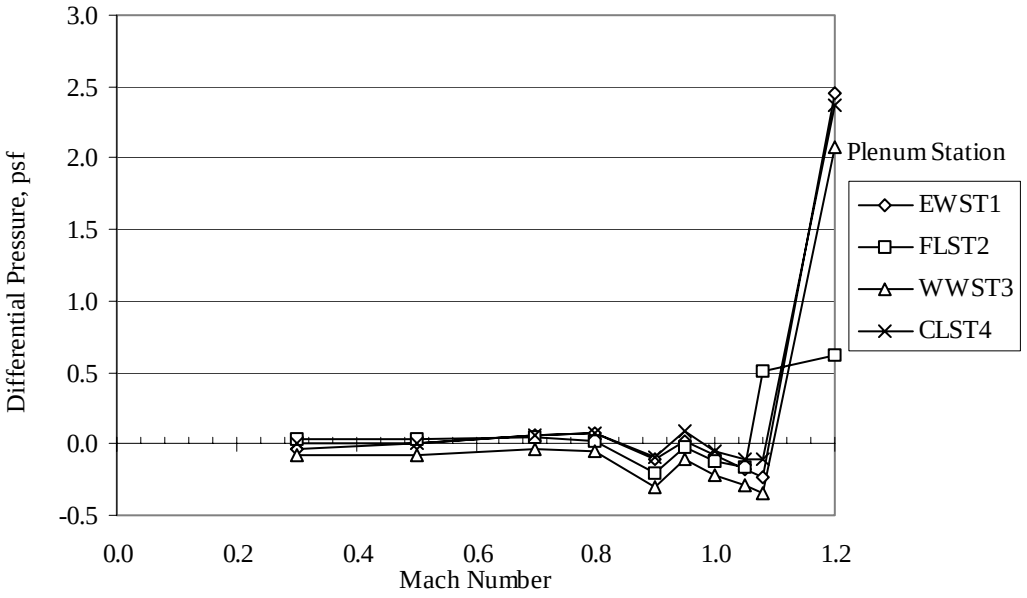

Figure 32. Plenum chamber differential static pressures versus Mach number in R-134a for wind-off tunnel pressure of 500 psf.

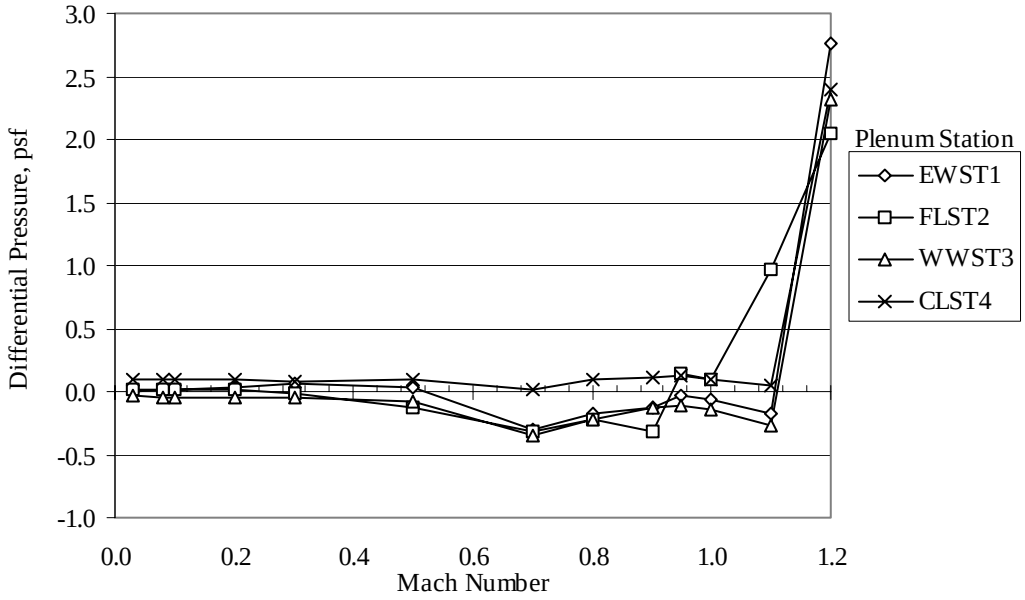

Figure 33. Plenum chamber differential static pressures versus Mach number in R-134a for wind-off tunnel pressure of 700 psf.

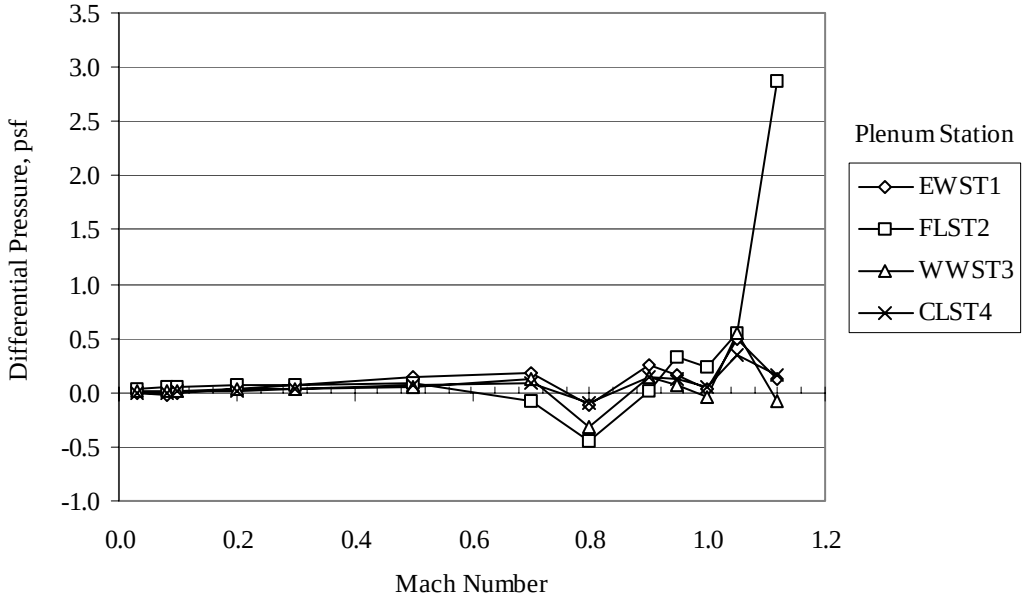

Figure 34. Plenum chamber differential static pressures versus Mach number in R-134a for wind-off tunnel pressure of 1000 psf.

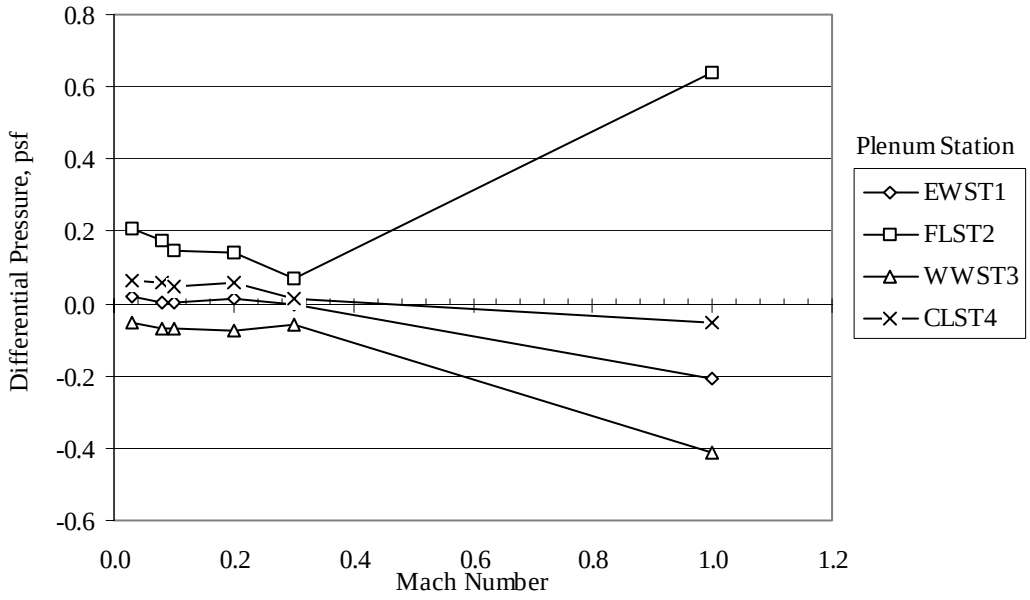

Figure 35. Plenum chamber differential static pressures versus Mach number in R-134a for wind-off tunnel pressure of 1400 psf.

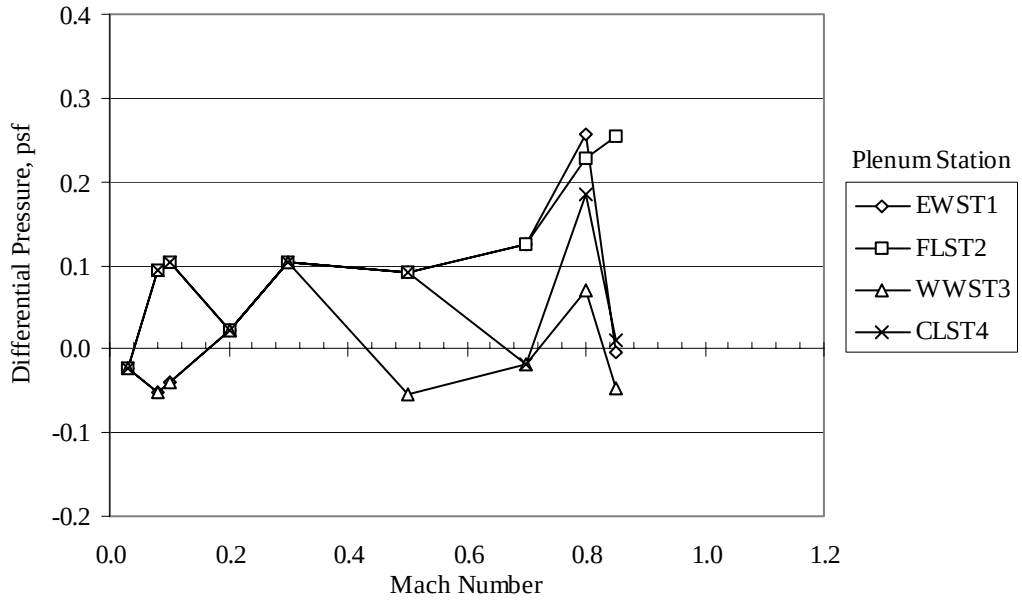

Figure 36. Plenum chamber differential static pressures versus Mach number in R-134a for wind-off tunnel pressure of 1800 psf.

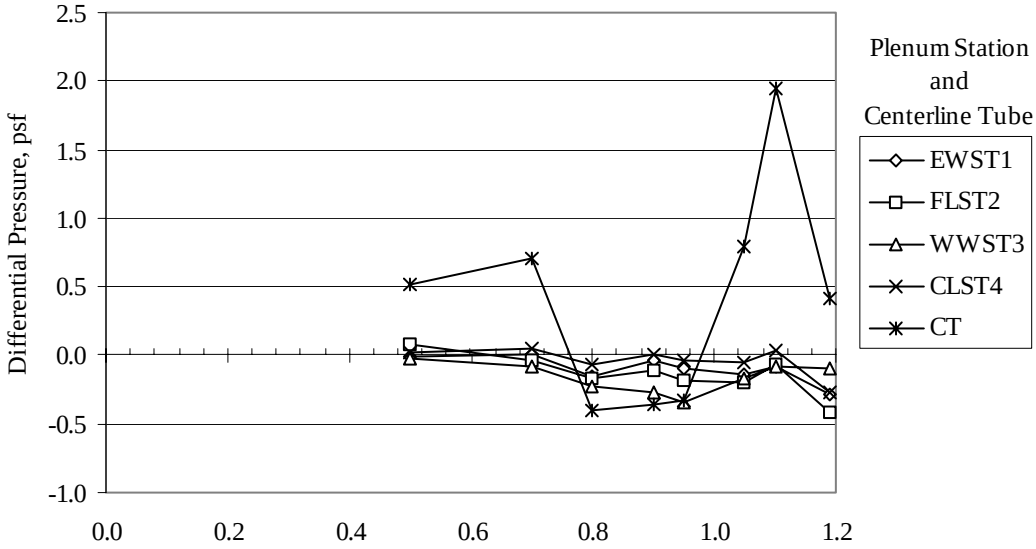

Figure 37. Plenum chamber and centerline tube differential static pressures versus Mach number in R-134a for constant tunnel dynamic pressures of 100 psf.

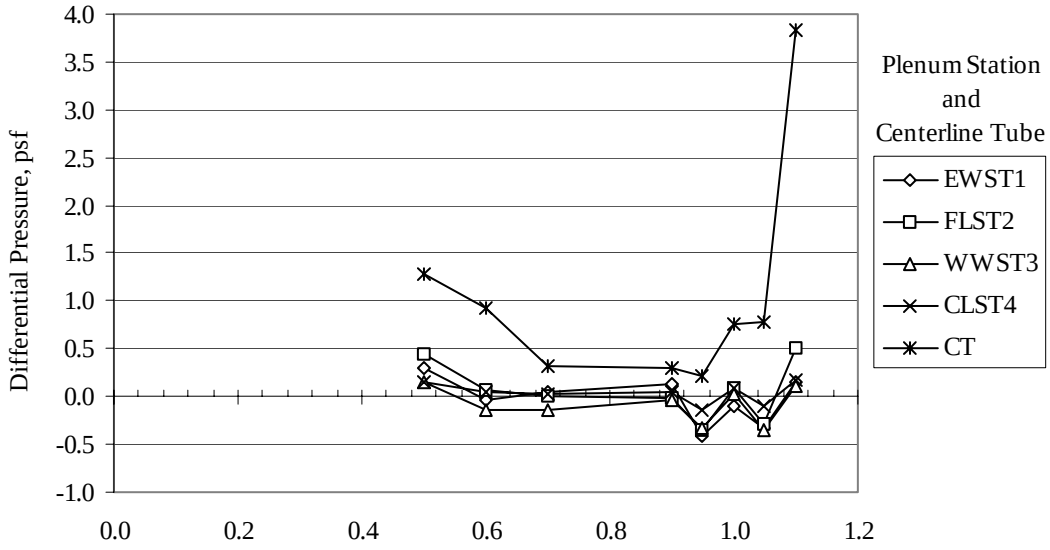

Figure 38. Plenum chamber and centerline tube differential static pressures versus Mach number in R-134a for constant tunnel dynamic pressures of 225 psf.

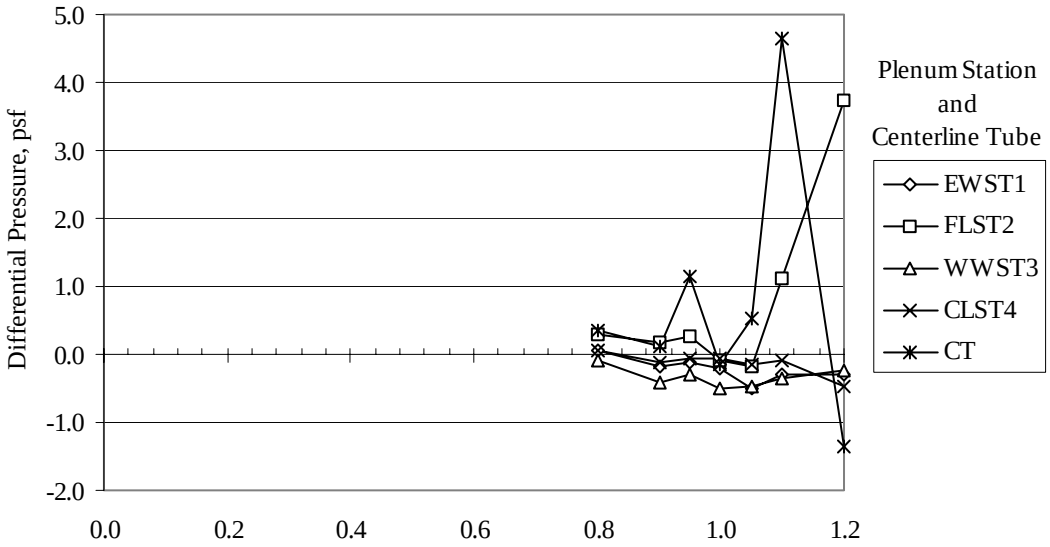

Figure 39. Plenum chamber and centerline tube differential static pressures versus Mach number in R-134a for constant tunnel dynamic pressures of 350 psf.

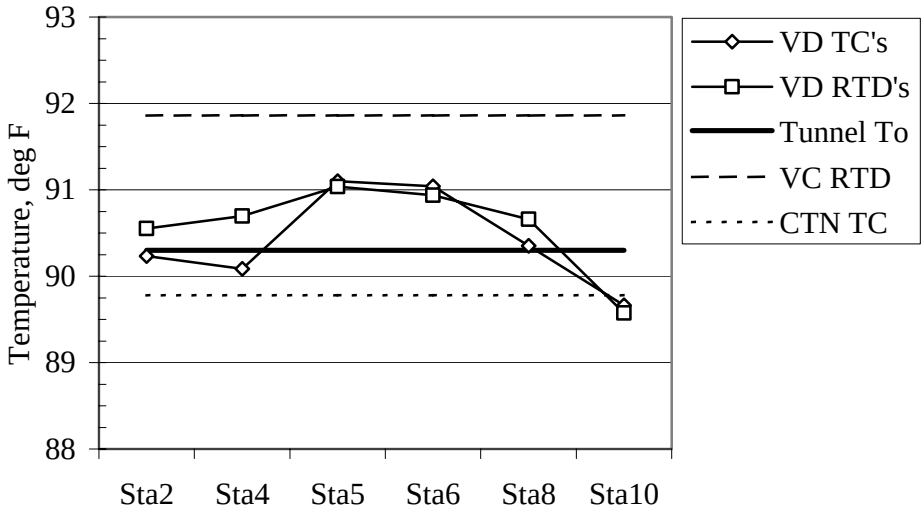

Figure 40. Stagnation temperature measurements at Q=125 psf and Mach 0.30 in air.

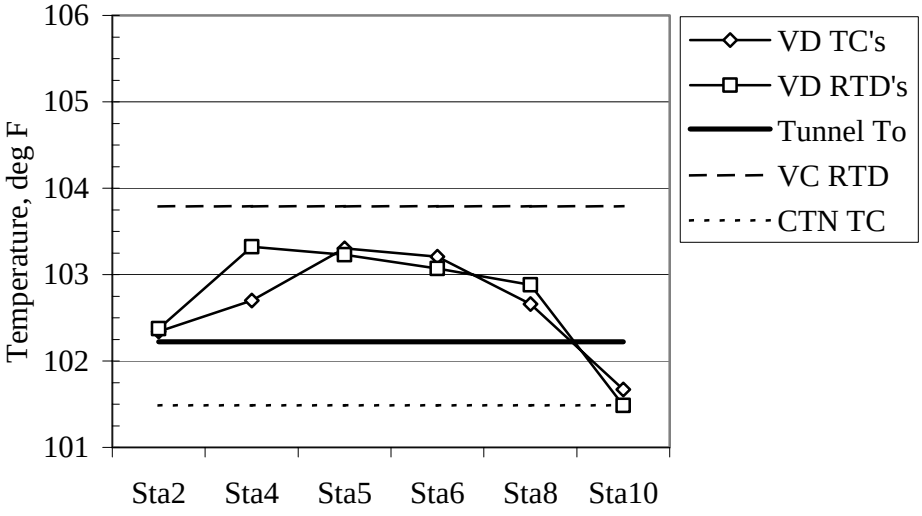

Figure 41. Stagnation temperature measurements at Q=125 psf and Mach 0.50 in air.

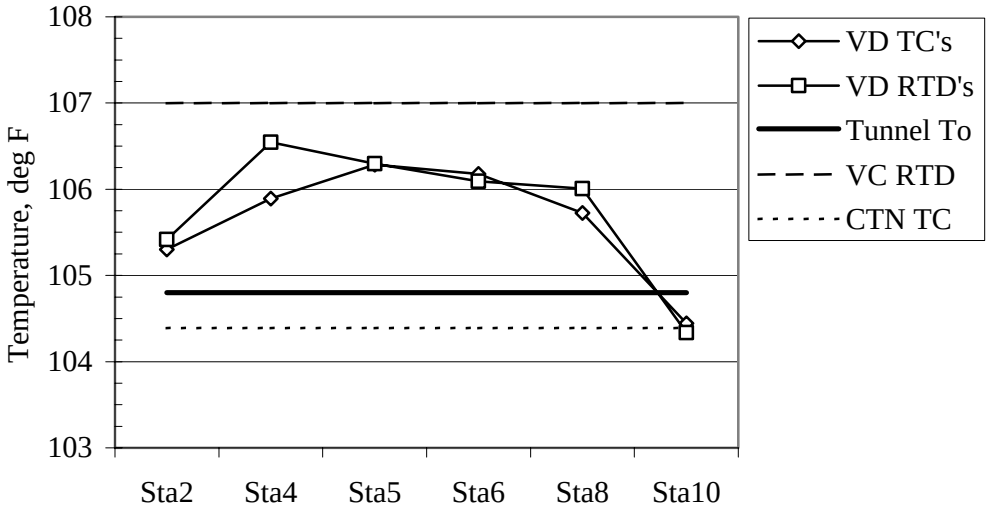

Figure 42. Stagnation temperature measurements at Q=125 psf and Mach 0.60 in air.

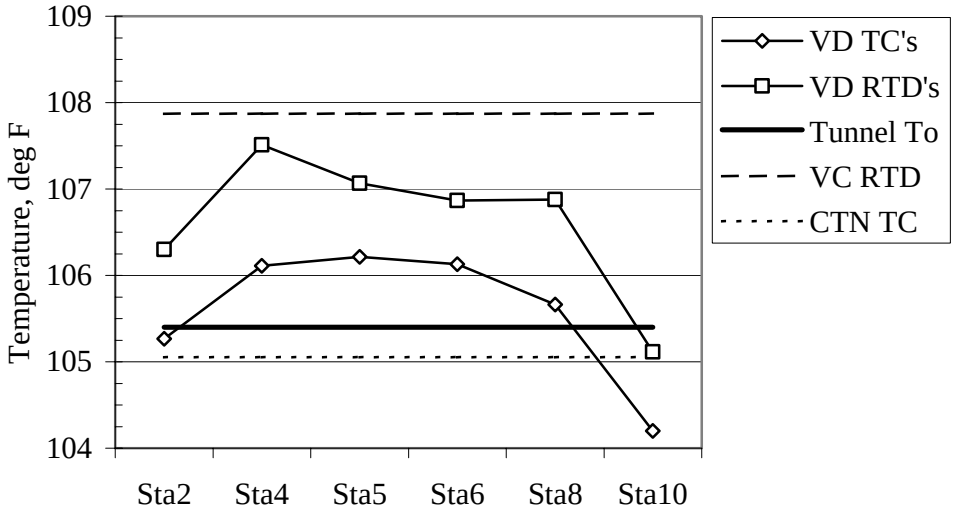

Figure 43. Stagnation temperature measurements at Q=125 psf and Mach 0.70 in air.

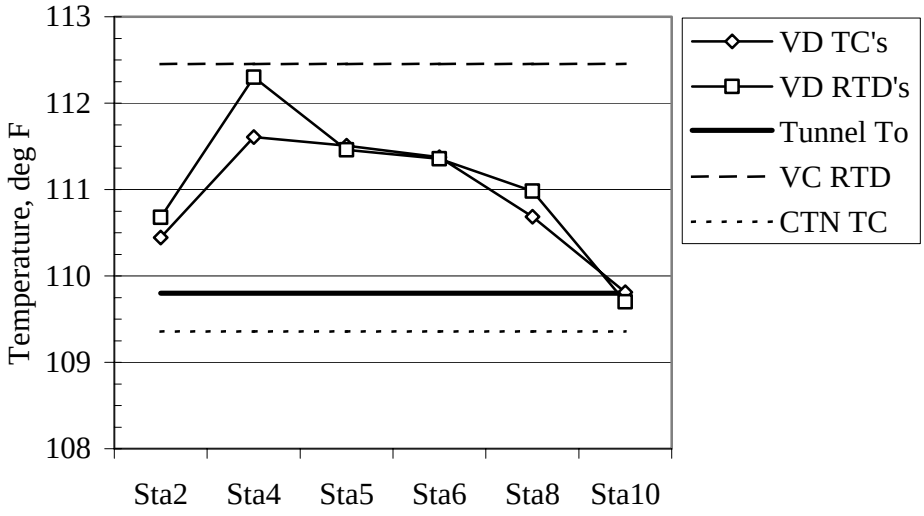

Figure 44. Stagnation temperature measurements at Q=125 psf and Mach 0.80 in air.

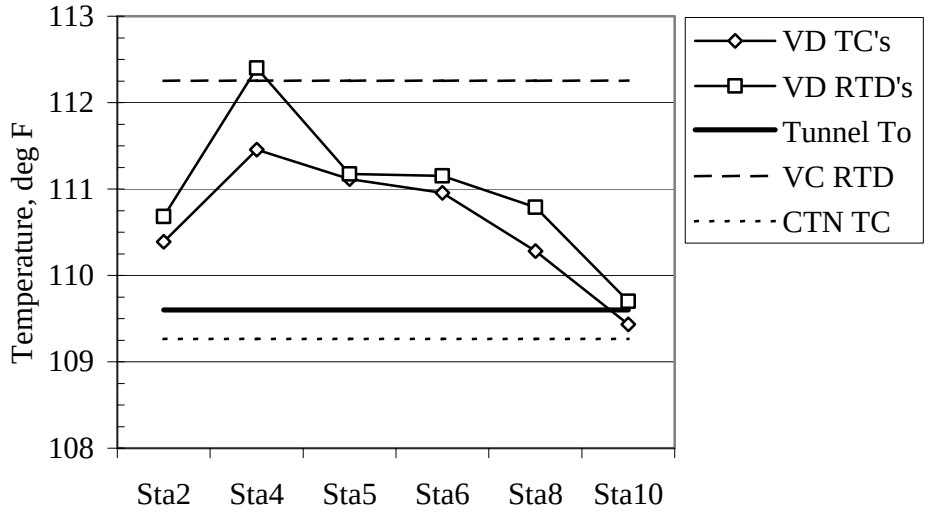

Figure 45. Stagnation temperature measurements at Q=125 psf and Mach 0.85 in air.

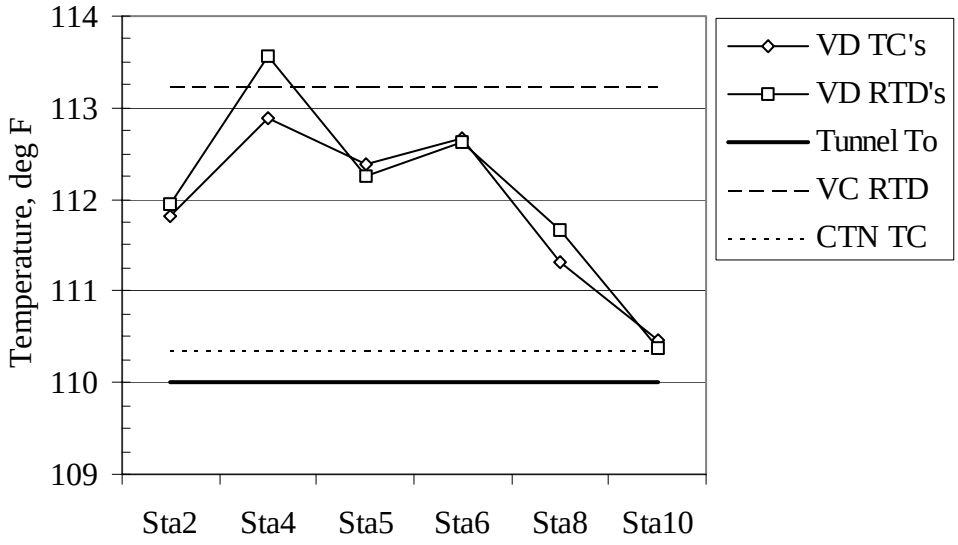

Figure 46. Stagnation temperature measurements at Q=125 psf and Mach 0.90 in air.

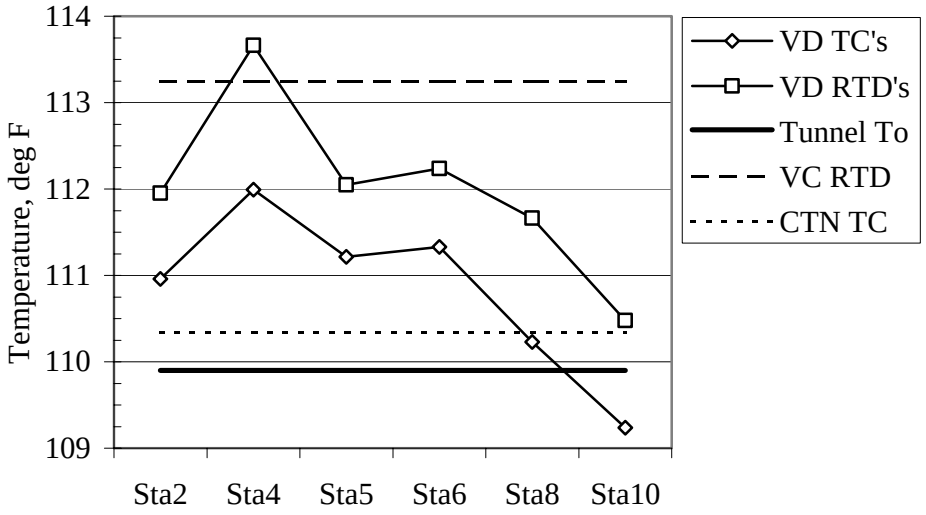

Figure 47. Stagnation temperature measurements at Q=125 psf and Mach 0.95 in air.

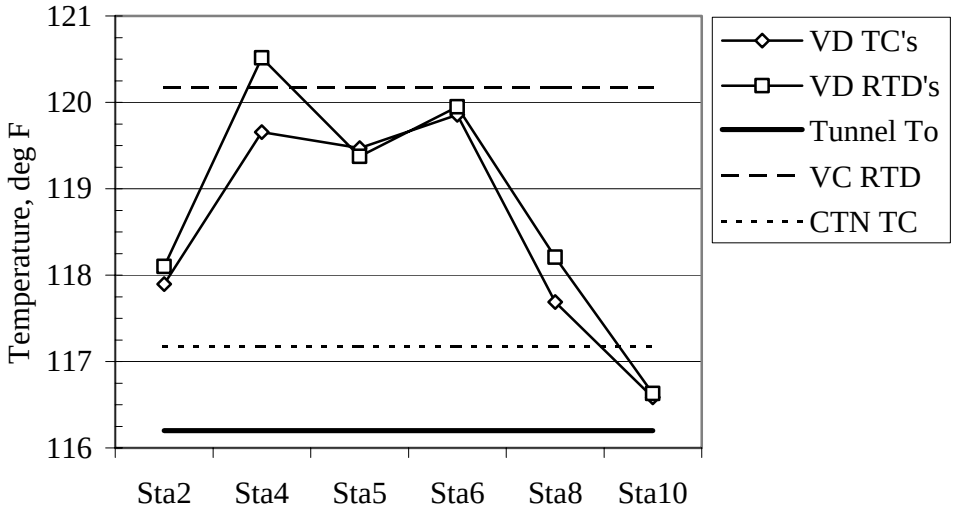

Figure 48. Stagnation temperature measurements at Q=125 psf and Mach 1.05 in air.

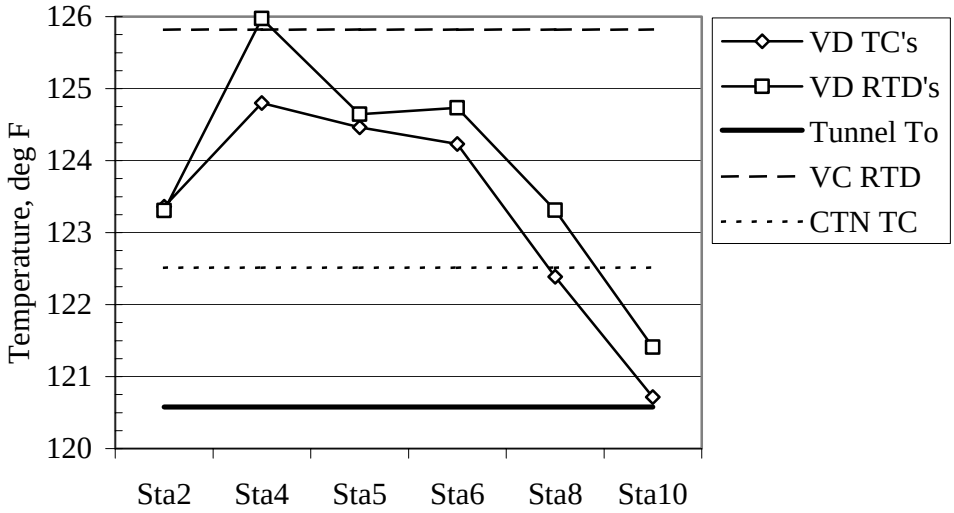

Figure 49. Stagnation temperature measurements at Q=125 psf and Mach 1.15 in air.

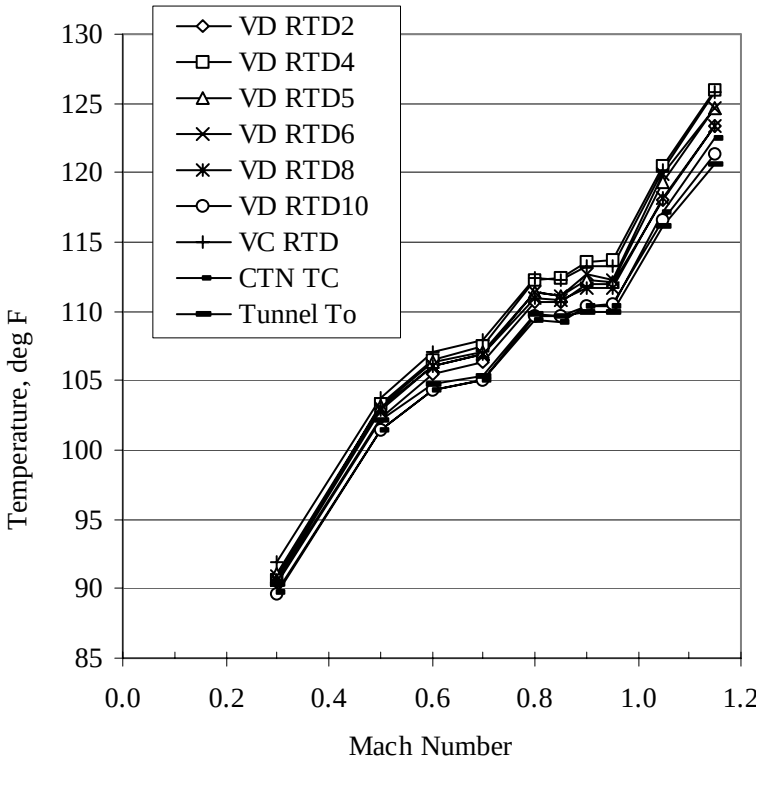

Figure 50a. Vane D RTD's, centerline tube thermocouple, and tunnel stagnation temperature versus Mach Number at constant dynamic pressure of 125 psf in air.

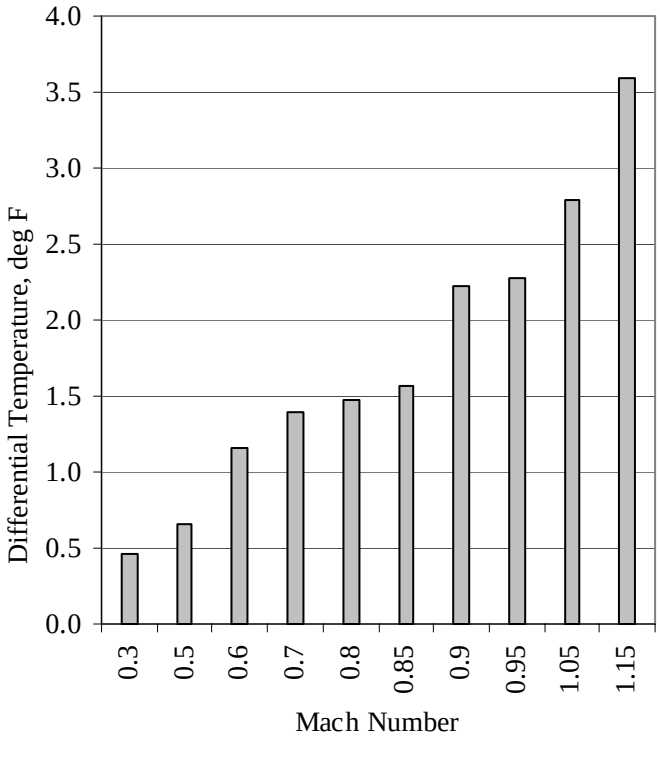

Figure 50b. Average differential Vane D RTD stagnation temperature versus Mach Number at constant dynamic pressure of 125 psf in air.

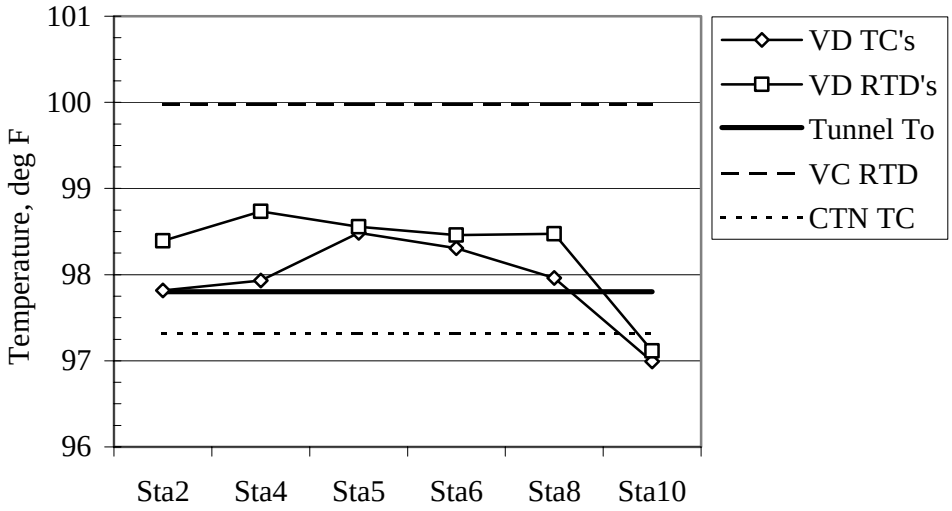

Figure 51. Stagnation temperature measurements at Q=200 psf and Mach =0.39 in air.

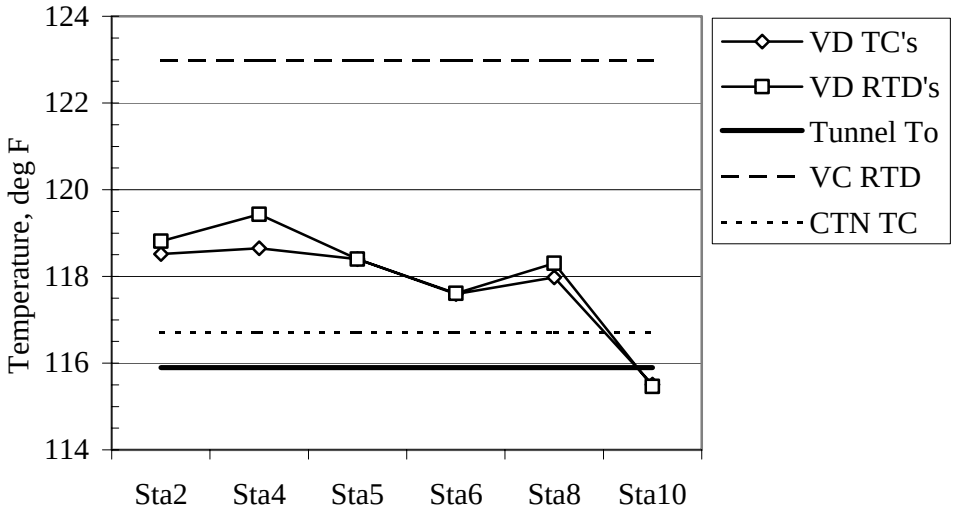

Figure 52. Stagnation temperature measurements at Q=200 psf and Mach 0.70 in air.

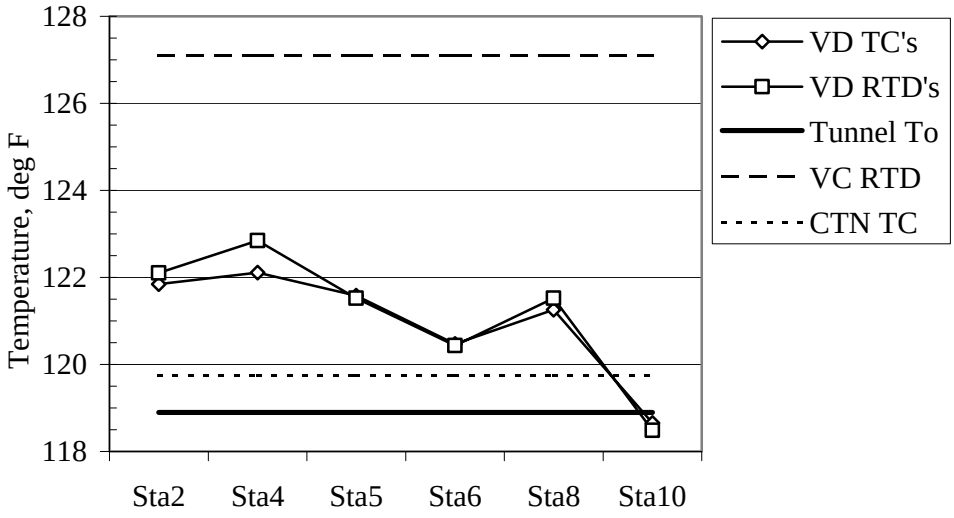

Figure 53. Stagnation temperature measurements at Q=200 psf and Mach 0.80 in air.

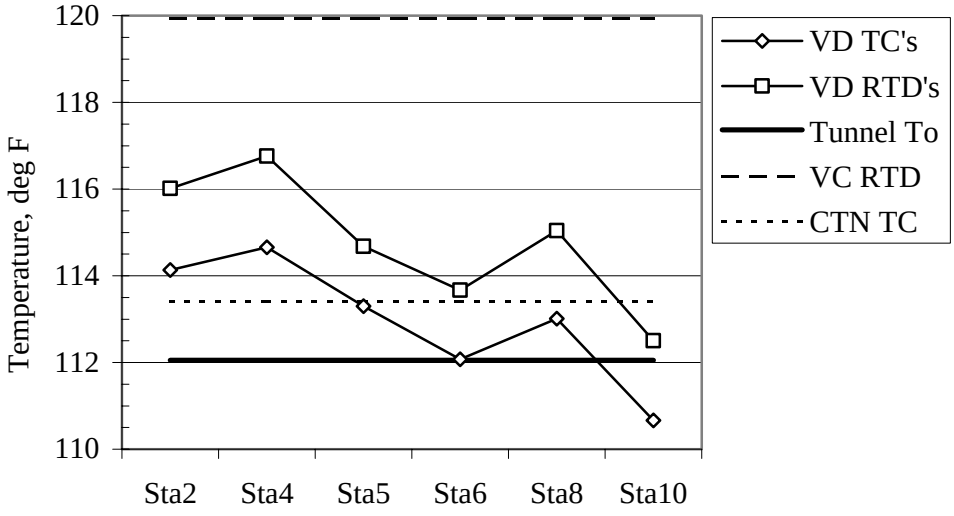

Figure 54. Stagnation temperature measurements at Q=200 psf and Mach 0.85 in air.

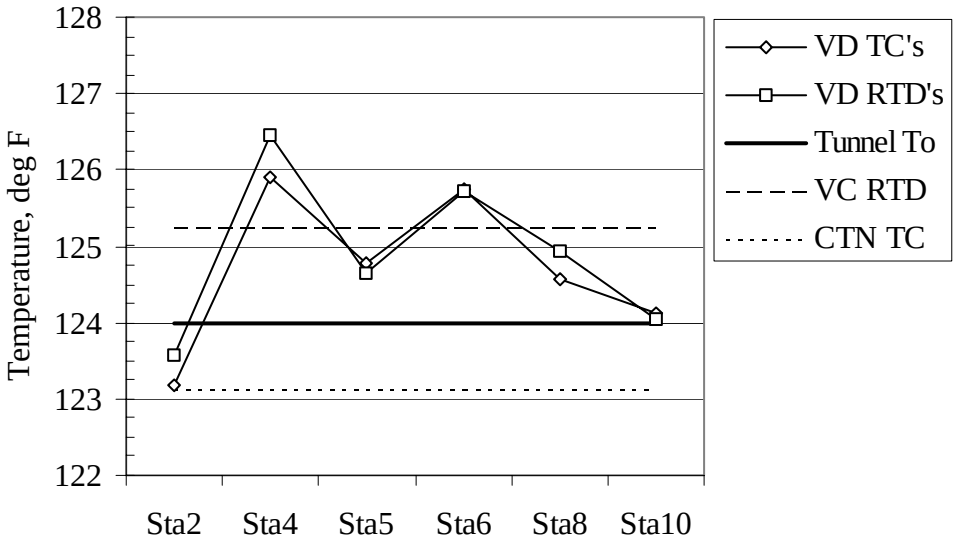

Figure 55. Stagnation temperature measurements at Q=200 psf and Mach 0.90 in air.

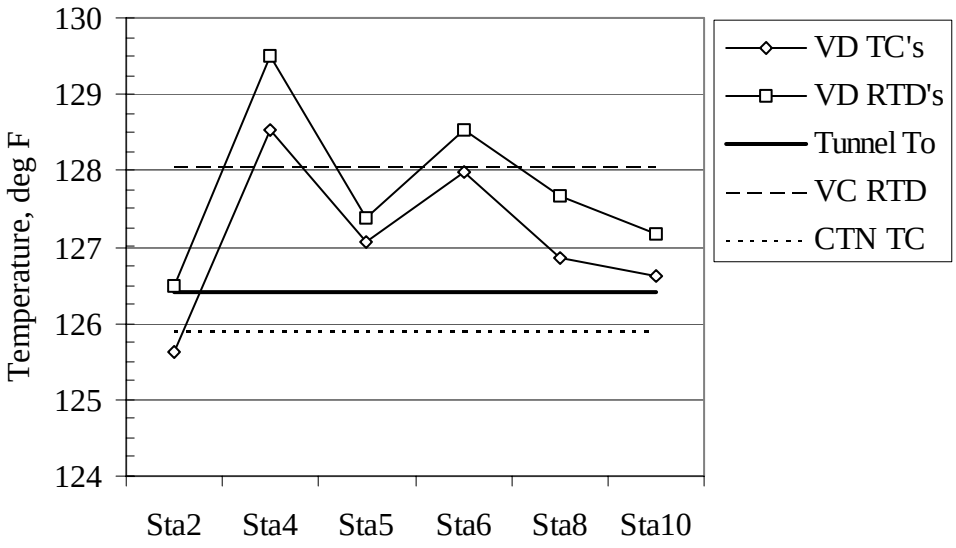

Figure 56. Stagnation temperature measurements at Q=200 psf and Mach 1.00 in air.

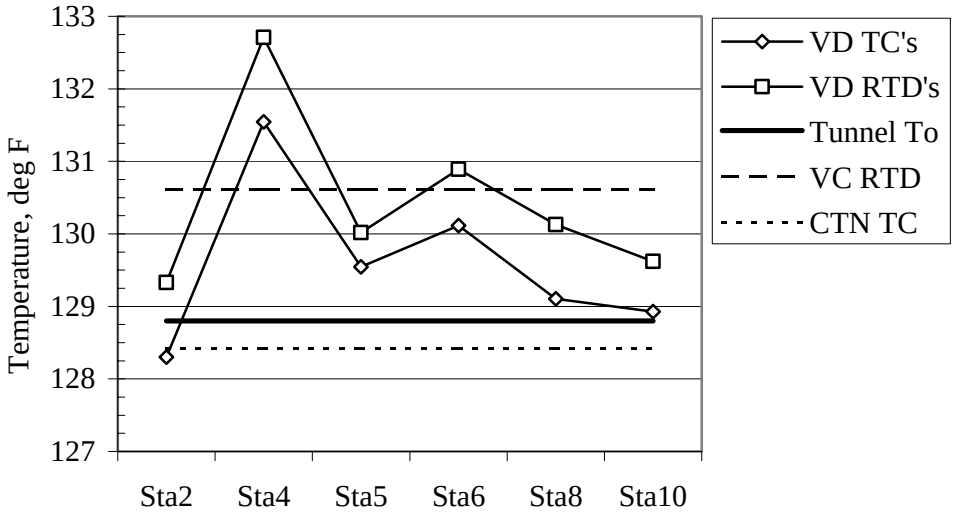

Figure 57. Stagnation temperature measurements at Q=200 psf and Mach 1.05 in air.

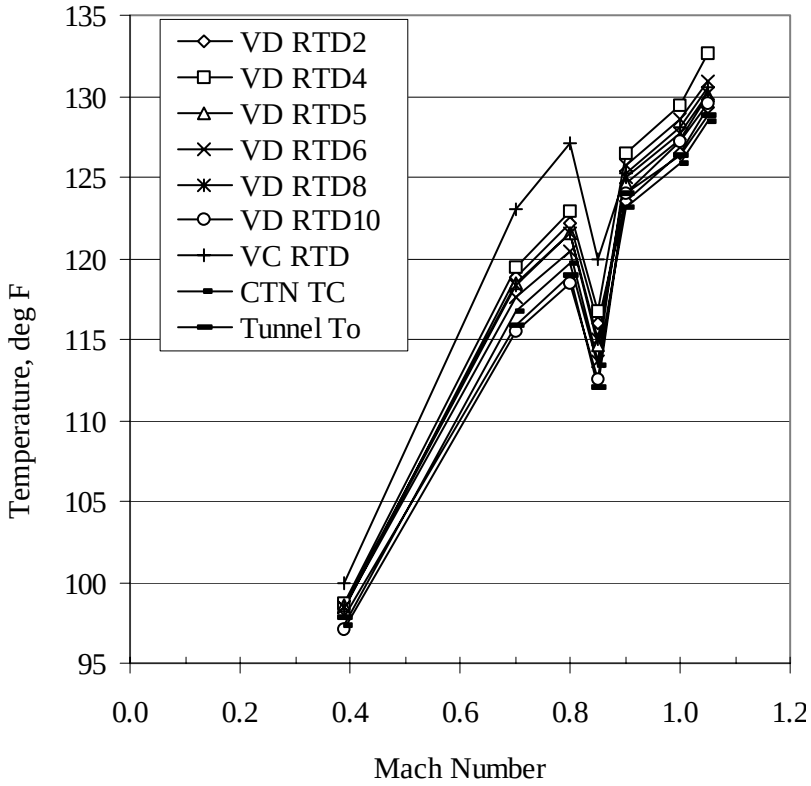

Figure 58a. Vane D RTD's, centerline tube thermocouple, and tunnel stagnation temperature versus Mach Number at constant dynamic pressure of 200 psf in air.

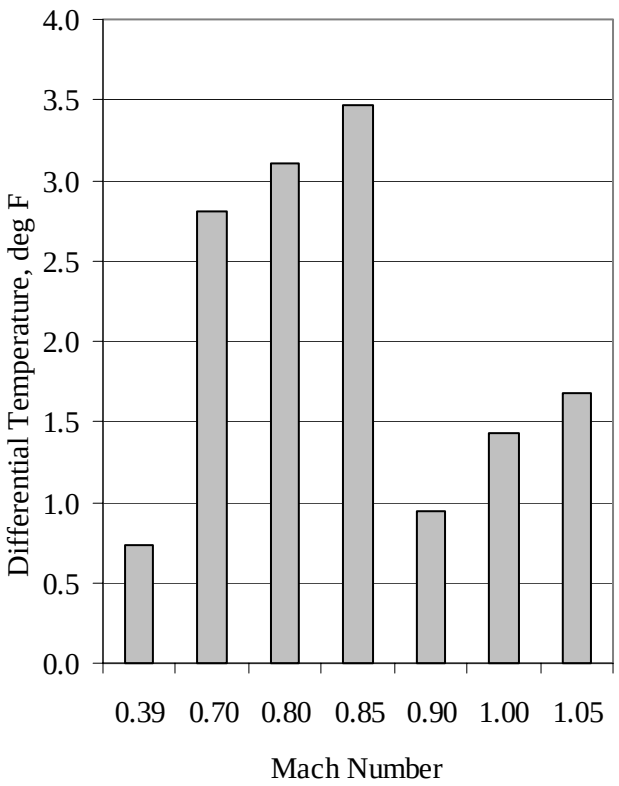

Figure 58b. Average differential Vane D RTD stagnation temperature versus Mach Number at constant dynamic pressure of 200 psf in air.

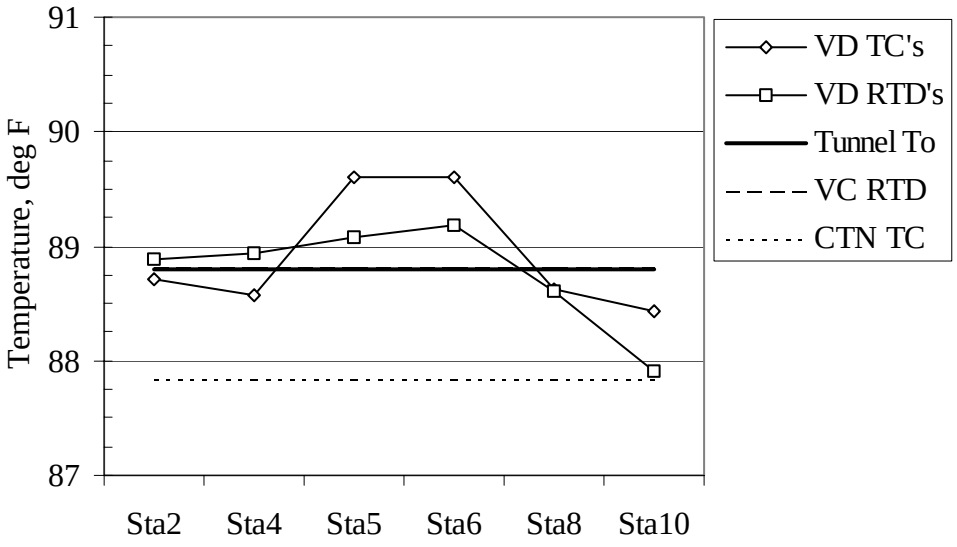

Figure 59. Stagnation temperature measurements at Q=100 psf and Mach 0.50 in R-134a.

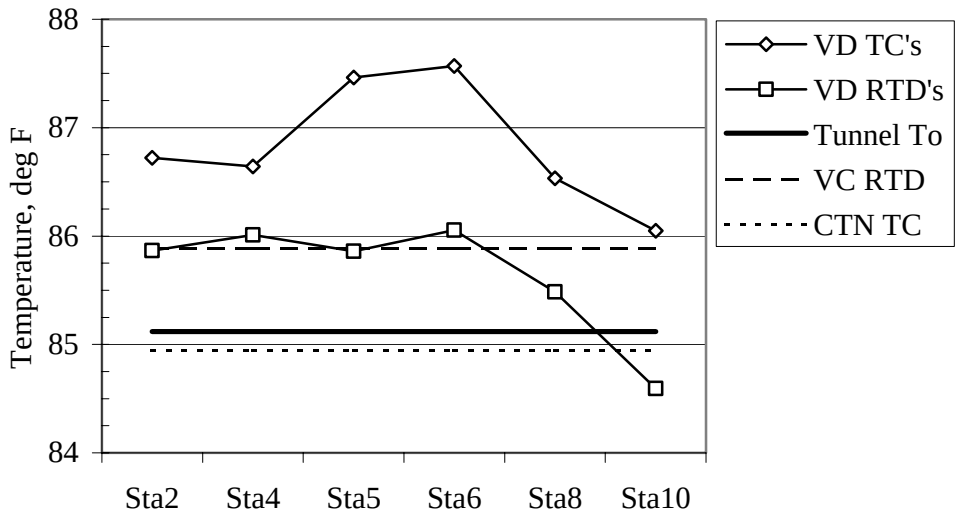

Figure 60. Stagnation temperature measurements at Q=100 psf and Mach 0.70 in R-134a.

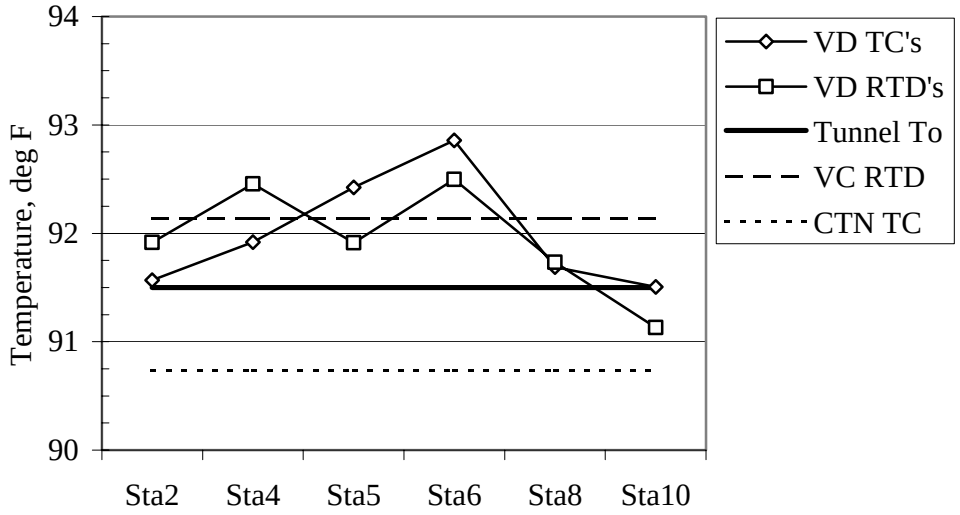

Figure 61. Stagnation temperature measurements at Q=100 psf and Mach 0.80 in R-134a.

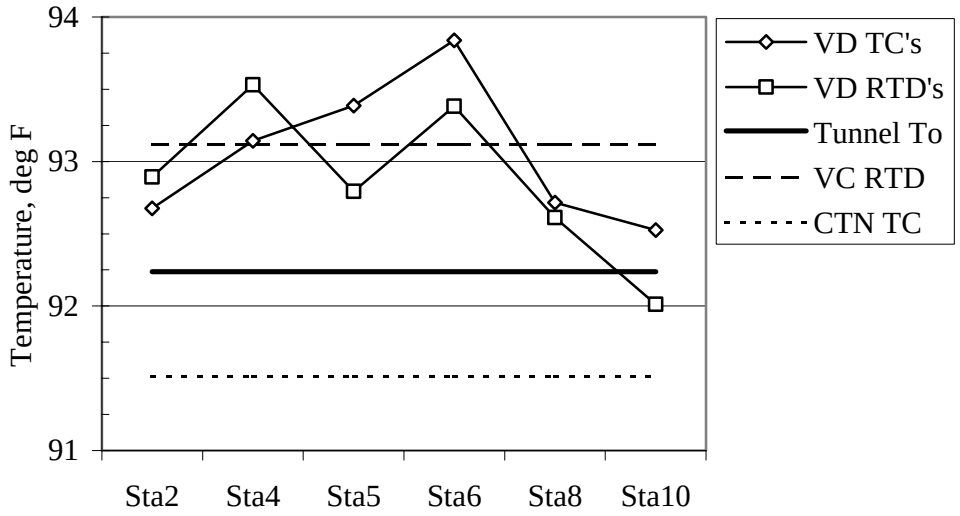

Figure 62. Stagnation temperature measurements at Q=100 psf and Mach 0.90 in R-134a.

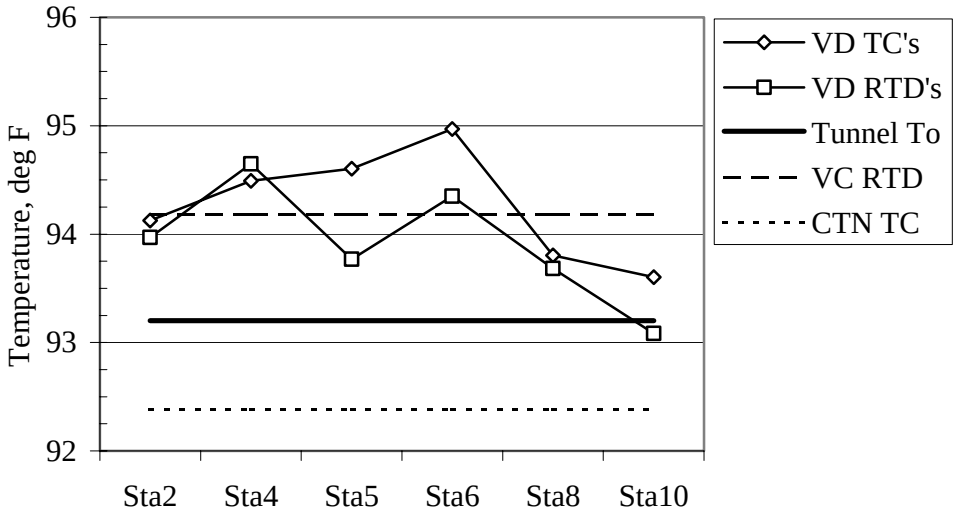

Figure 63. Stagnation temperature measurements at Q=100 psf and Mach 0.95 in R-134a.

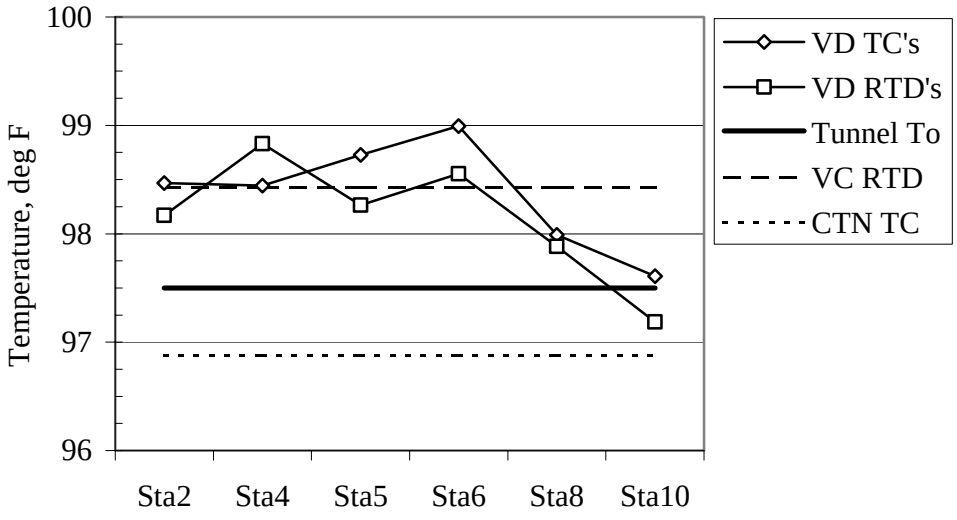

Figure 64. Stagnation temperature measurements at Q=100 psf and Mach 1.05 in R-134a.

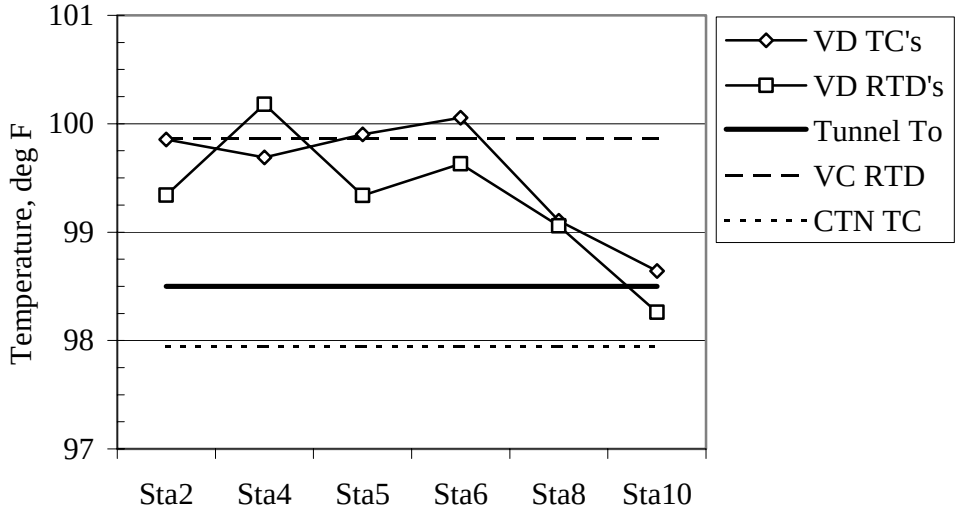

Figure 65. Stagnation temperature measurements at Q=100 psf and Mach 1.10 in R-134a.

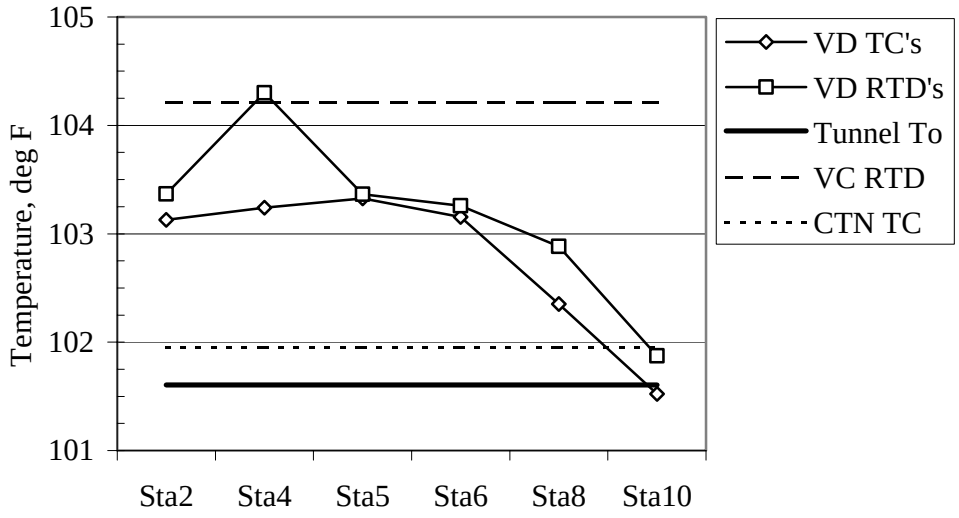

Figure 66. Stagnation temperature measurements at Q=100 psf and Mach 1.19 in R-134a.

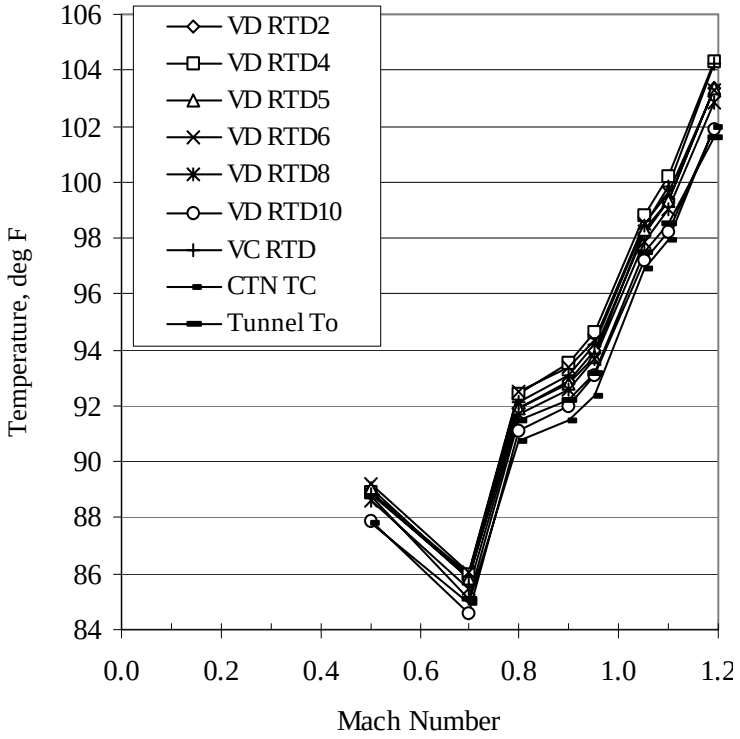

Figure 67a. Vane D RTD's, centerline tube thermocouple, and tunnel stagnation temperature versus Mach Number at constant dynamic pressure of 100 psf in R-134a.

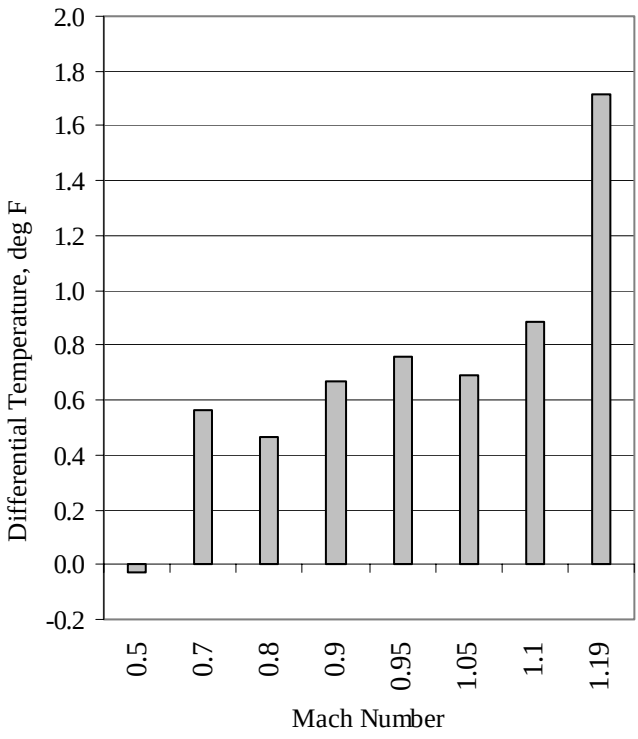

Figure 67b. Average differential Vane D RTD stagnation temperature versus Mach Number at constant dynamic pressure of 100 psf in R-134a.

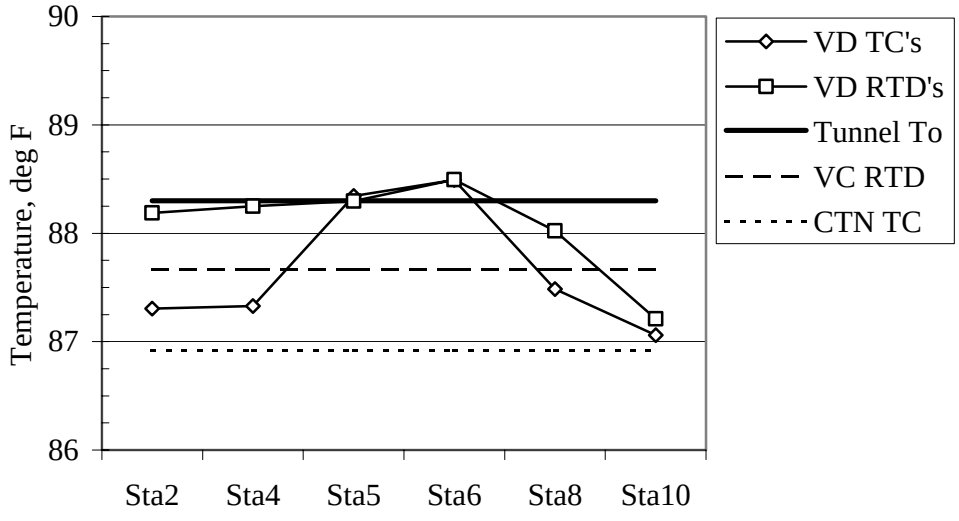

Figure 68. Stagnation temperature measurements at Q=225 psf and Mach 0.5 in R-134a.

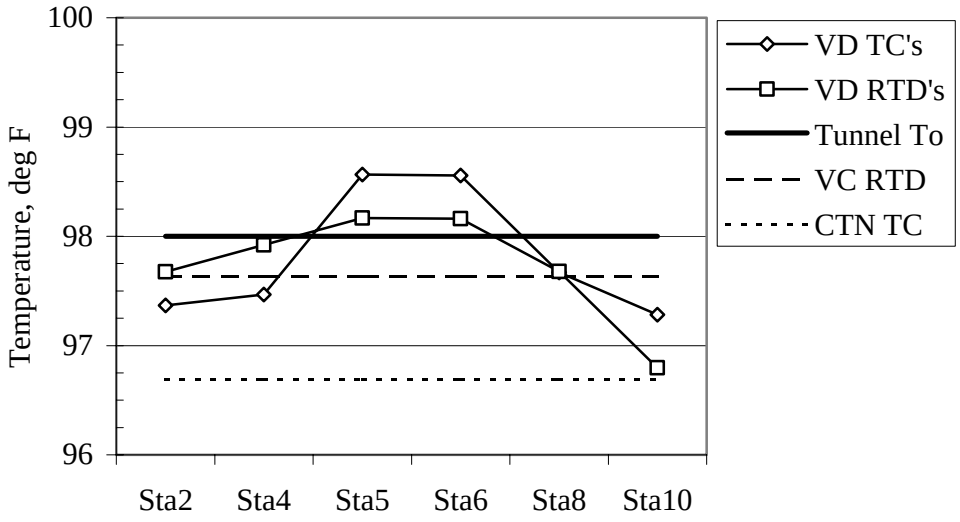

Figure 69. Stagnation temperature measurements at Q=225 psf and Mach 0.6 in R-134a.

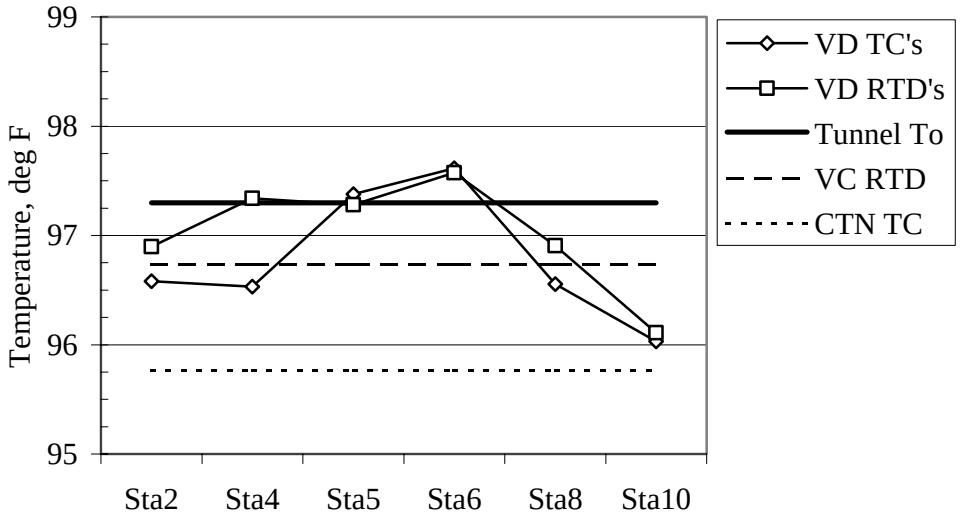

Figure 70. Stagnation temperature measurements at Q=225 psf and Mach 0.7 in R-134a.

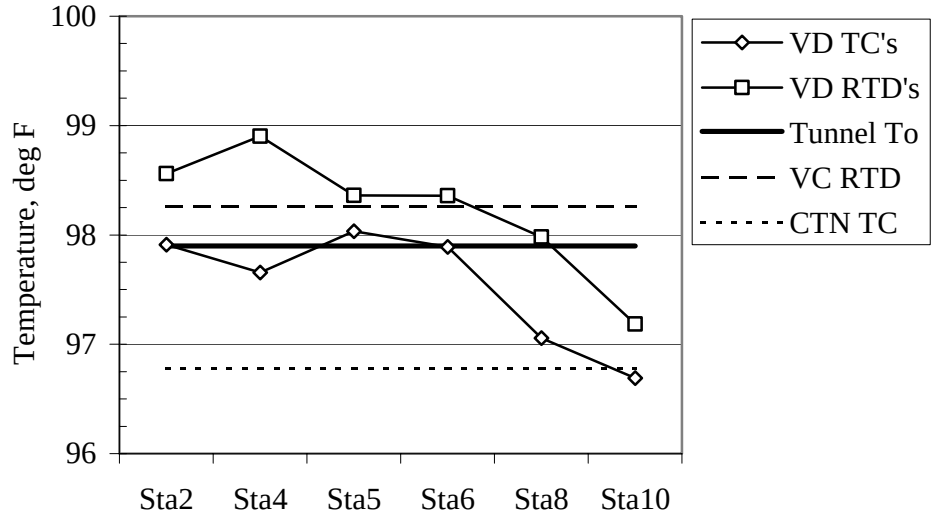

Figure 71. Stagnation temperature measurements at Q=225 psf and Mach 0.90 in R-134a.

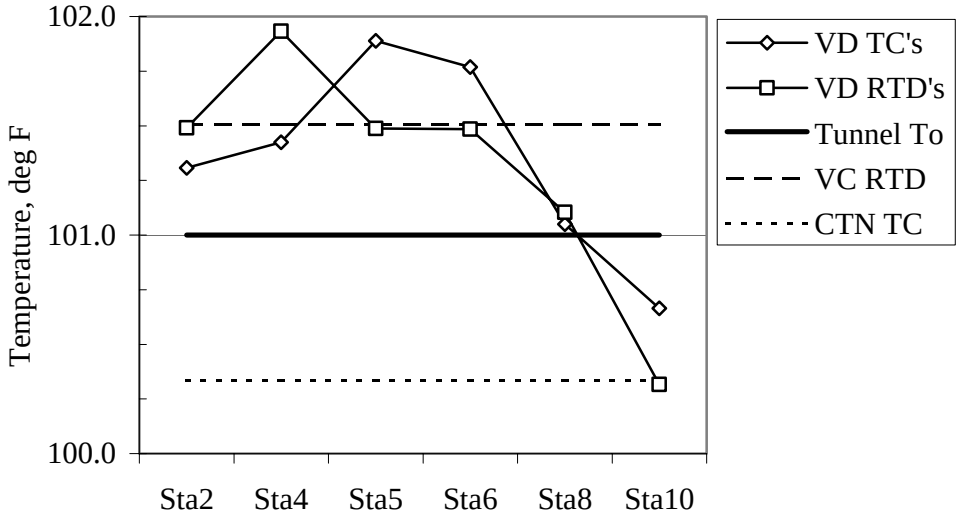

Figure 72. Stagnation temperature measurements at Q=225 psf and Mach 0.95 in R-134a.

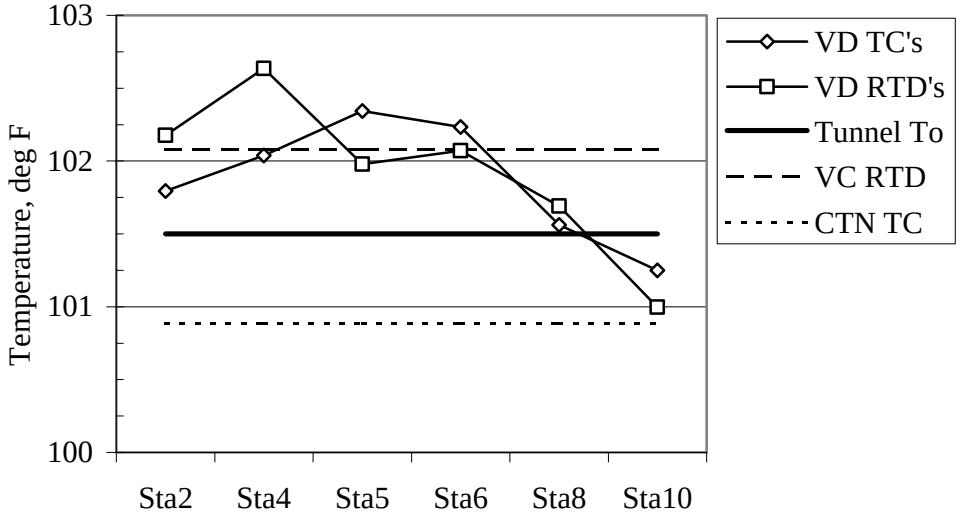

Figure 73. Stagnation temperature measurements at Q=225 psf and Mach 1.00 in R-134a.

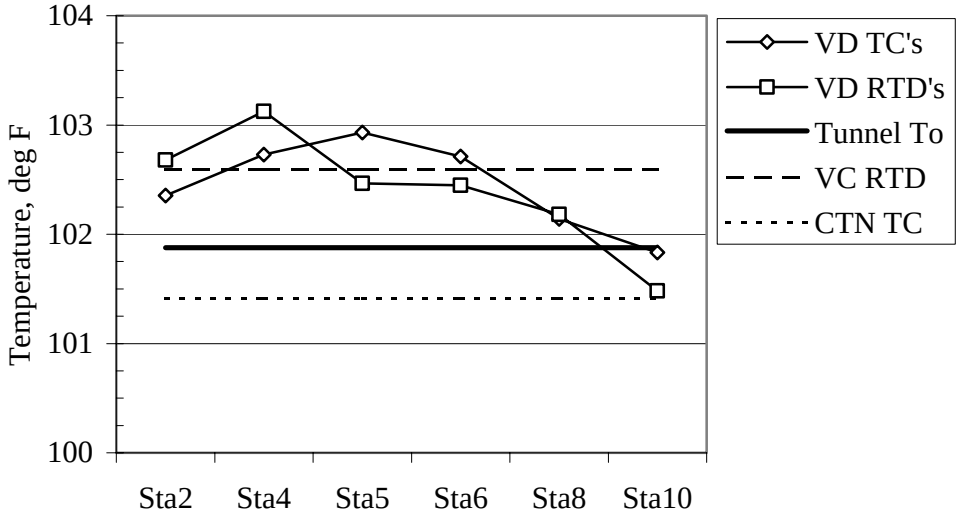

Figure 74. Stagnation temperature measurements at Q=225 psf and Mach 1.05 in R-134a.

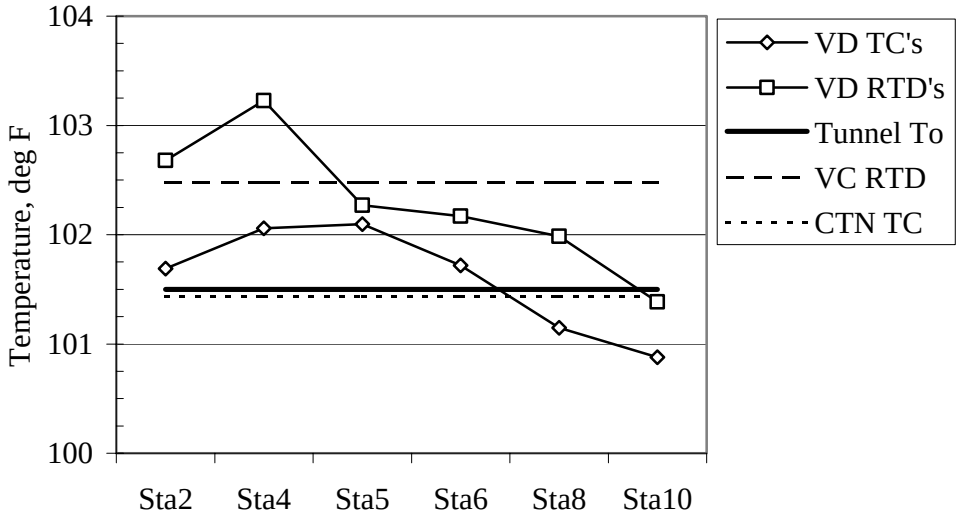

Figure 75. Stagnation temperature measurements at Q=225 psf and Mach 1.10 in R-134a.

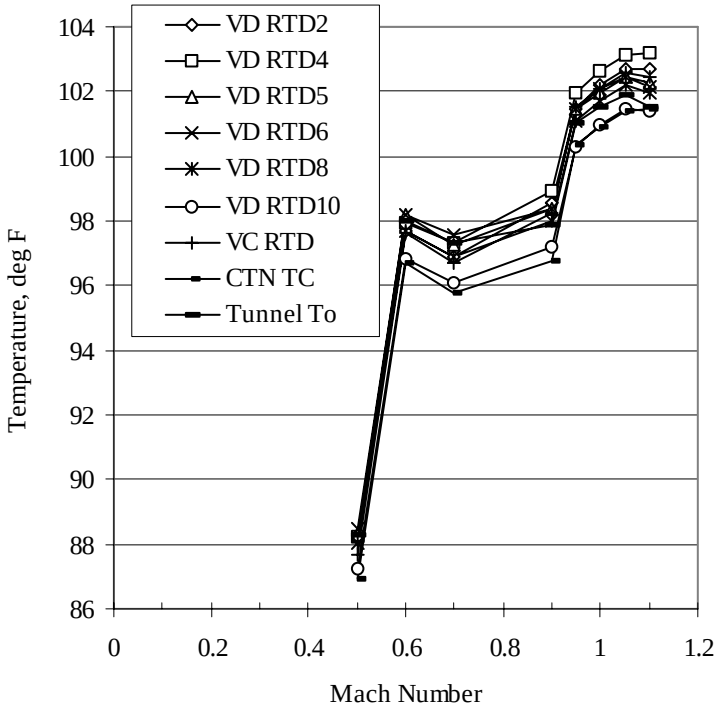

Figure 76a. Vane D RTD's, centerline tube thermocouple, and tunnel stagnation temperature versus Mach Number at constant dynamic pressure of 225 psf in R-134a.

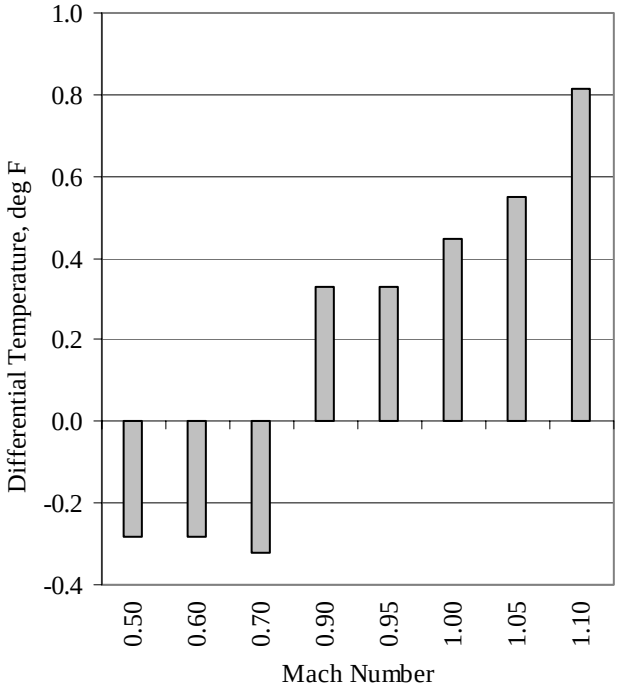

Figure 76b. Average differential Vane D RTD stagnation temperature versus Mach Number at constant dynamic pressure of 225 psf in R-134a.

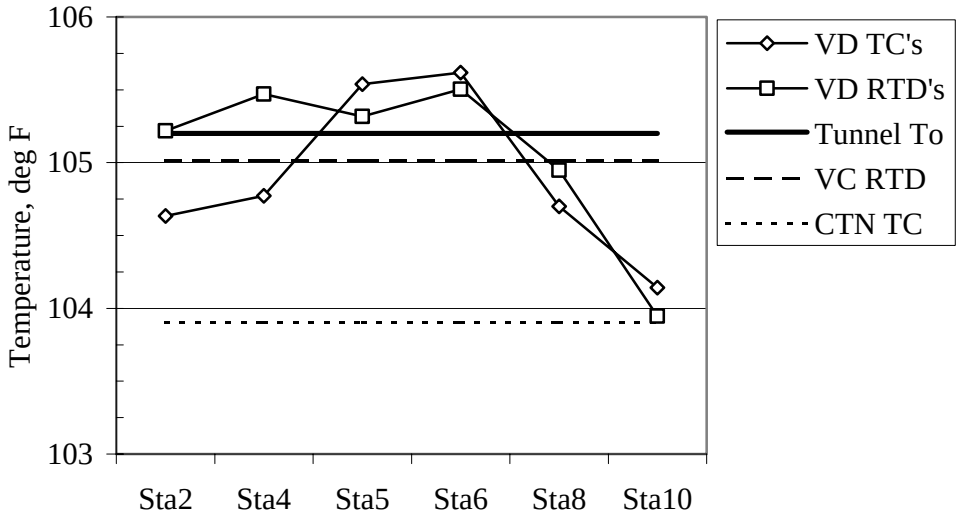

Figure 77. Stagnation temperature measurements at Q=350 psf and Mach 0.80 in R-134a.

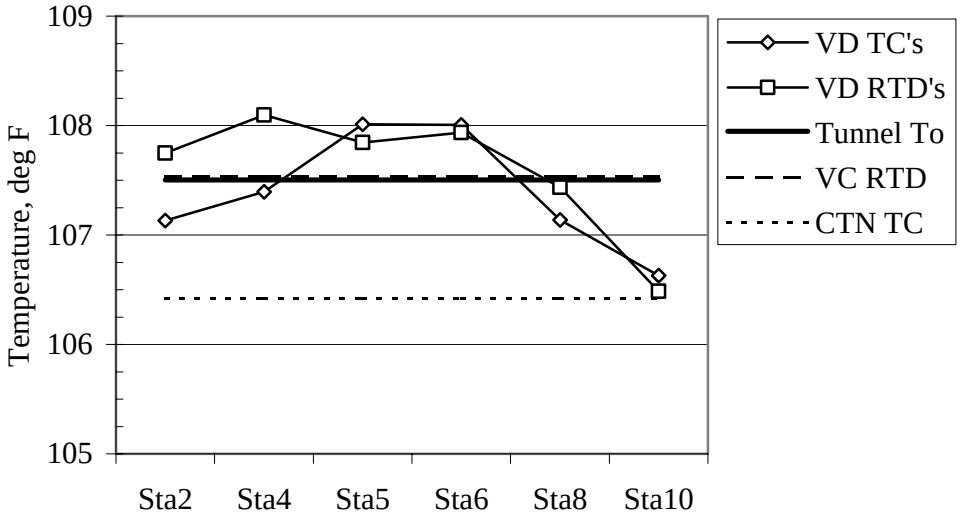

Figure 78. Stagnation temperature measurements at Q=350 psf and Mach 0.90 in R-134a.

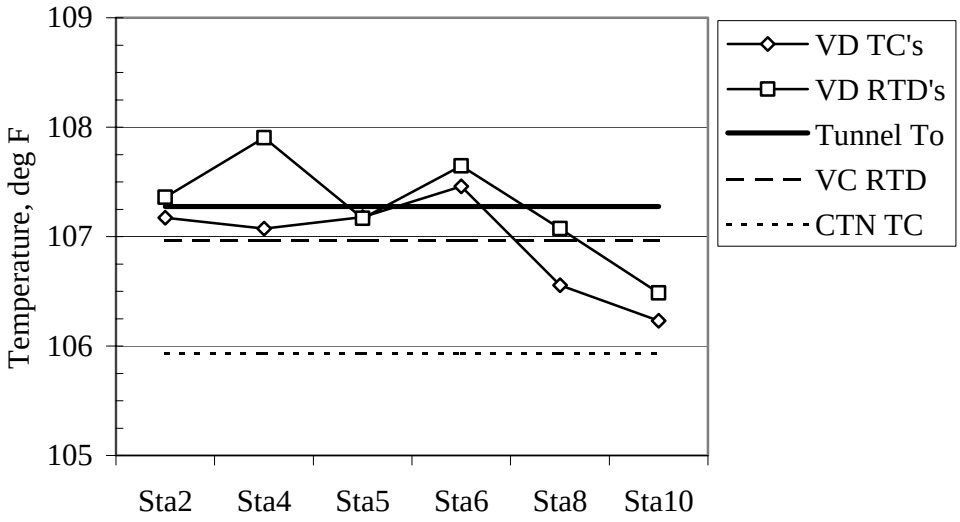

Figure 79. Stagnation temperature measurements at Q=350 psf and Mach 0.95 in R-134a.

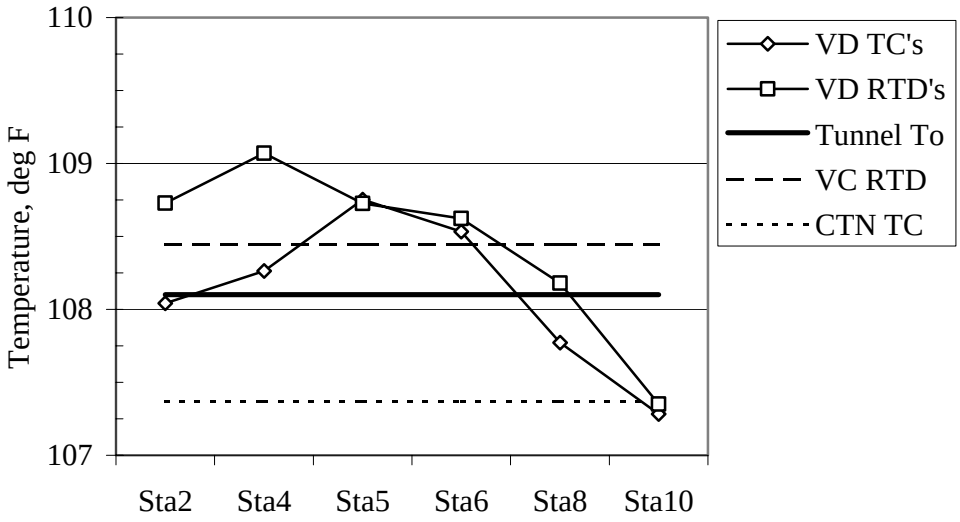

Figure 80. Stagnation temperature measurements at Q=353 psf and Mach 1.00 in R-134a.

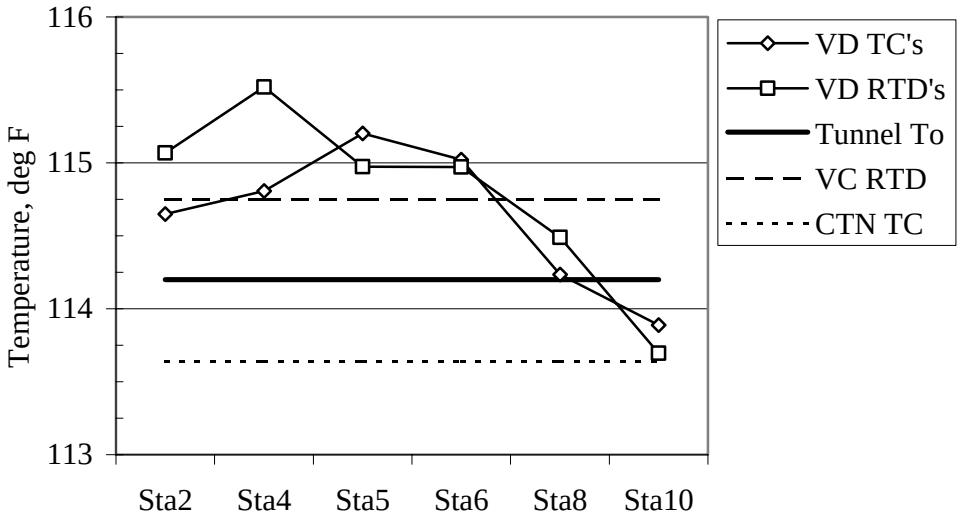

Figure 81. Stagnation temperature measurements at Q=350 psf and Mach 1.05 in R-134a.

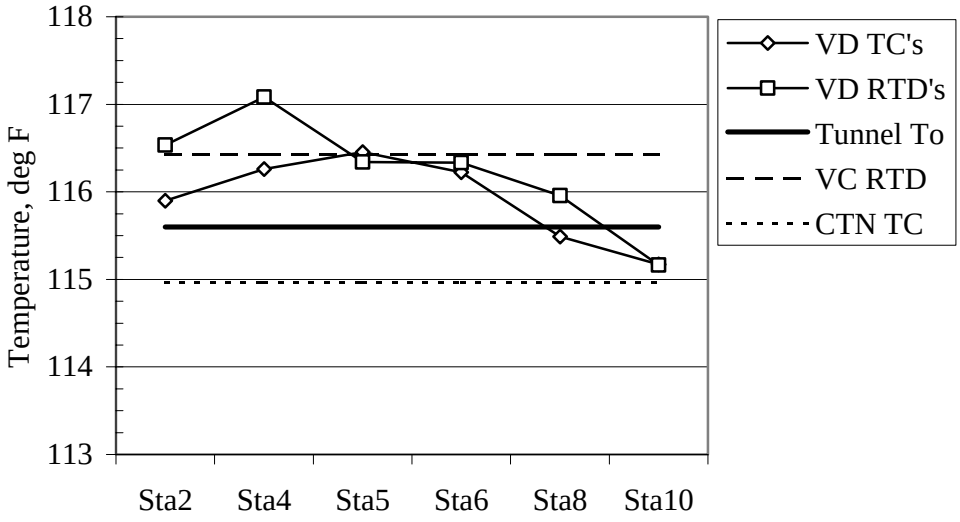

Figure 82. Stagnation temperature measurements at Q=350 psf and Mach 1.10 in R-134a.

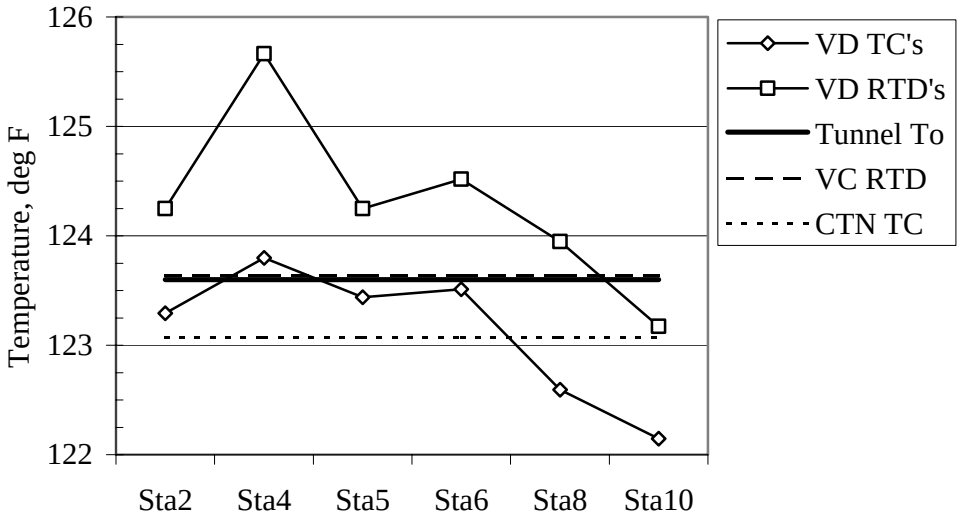

Figure 83. Stagnation temperature measurements at Q=350 psf and Mach 1.20 in R-134a.

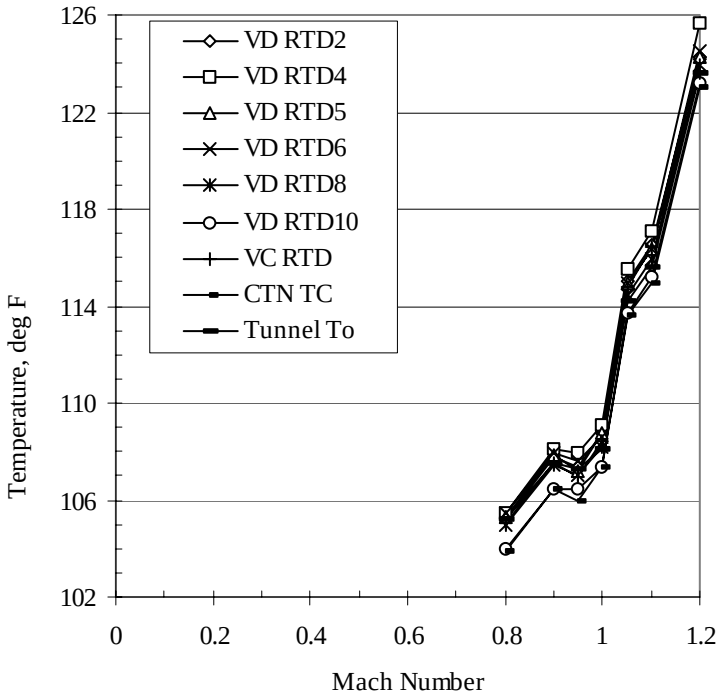

Figure 84a. Vane D RTD's, centerline tube thermocouple, and tunnel stagnation temperature versus Mach Number at constant dynamic pressure of 350 psf in R-134a.

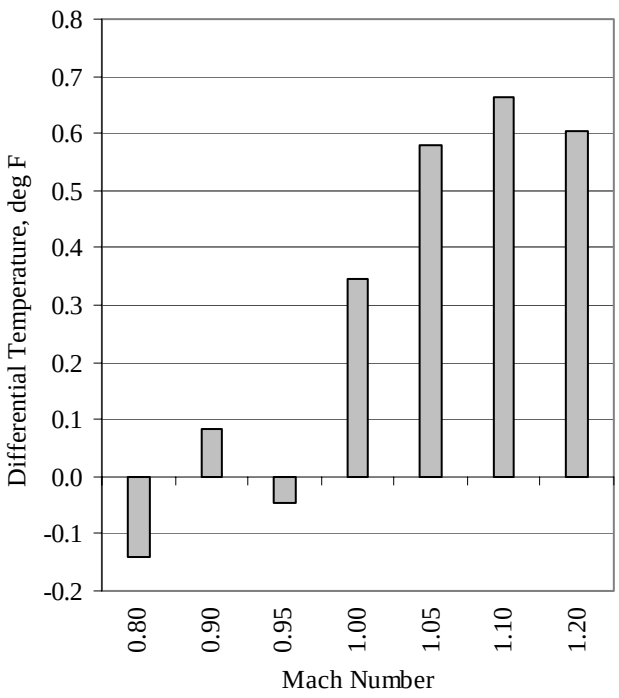

Figure 84b. Average differential Vane D RTD stagnation temperature versus Mach Number at constant dynamic pressure of 350 psf in R-134a.

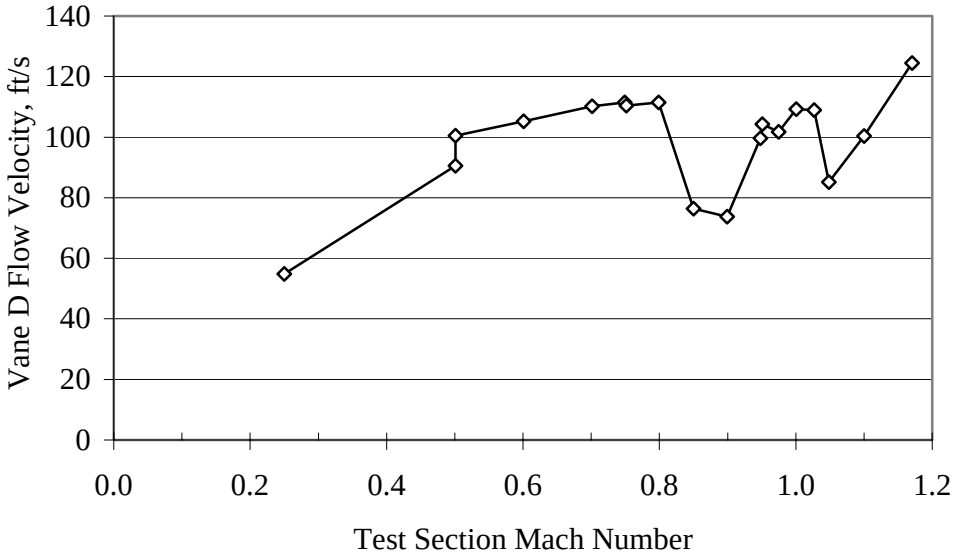

Figure 85. Vane D pitot probe flow velocity versus test section Mach number for a wind-off tunnel pressure of 200 psf in air.

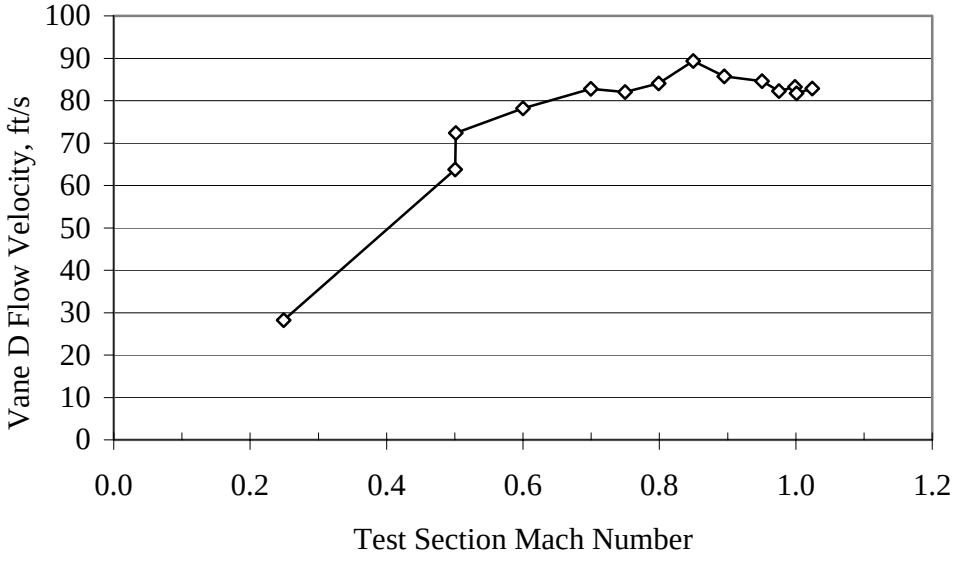

Figure 86. Vane D pitot probe flow velocity versus test section Mach number for a wind-off tunnel pressure of 400 psf in air.

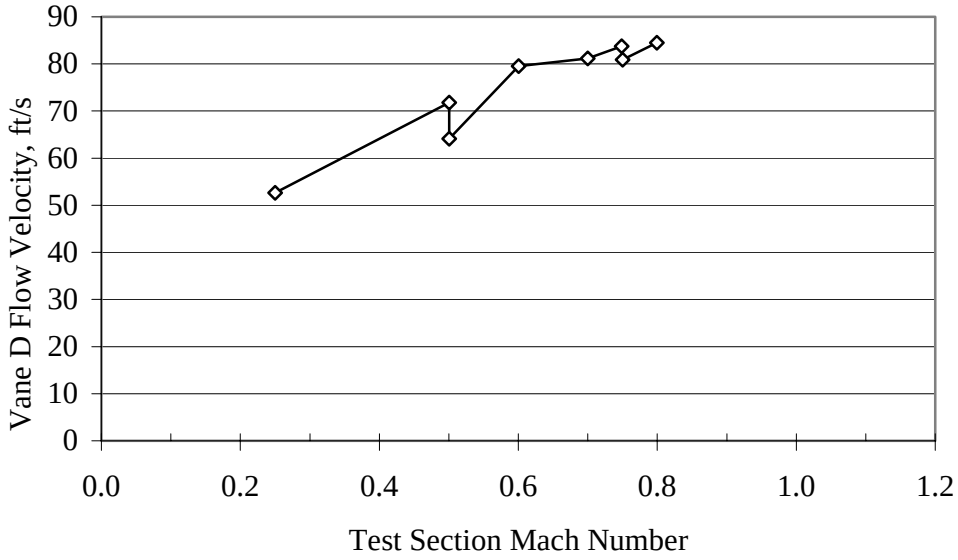

Figure 87. Vane D pitot probe flow velocity versus test section Mach number for a wind-off tunnel pressure of 700 psf in air.

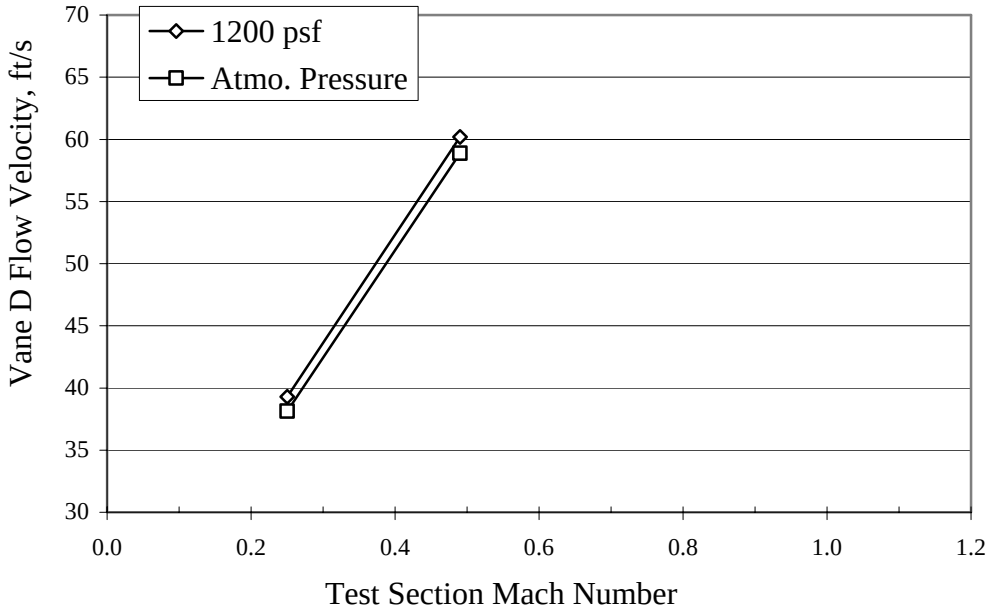

Figure 88. Vane D pitot probe flow velocity versus test section Mach number for a wind-off tunnel pressure of 1200 psf and atmospheric pressure in air.

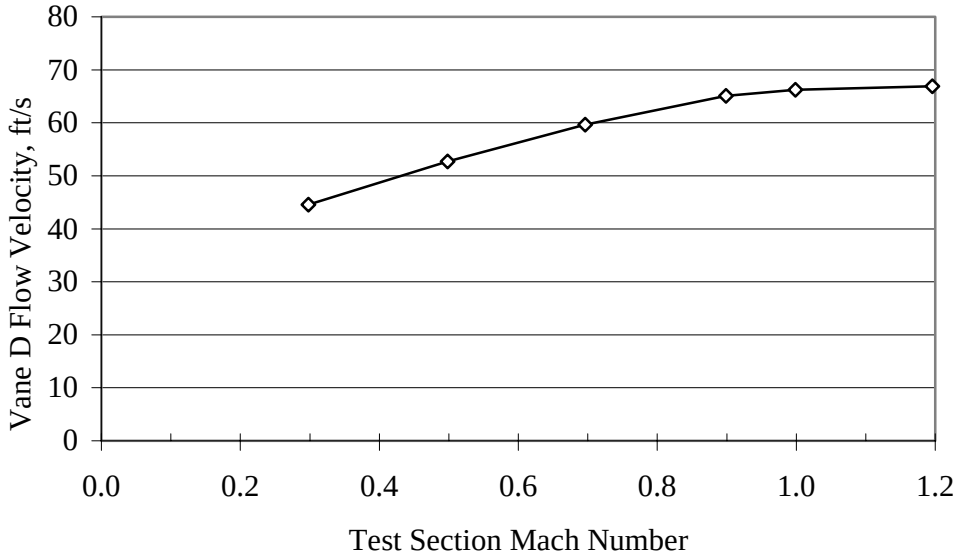

Figure 89. Vane D pitot probe flow velocity versus test section Mach number for a wind-off tunnel pressure of 200 psf in R134a.

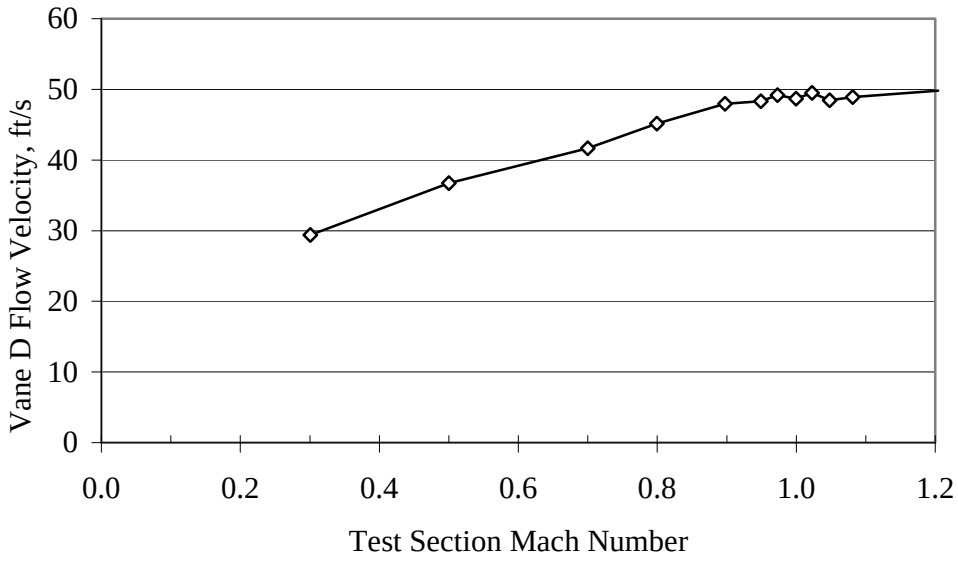

Figure 90. Vane D pitot probe flow velocity versus test section Mach number for a wind-off tunnel pressure of 500 psf in R134a.

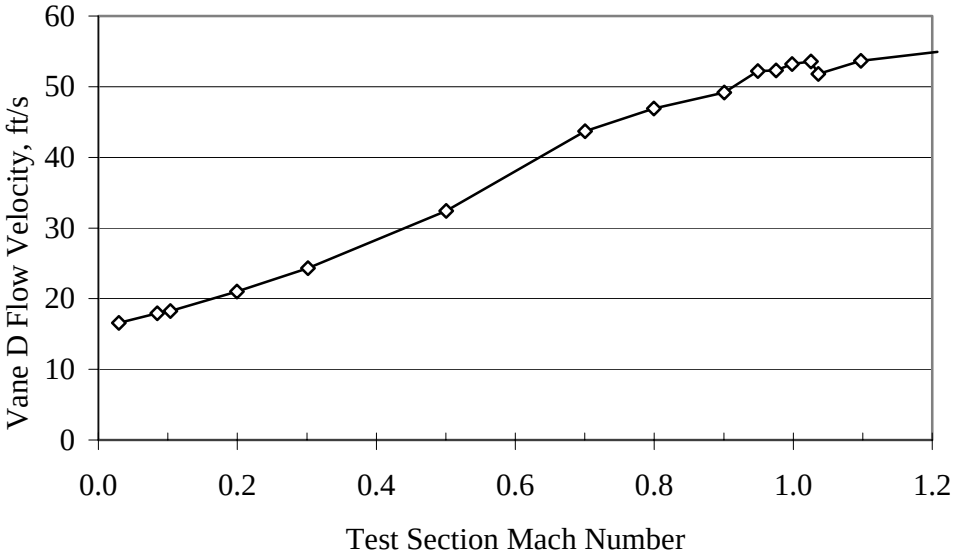

Figure 91. Vane D pitot probe flow velocity versus test section Mach number for a wind-off tunnel pressure of 700 psf in R134a.

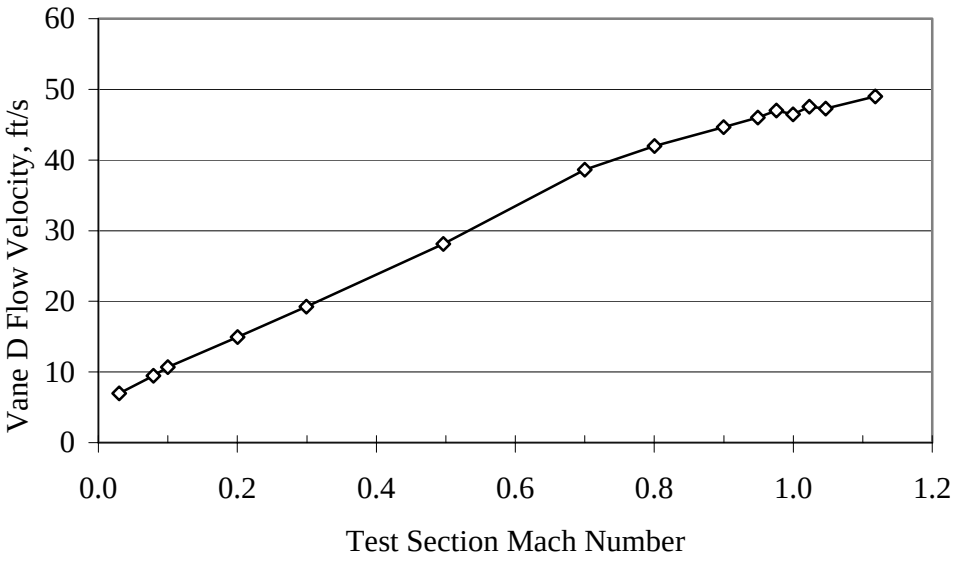

Figure 92. Vane D pitot probe flow velocity versus test section Mach number for a wind-off tunnel pressure of 1000 psf in R134a.

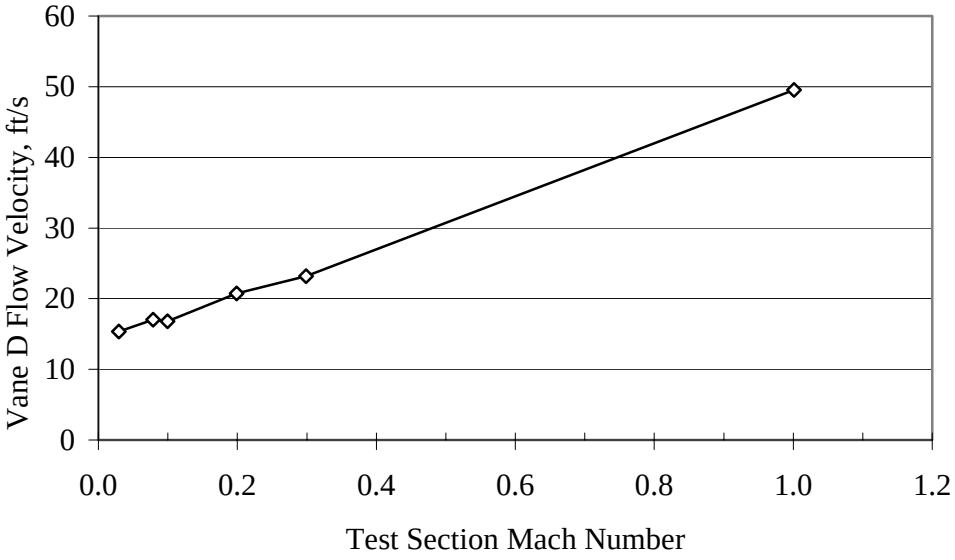

Figure 93. Vane D pitot probe flow velocity versus test section Mach number for a wind-off tunnel pressure of 1400 psf in R134a.

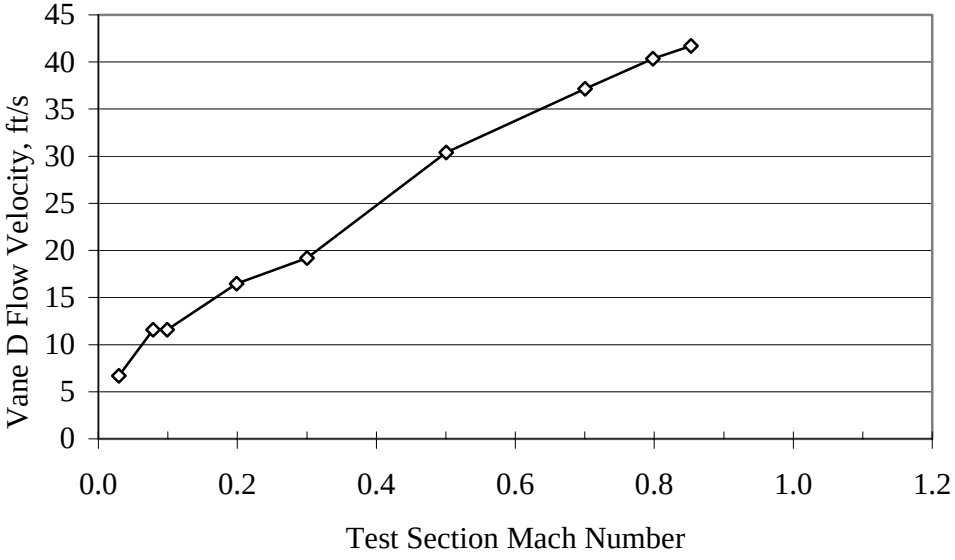

Figure 94. Vane D pitot probe flow velocity versus test section Mach number for a wind-off tunnel pressure of 1800 psf in R134a.

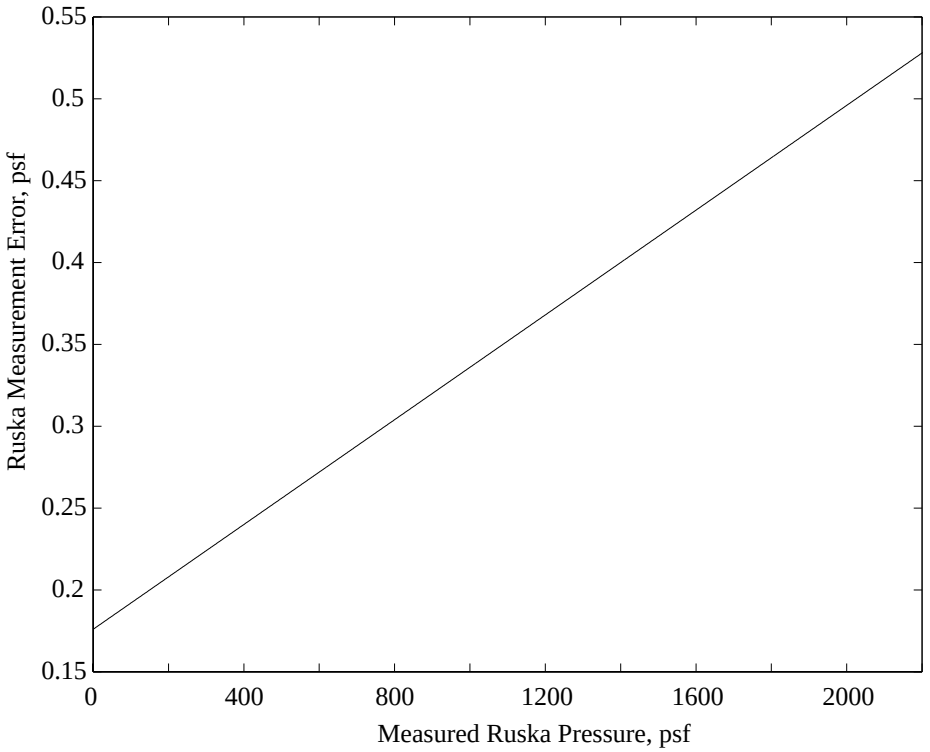

Figure 95. Ruska measurement error versus measured pressure.

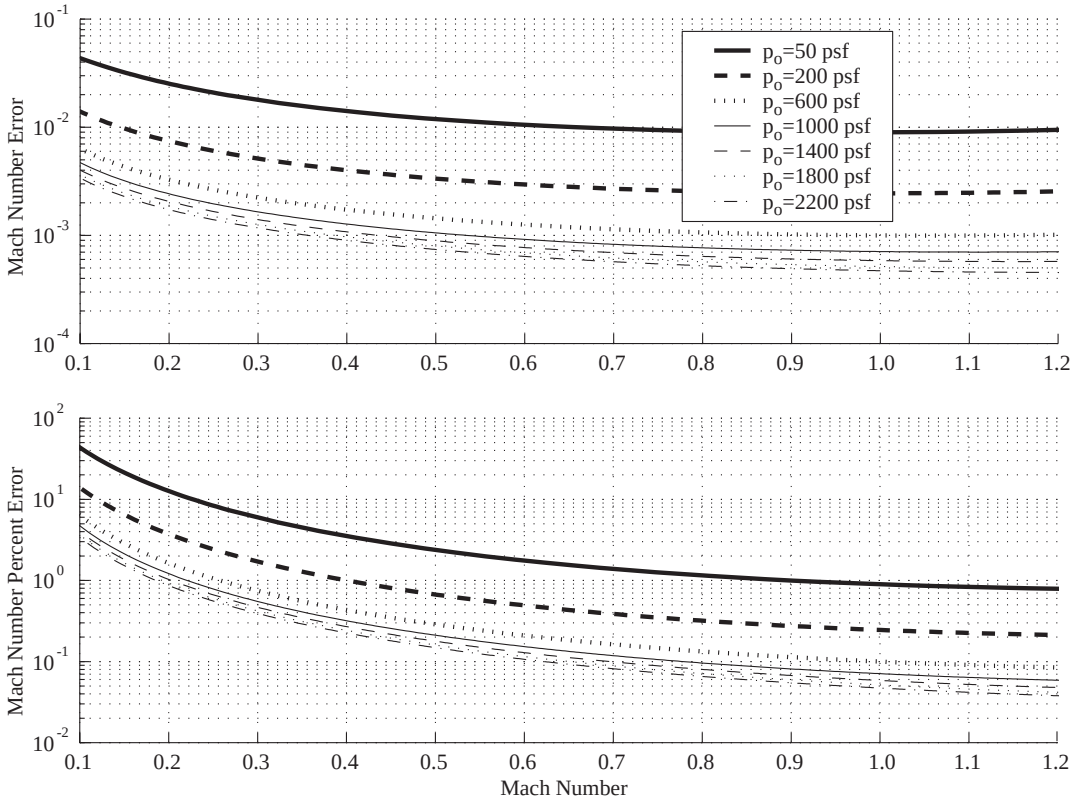

Figure 96. Mach number error and percent error versus Mach number in air due to Ruska error in primary tunnel stagnation and plenum pressures.

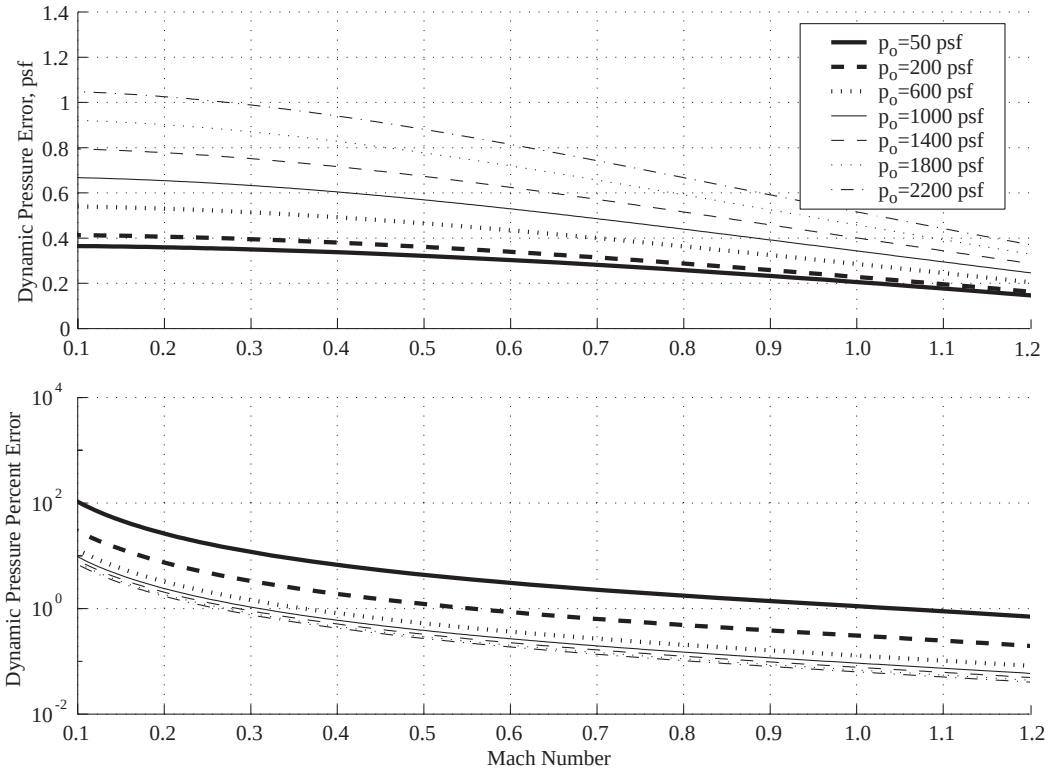

Figure 97. Dynamic pressure error and percent error versus Mach number in air due to Ruska error in primary tunnel stagnation and plenum pressures.

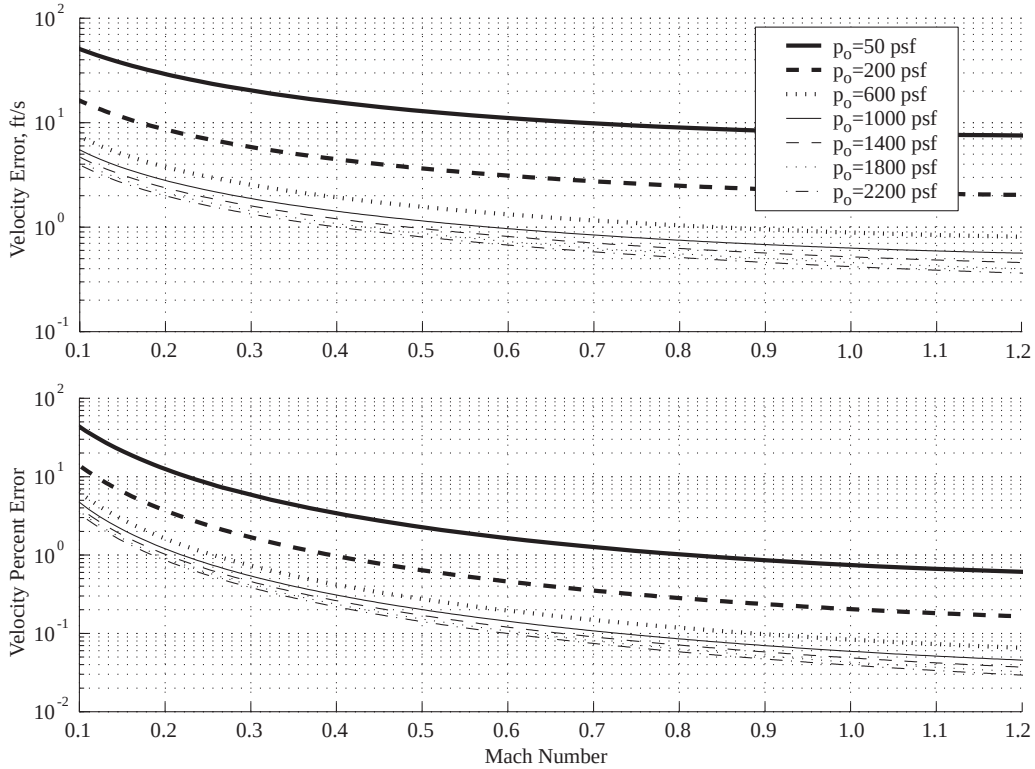

Figure 98. Velocity error and percent error versus Mach number in air due to Ruska error in primary tunnel stagnation and plenum pressures.

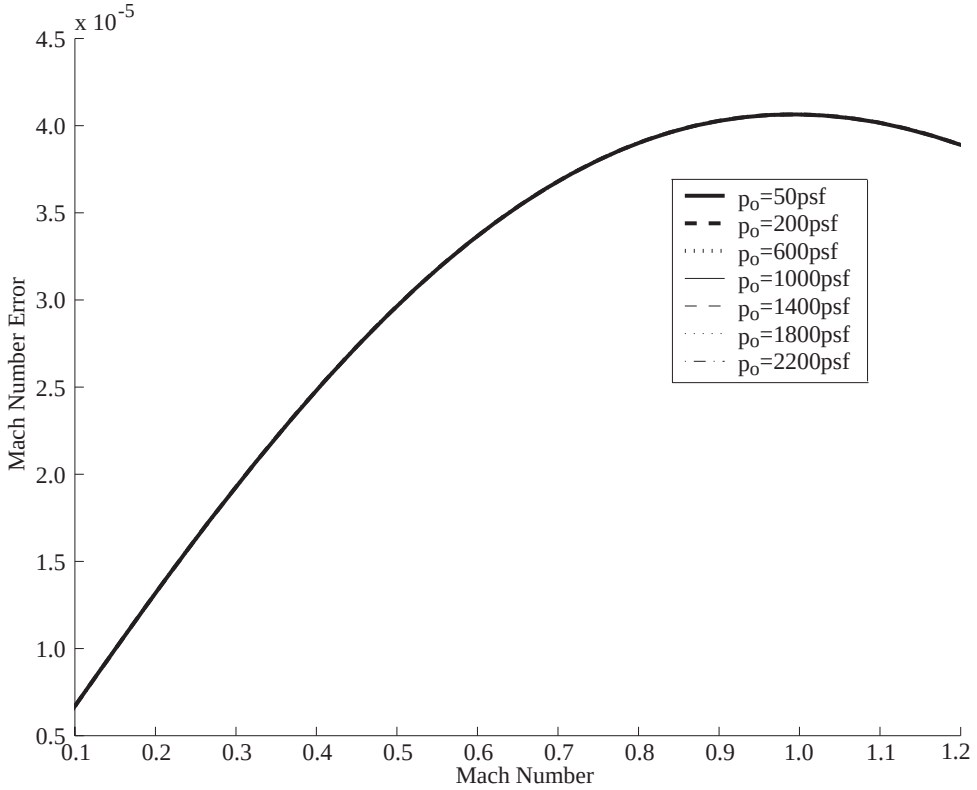

Figure 99. Mach number error versus Mach number in air due to error in primary tunnel stagnation temperature measurement.

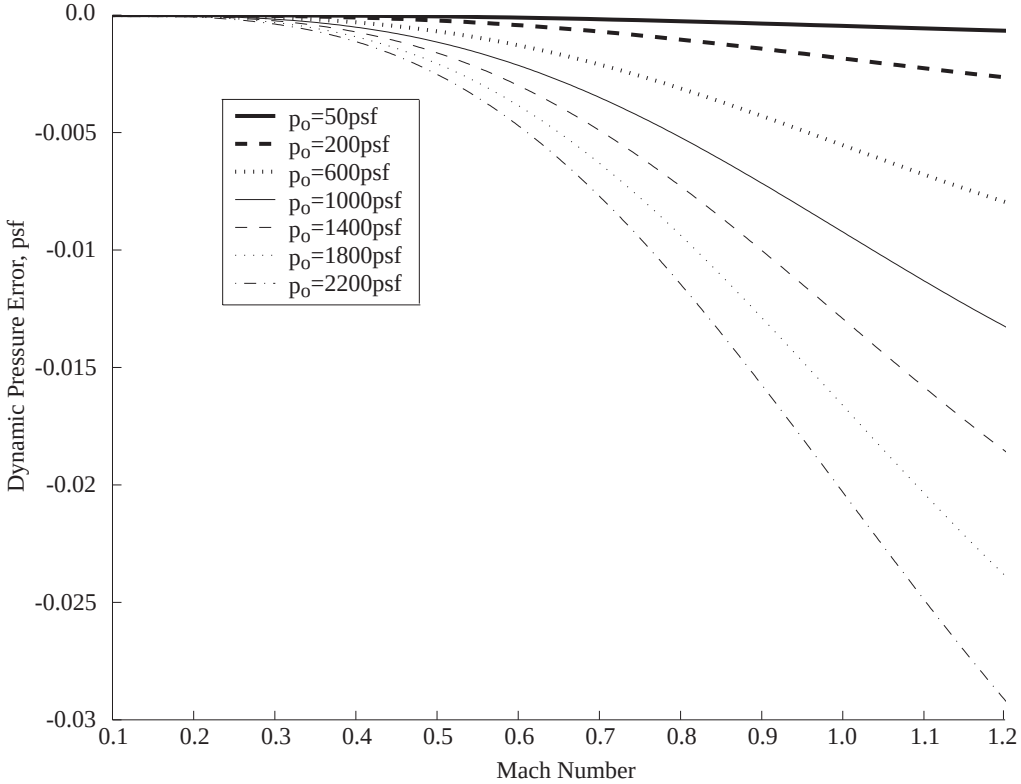

Figure 100. Dynamic pressure error versus Mach number in air due to error in primary tunnel stagnation temperature measurement.

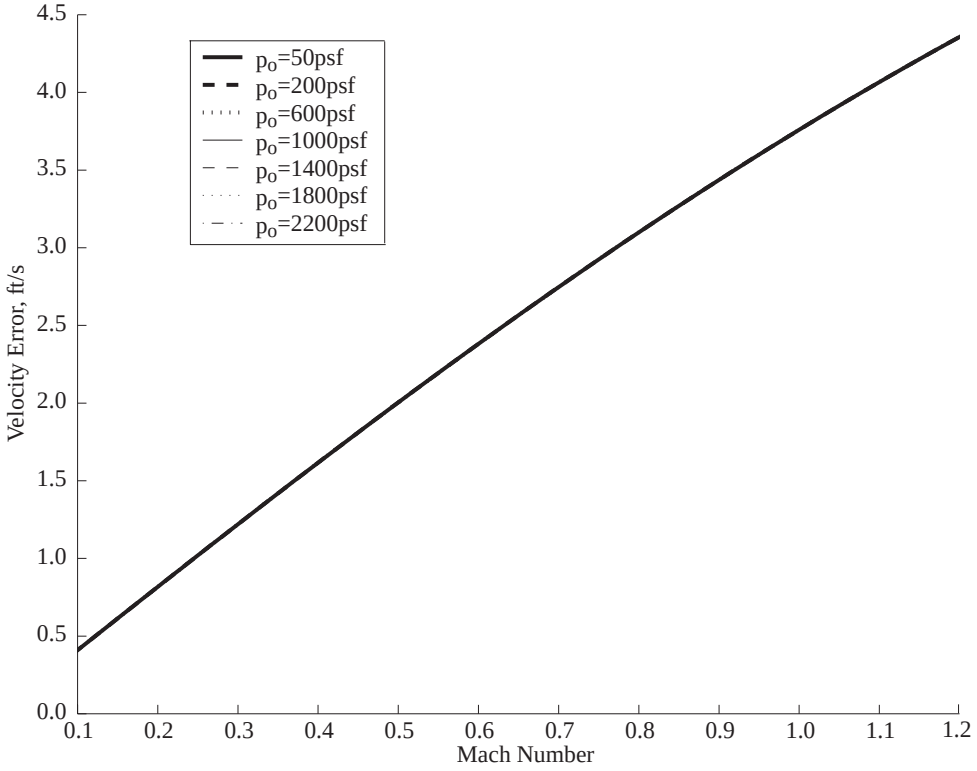

Figure 101. Velocity error versus Mach number in air due to error in primary tunnel stagnation temperature measurement.

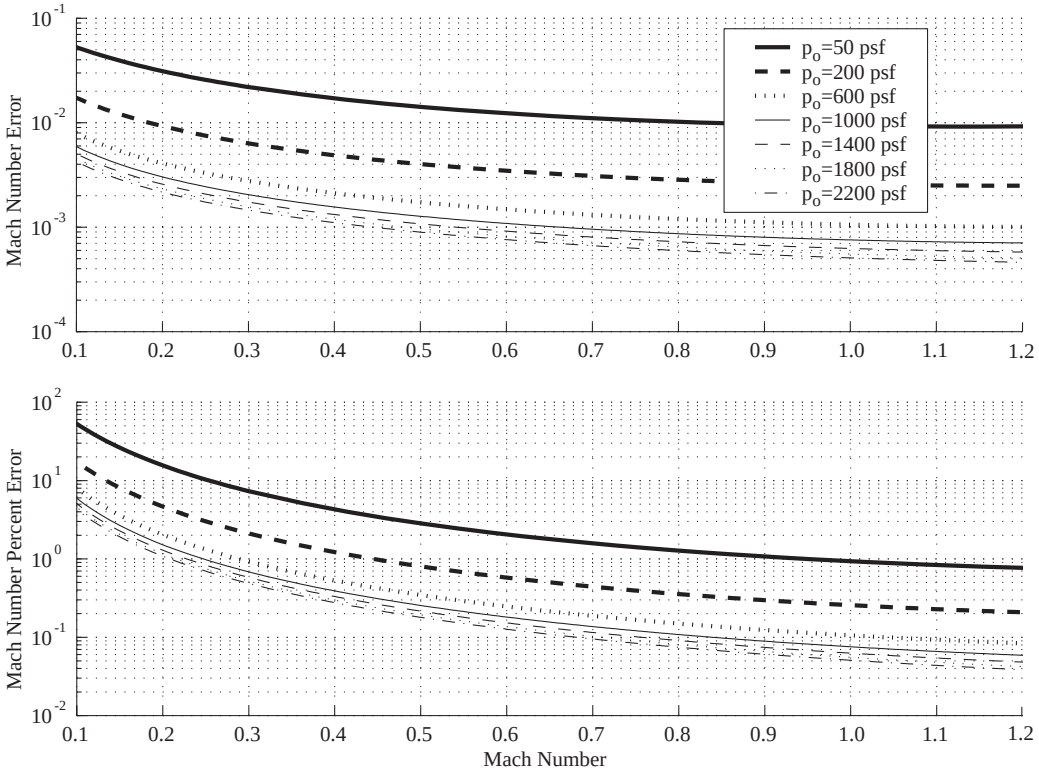

Figure 102. Mach number error and percent error versus Mach number in R-134a due to Ruska error in primary tunnel stagnation and plenum pressure.

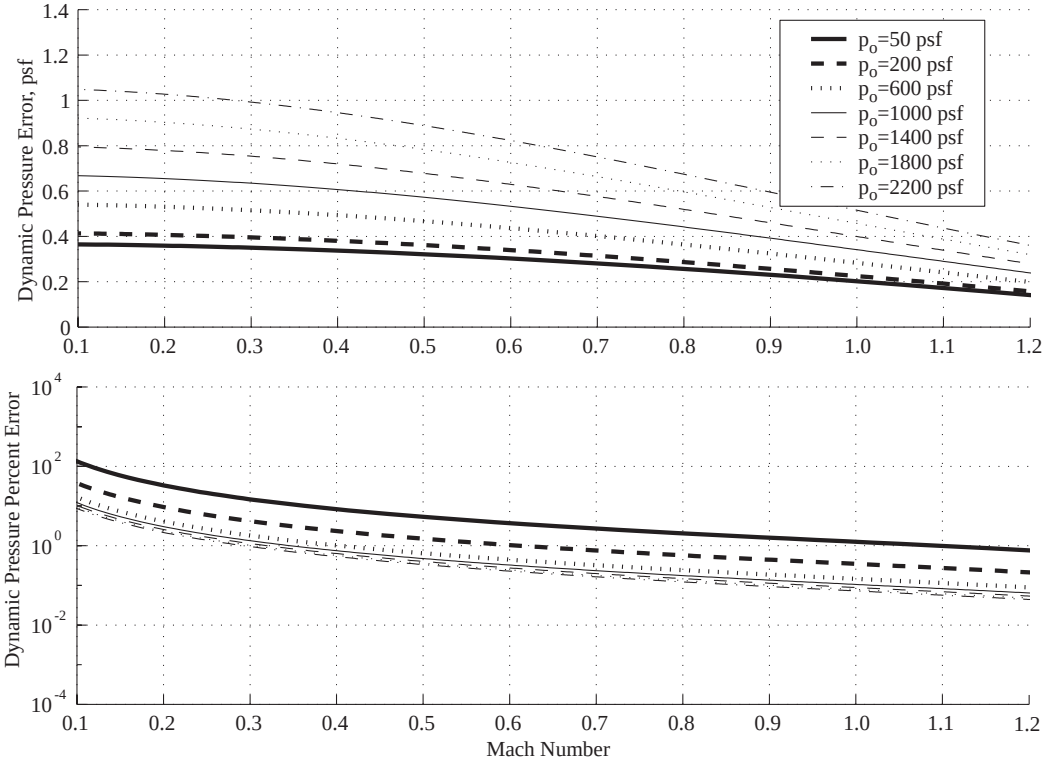

Figure 103. Dynamic pressure error and percent error versus Mach number in R-134a due to Ruska error in primary tunnel stagnation and plenum pressure.

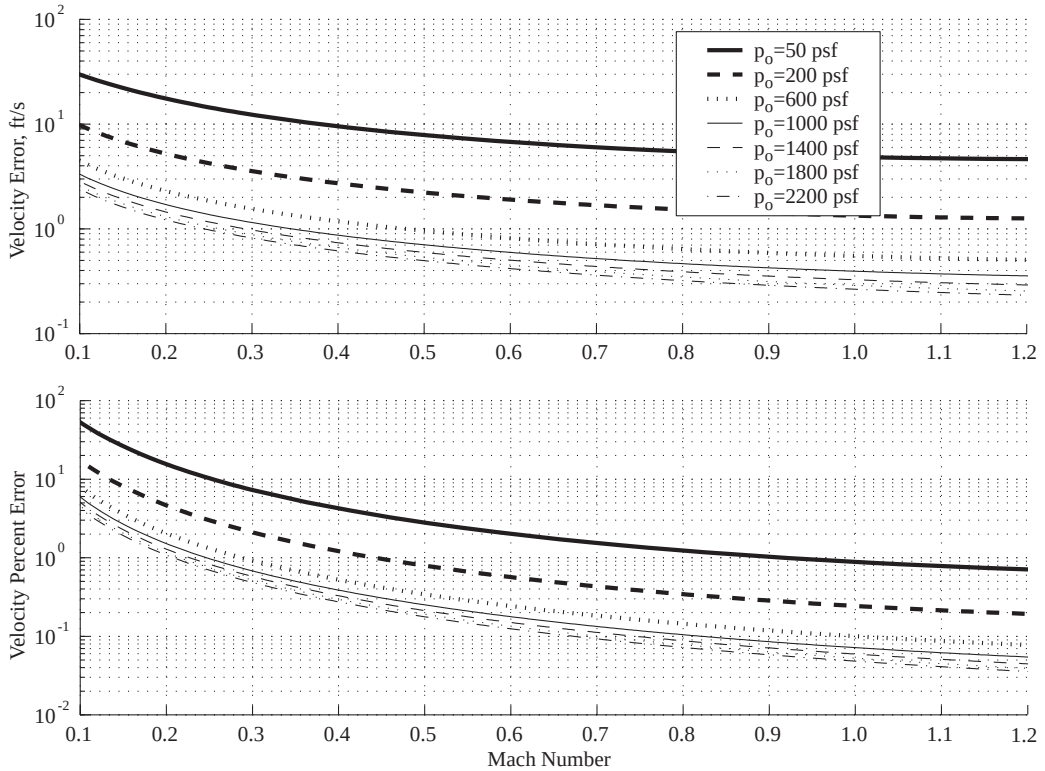

Figure 104. Velocity error and percent error versus Mach number in R-134a due to Ruska error in primary tunnel stagnation and plenum pressure.

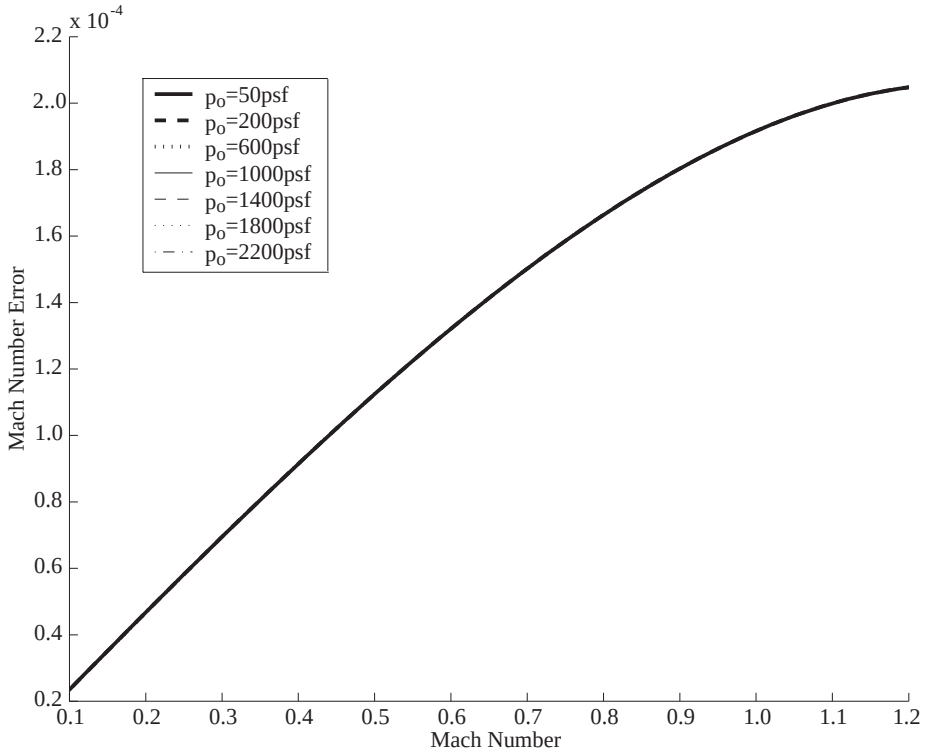

Figure 105. Mach number error versus Mach number in R-134a due to error in primary tunnel stagnation temperature.

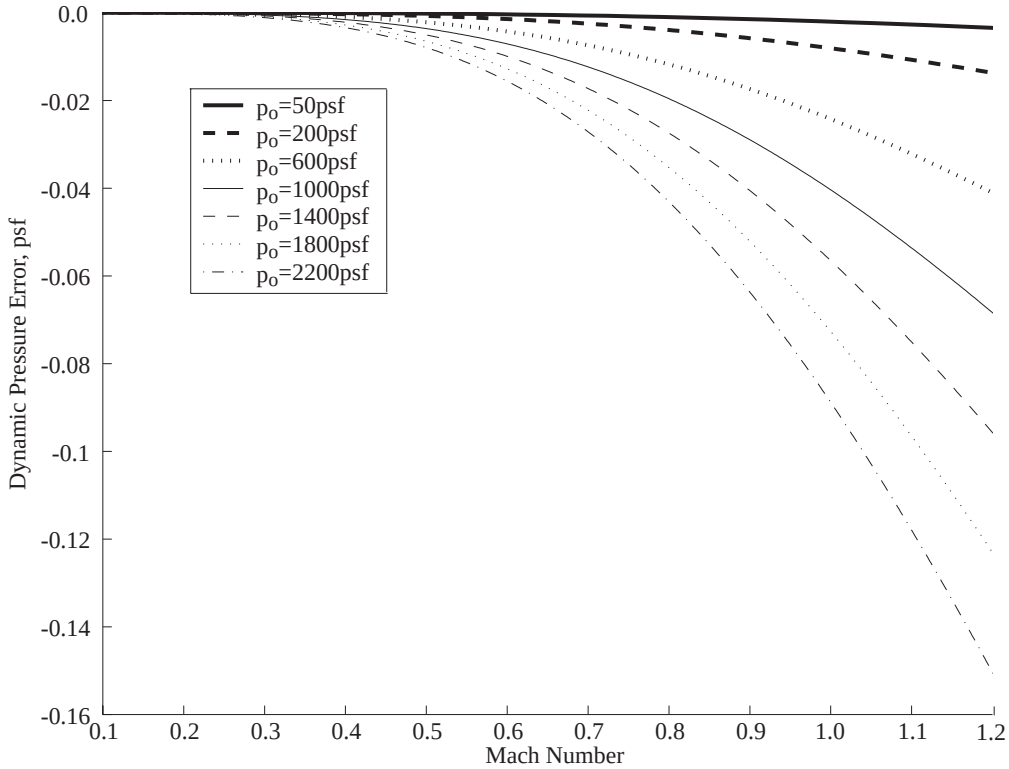

Figure 106. Dynamic pressure error versus Mach number in R-134a due to error in primary tunnel stagnation temperature.

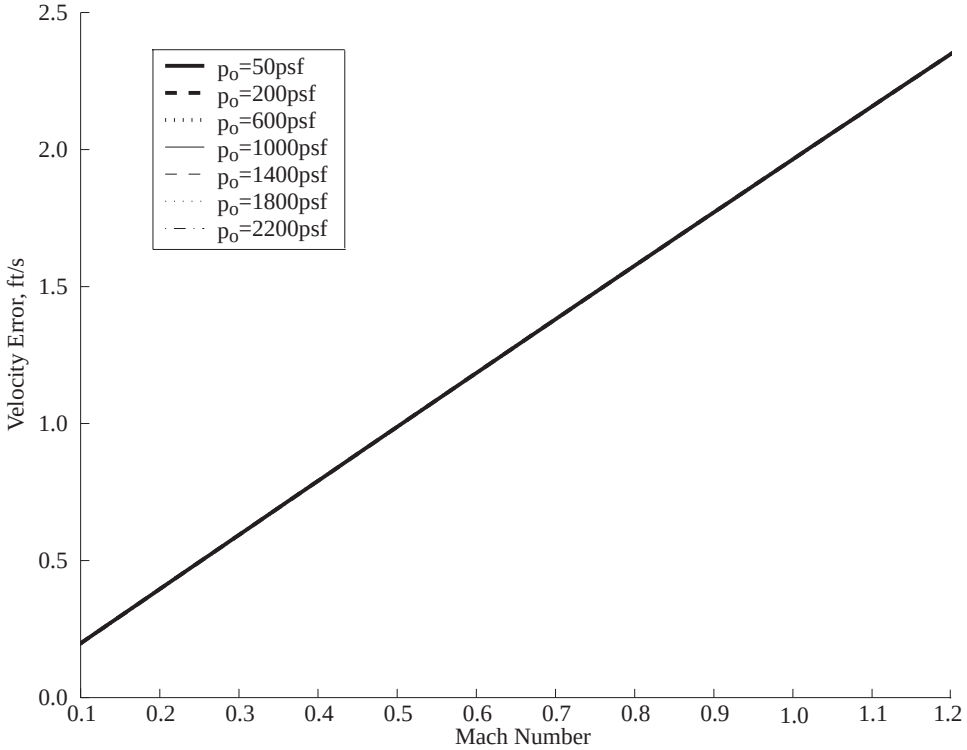

Figure 107. Velocity error versus Mach number in R-134a due to error in primary tunnel stagnation temperature.

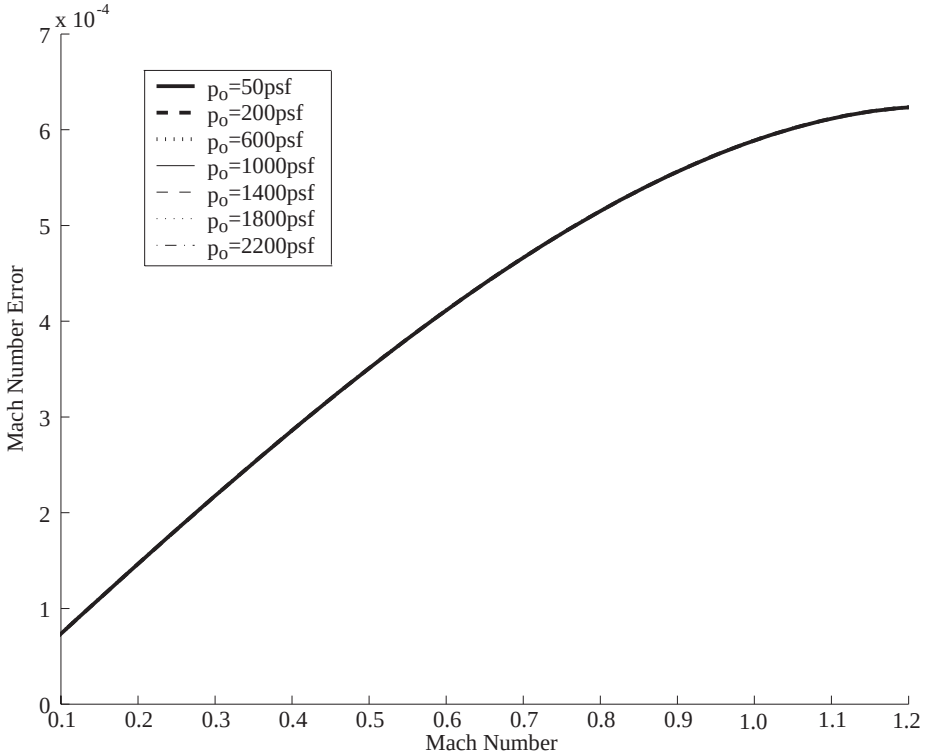

Figure 108. Mach number error versus Mach number in R-134a due to a 2% error in R-134a gas purity measurement.

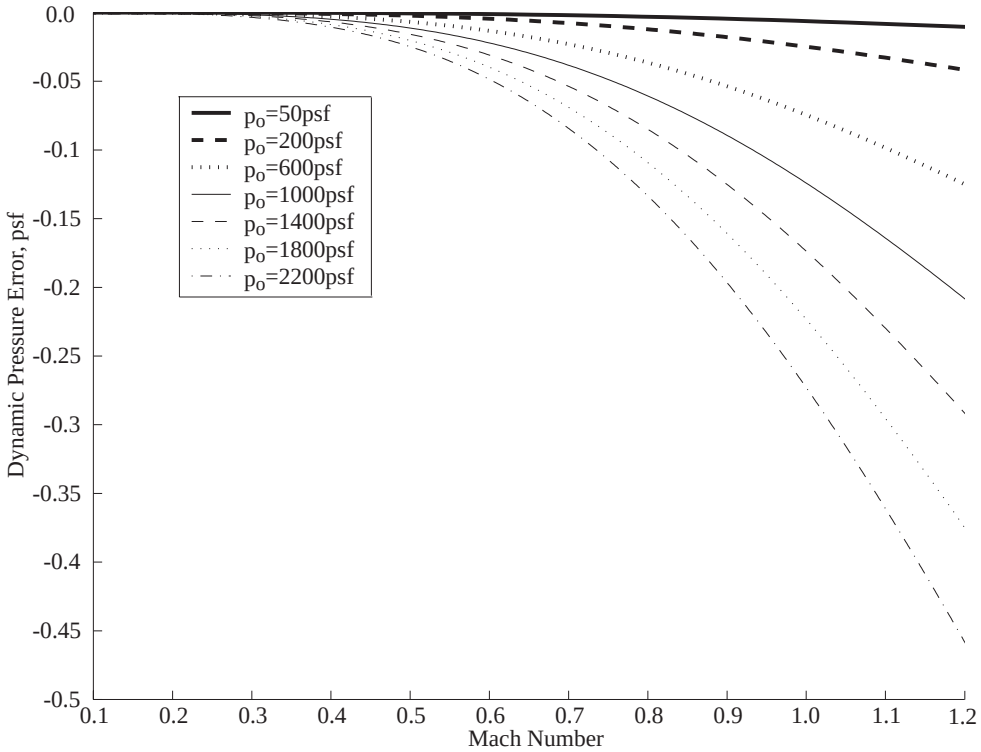

Figure 109. Dynamic pressure error versus Mach number in R-134a due to a 2% error in R-134a gas purity measurement.

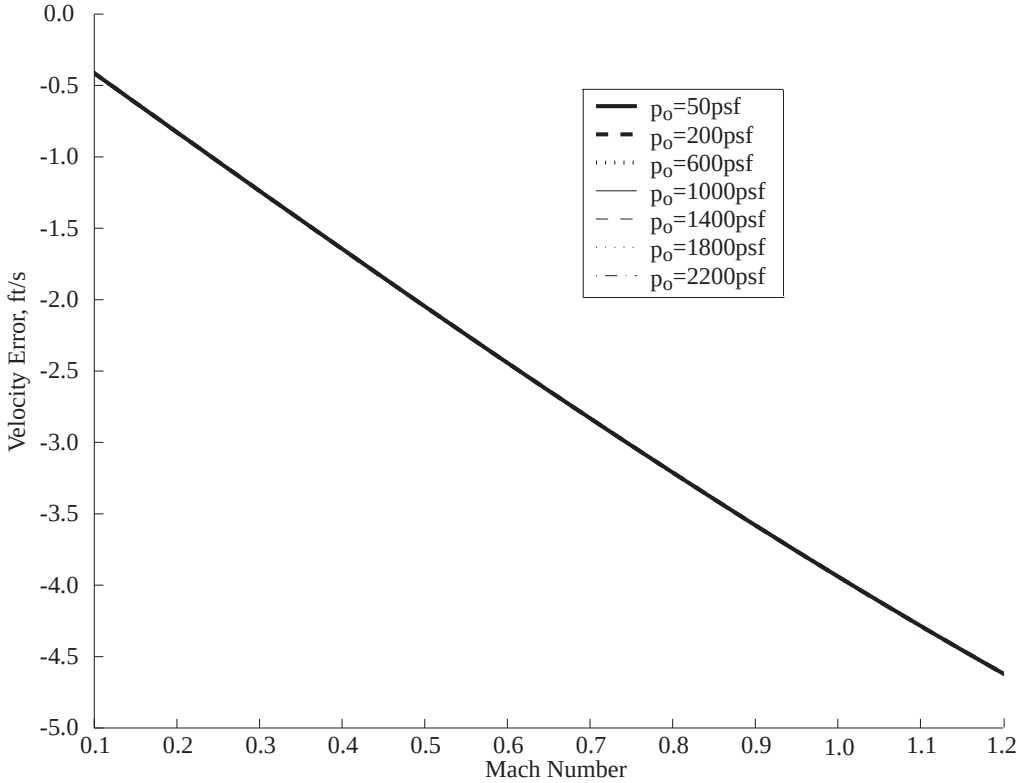

Figure 110. Velocity error versus Mach number in R-134a due to a 2% error in R-134a gas purity measurement.

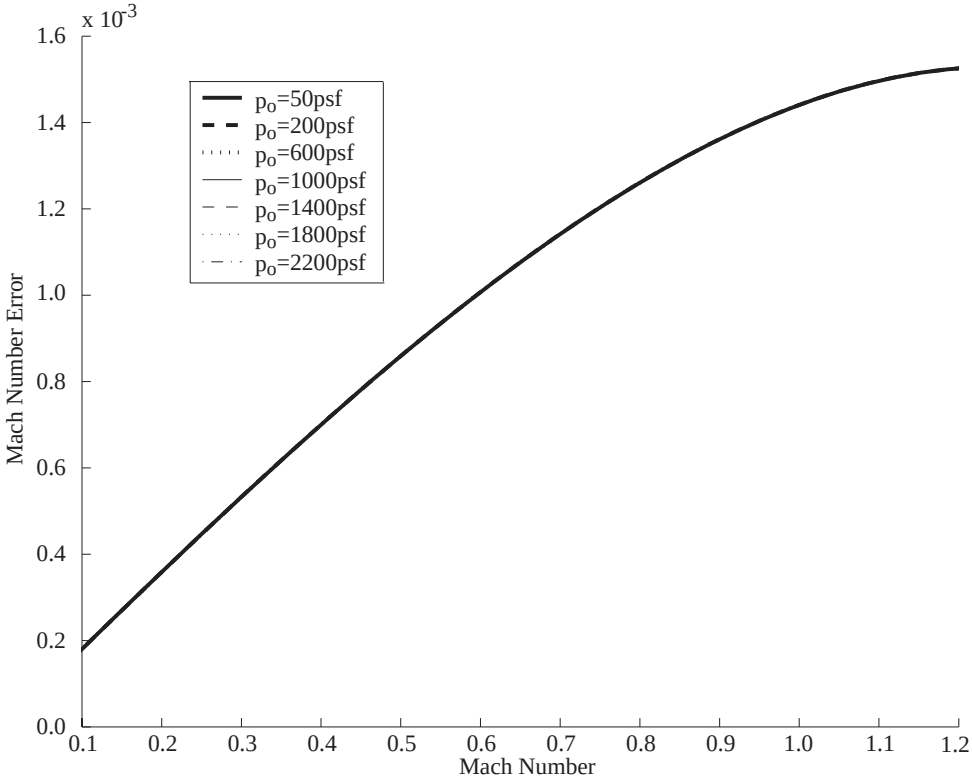

Figure 111. Mach number error versus Mach number in R-134a due to a 5% error in R-134a gas purity measurement.

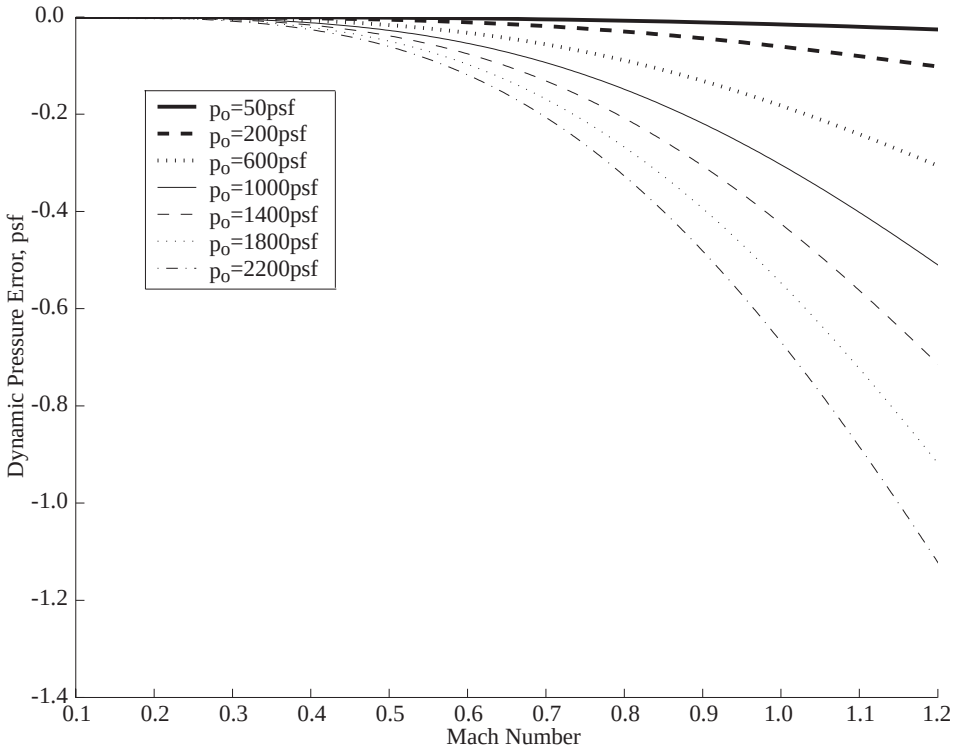

Figure 112. Dynamic pressure error versus Mach number in R-134a due to a 5% error in R-134a gas purity measurement.

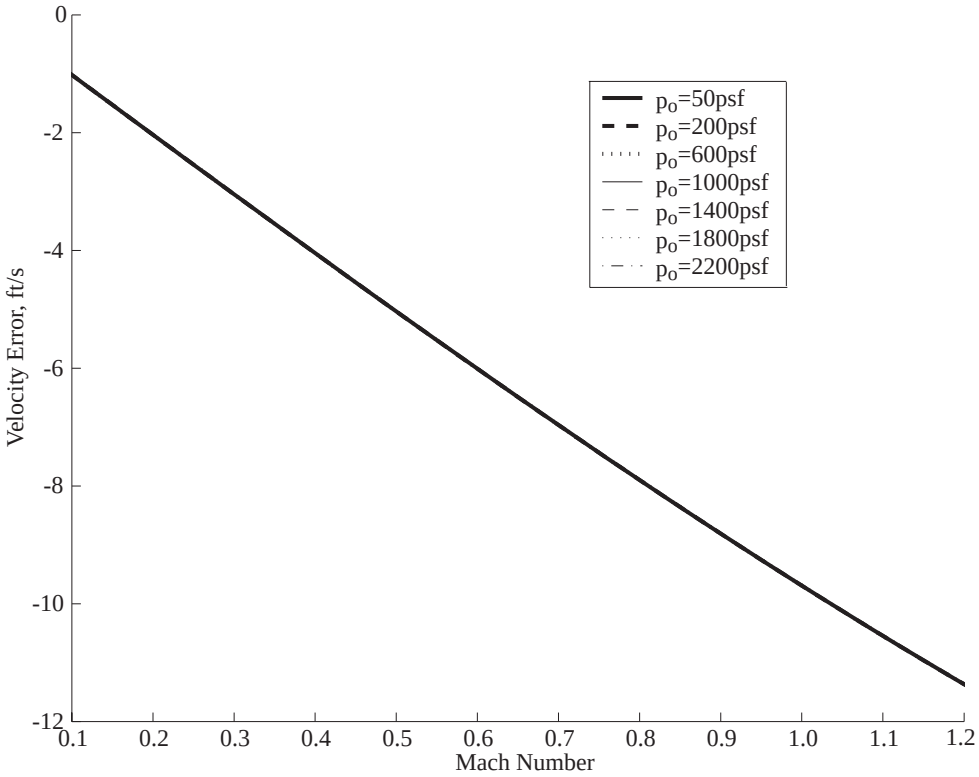

Figure 113. Velocity error versus Mach number in R-134a due to a 5% error in R-134a gas purity measurement.

REPORT DOCUMENTATION PAGE

Form Approved
OMB No. 0704-0188

1. AGENCY USE ONLY (*Leave blank*)	2. REPORT DATE	3. REPORT TYPE AND DATES COVERED
	June 2003	Technical Memorandum

4. TITLE AND SUBTITLE
Survey of Primary Flow Measurement Parameters at the NASA Langley Transonic Dynamics Tunnel

5. FUNDING NUMBERS
762-20-41-02

6. AUTHOR(S)
David J. Piatak

7. PERFORMING ORGANIZATION NAME(S) AND ADDRESS(ES)
NASA Langley Research Center
Hampton, VA 23681-2199

8. PERFORMING ORGANIZATION REPORT NUMBER
L-18282

9. SPONSORING/MONITORING AGENCY NAME(S) AND ADDRESS(ES)
National Aeronautics and Space Administration
Washington, DC 20546-0001

10. SPONSORING/MONITORING AGENCY REPORT NUMBER
NASA/TM-2003-212413

11. SUPPLEMENTARY NOTES

12a. DISTRIBUTION/AVAILABILITY STATEMENT
Unclassified-Unlimited
Subject Category 05 Distribution: Standard
Availability: NASA CASI (301) 621-0390

12b. DISTRIBUTION CODE

13. ABSTRACT *(Maximum 200 words)*
An assessment of the methods and locations used to measure the primary flow conditions in the NASA Langley Transonic Dynamics Tunnel was conducted during calibration activities following the facility conversion from a Freon-12 heavy-gas test medium to R-134a. A survey of stagnation pressure, plenum static pressure, and stagnation temperature was undertaken at many pertinent locations in the settling chamber, plenum, and contraction section of the wind tunnel and these measurements were compared to those of the existing primary flow measurement systems. Local flow velocities were measured in the settling chamber using a pitot probe. Results illustrate that small discrepancies exist between measured primary tunnel flow conditions and the survey measurements. These discrepancies in tunnel stagnation pressure, plenum pressure, and stagnation temperature were found to be approximately +/- 1-3 psf and 2-3 degrees Fahrenheit. The propagation of known instrument errors in measured primary flow conditions and its impact on tunnel Mach number, dynamic pressure, flow velocity, and Reynolds number have been investigated analytically and shown to require careful attention when considering the uncertainty in measured test section conditions.

14. SUBJECT TERMS
Wind tunnel flow measurements; Transonic wind tunnel; Transonic flow; R-134a;

15. NUMBER OF PAGES
81

16. PRICE CODE

17. SECURITY CLASSIFICATION OF REPORT	18. SECURITY CLASSIFICATION OF THIS PAGE	19. SECURITY CLASSIFICATION OF ABSTRACT	20. LIMITATION OF ABSTRACT
Unclassified	Unclassified	Unclassified	UL